

# **Geostatistical analysis of air pollution using models, in situ and remote sensed data**

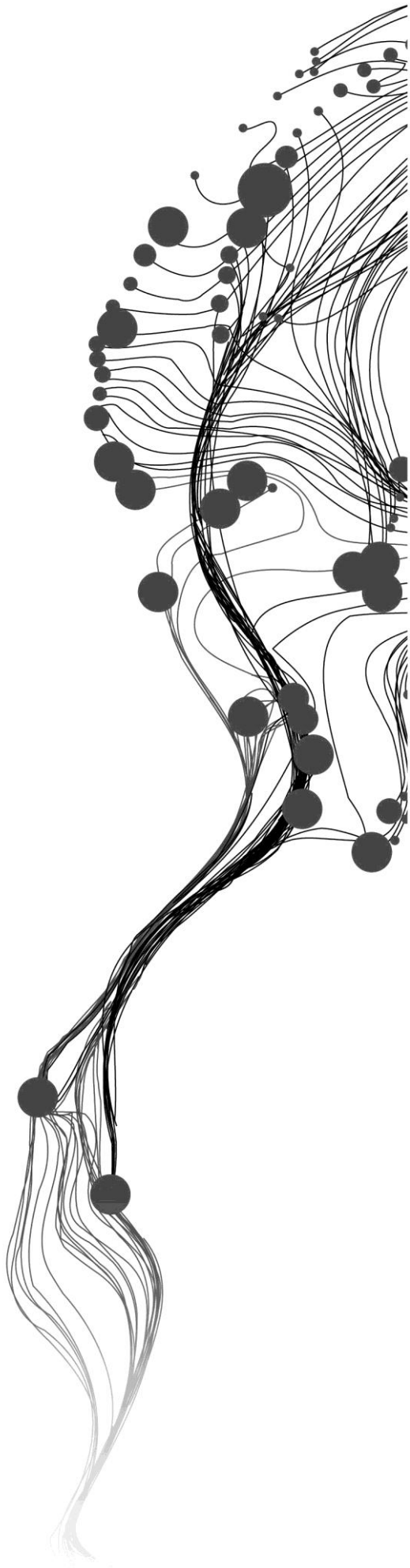
LEONS PETER MWENDA

March, 2011

SUPERVISORS:

Dr. N. A. S. Hamm

Prof. Dr. Ir. A. Stein



# **Geostatistical analysis of air pollution using models, in situ and remote sensed data**

**LEONS PETER MWENDA**

**Enschede, The Netherlands, March, 2011**

Thesis submitted to the Faculty of Geo-Information Science and Earth Observation of the University of Twente in partial fulfilment of the requirements for the degree of Master of Science in Geo-information Science and Earth Observation.

Specialization: Geoinformatics

**SUPERVISORS:**

Dr. N. A. S. Hamm

Prof. Dr. Ir. A. Stein

**THESIS ASSESSMENT BOARD:**

Chair: Prof. Dr. Ir. A. Stein

External Examiner : Prof. Dr. F. D. Van der Meer

#### DISCLAIMER

This document describes work undertaken as part of a programme of study at the Faculty of Geo-Information Science and Earth Observation of the University of Twente. All views and opinions expressed therein remain the sole responsibility of the author, and do not necessarily represent those of the Faculty.

## ABSTRACT

Understanding the status of air pollution concentration is of great importance due to severe effects to human health and environments. Different countries in Europe have several monitoring stations that collect information about pollutants continuously in time. These stations use different measurement techniques and different calibration practices are usually applied to measurements. However due to cost implication these stations are limited in space and therefore knowing air pollution at every point in space requires interpolation techniques. Geostatistical methods have been reported in various research to produce accurate maps because they incorporate spatial variability in observations. Recent research have shown that incorporating information that are correlated with in situ observations using appropriate techniques increases accuracy of resulting maps.

Country by country PM<sub>10</sub> daily annual mean concentration for 2006 were explored to understand effect of combining data from different countries. Two groups of data were explored; combined data from different countries measured by all techniques and combined data from different countries measured by one technique (beta ray attenuation) followed by country to country data exploration. Results shows that there are slightly differences in variability between two groups but relatively have similar spatial structures. It was difficult to obtain reliable spatial structure for some country due to small number of measurements.

Geostatistical methods known as regression kriging (RK) and cokriging (CK) were applied to integrate in situ measurements (PM<sub>10</sub>), models (PM<sub>2.5</sub>) and remotely sensed data (AOT) to predict PM<sub>10</sub> daily annual mean concentration for the year 2003. Accuracy assessment done at validation points has shown that regression kriging (RK) gave better results having lower RMSE equals 0.096 as compared to RMSE 0.099 obtained by CK. RK increased R from 0.40 to 0.71. Comparing to performance of ordinary kriging (OK) and universal kriging (UK), results shows that both RK and UK gave similar results of RMSE (0.096) and correlation (0.72). But RK was less biased as compared to UK. These results were obtained using exponential model.

Hole effect model was used in this study due to hole effect emerged on estimated variograms. Hole effect model fitted better the estimated variograms than exponential model at shorter distance but gave poor prediction results as compared to exponential model. RK of PM<sub>10</sub> on AOT and PM<sub>2.5</sub> using exponential model resulted to RMSE equals 0.096 as compared to RMSE value equals to 0.105 when hole effect model were used. However hole effect model was less biased as compared to exponential model.

Change of support was evaluated using universal block kriging. The results showed that lower RMSE were obtained for block sizes less or equal to 10 km by 10 km and high RMSE for block sizes greater than 10 km by 10 km. SSE was more sensitive to change of block size as compared to RMSE.

**Key words:** Air pollution, *Cokriging, Regression kriging, hole effect model, exponential model, block kriging, universal kriging, ordinary kriging.*

## ACKNOWLEDGEMENTS

To God be the glory for gift of life, blessings and protection.

I would like to appreciate my supervisor Dr. Nicholas Hamm for his guidance during the whole period of this study. Dr. Hamm did not only give his valuable advice and encouragement but also let me learn and discover processes on my own. His door was always opened for consultations sometimes even without an appointment. Importantly his criticisms during the whole research time made this study successful. Dr. Hamm thank you very much for the gift of geostatistical methods.

Second appreciation goes to my second supervisor Prof. Alfred Stein. I sincerely appreciate for your quick response and critical view on results which I provided at different stages. It helped me in detecting and correcting errors done in processes. Thank you indeed Prof. Stein.

I am thankful to van de Kasstele for provision of secondary data for the year 2003 used in this study.

I am grateful to my sponsor (NUFFIC) and my employer for allowing me to study.

I appreciate my fellow Tanzanian students who are studying in ITC and GFM 2009-2011 classmates for their cooperation at all moments. You are all part of this success.

I am indebted to my parents for raising me in good morals; My mother Antonia Samkongwa and my late father Petro Malipulla who passed away while I was studying for this MSc. May your soul rest in eternal peace.

I am thankful to my lovely family; my wife Modesta Mpoma and my children Josephina and Baraka for your encouragement and prayers. To my uncle Alphonse Mkongwa, you have been always light to my success.

I understand it is difficult to mention names of all individuals who in one way or another made all these possible, I am grateful for all your efforts. God bless you all.

# TABLE OF CONTENTS

---

Abstract .....	i
Acknowledgements .....	ii
List of figures .....	v
List of tables .....	vii
1. Introduction .....	1
1.1. Motivation and problem statement .....	1
1.2. Research objectives .....	2
1.2.1. Overall research objectives .....	3
1.2.2. Specific objectives .....	3
1.3. Research questions .....	3
1.4. Innovation .....	3
1.5. Thesis structure .....	3
2. Geostatistical methods .....	5
2.1. Introduction .....	5
2.2. Kriging of target variable only .....	5
2.3. Kriging the target variable using ancillary information .....	5
2.3.1. Ordinary linear regression .....	6
2.3.2. Regression kriging (RK) .....	6
2.3.3. Cokriging (CK) .....	7
2.4. Change of support .....	7
3. Study area and data description .....	9
3.1. Introduction .....	9
3.2. Study area .....	9
3.3. Data description .....	10
3.3.1. In situ measurements (PM10) .....	10
3.3.2. Satellite image data (AOT) .....	11
3.3.3. Model outputs (PM2.5) .....	12
4. Methodology .....	15
4.1. Data preprocessing .....	15
4.2. Data projection .....	15
4.3. Data exploration .....	15
4.4. Country by country data exploration for 2006 .....	15
4.5. Subsetting in situ measurements .....	15
4.6. Modelling .....	16
4.6.1. Empirical variograms .....	16
4.6.2. Modelling the variograms .....	16
4.6.3. Selection of variograms model .....	16
4.6.4. Modelling the hole effect .....	16
4.7. Prediction .....	17
4.7.1. Kriging of PM10 only .....	17
4.7.2. Universal block kriging .....	17
4.7.3. Ordinary linear regression .....	17
4.7.4. Regression kriging (RK) .....	17
4.7.5. Cokriging (CK) .....	19
4.8. Uncertainty assessment .....	20
5. Results .....	21
5.1. Country by country data analysis for 2006 .....	21

5.2.	Data exploration for 2003.....	23
5.2.1.	PM10 daily annual mean concentration for 2003.....	24
5.2.2.	PM2.5 monthly annual mean averages for 2003.....	24
5.2.3.	AOT daily annual averages for 2003 .....	25
5.3.	Spatial data analysis .....	26
5.4.	Variogram models .....	26
5.4.1.	Selection of variograms model .....	26
5.4.2.	Exponential variograms model of PM10 daily annual mean concentration for the year 2003..	27
5.5.	Kriging of PM10 only .....	27
5.6.	Universal block kriging .....	28
5.7.	Kriging of PM10 using ancillary data.....	29
5.7.1.	Ordinary linear regression .....	29
5.7.2.	Regression kriging using exponential model.....	31
5.7.3.	Kriging using hole effect model.....	35
5.7.4.	Cokriging (CK).....	38
5.8.	Using coarse model outputs .....	42
5.8.1.	RK of PM10 regressed on coarser PM2.5.....	42
5.8.2.	Cokriging of PM10 with coarser PM2.5 .....	44
5.9.	Accuracy assessment.....	45
5.9.1.	Prediction using exponential model .....	45
5.9.2.	Prediction using hole effect model .....	45
5.9.3.	Block kriging.....	46
5.9.4.	Ordinary linear regression and RK.....	46
6.	Discussion.....	49
7.	Conclusion and recommendations .....	53
7.1.	Conclusions .....	53
7.2.	Recommendations .....	54
	List of appendices.....	55
	List of references .....	68

## LIST OF FIGURES

---

Figure 3-1. Study area : Source (Google Earth).....	9
Figure 3-2. Locations of air pollution monitoring stations across Europe for the year 2003.....	11
Figure 3-3. AOT daily annual averages derived from MODIS projected to LAEA 1989 at spatial resolution of 10 km by 10 km square grid.....	12
Figure 3-4. Monthly annual averages PM2.5 modelled by LOTOS-EUROS for 2003 projected to LAEA 1989 coordinates system at 30 km by 30 km square grid (left) and to 10 km by 10 km square grid (right). ..	12
Figure 4-1. Overlay of PM10 daily annual mean concentration observations with secondary information for 2003; AOT overlaid with PM10 (left) and PM2.5 overlaid with PM10 (right) .....	17
Figure 4-2. Methodology for linear regression and regression kriging (Adopted from (Hengl et al., 2004)) .....	18
Figure 4-3. General methodology for kriging .....	19
Figure 5-1. Histograms for combined PM10 daily annual mean concentration measured by all techniques. A-raw data, B-log 10 .....	21
Figure 5-2. Histograms of combined PM10 daily annual mean concentration measured by beta ray technique for the year 2006.....	22
Figure 5-3. Log10 normal probability plots of PM10 daily annual mean concentration for 2006. (A) combined PM10 data measured by all techniques and (B) combined PM10 data measured by beta ray attenuation technique for the year 2006.....	22
Figure 5-4. Variograms models for PM10 concentration for the year 2006: A-for combined PM10 data measured by all techniques and B-for data measured by beta ray technique.....	23
Figure 5-5. Histograms of PM10 daily annual mean measurements for the year 2003; (a) raw data, (b) log10 and (c) natural log .....	24
Figure 5-6. Normal probability plots of PM10 daily annual mean measurements for the year 2003 (a) raw data, (b) log10 and (c) natural log.....	24
Figure 5-7. Histograms of PM2.5 monthly annual mean concentration averages for 2003. (A) is the PM2.5 raw data histogram which is positively skewed. (B) is the histogram of base-10 logarithm transformed PM2.5 showed to be normally distributed.....	25
Figure 5-8. Histogram of AOT daily annual averages for 2003.....	25
Figure 5-9. Bubble plot of insitu measurements showing PM10 concentration.....	26
Figure 5-10. Selecting variograms model for PM10 concentration for 2003.....	26
Figure 5-11. Exponential variograms model of PM10 daily annual mean concentration for the year 2003. ....	27
Figure 5-12. PM10 daily annual mean concentrations map for the year 2003 produced by OK of in situ measurements.....	27
Figure 5-13. PM10 daily annual mean concentrations map for the year 2003 produced by UK of in situ measurements.....	28
Figure 5-14. PM10 daily annual mean concentrations map for the year 2003 produced by universal block kriging of in situ measurements at the block size of 10 km by 10 km. (A) is the prediction map at area support (B) is the kriging variance.....	28
Figure 5-15. PM10 daily annual mean concentrations map for the year 2003 produced by universal block kriging of in situ measurements at the block size of 30 km by 30 km. (A) is the prediction map at area support (B) is the kriging variance.....	29
Figure 5-16. PM10 daily annual mean concentration map for 2003 produced by ordinary linear regression of PM10 regressed on AOT. AOT was an input to equation 5-1.....	30

Figure 5-17. PM10 daily annual mean concentration map for 2003 produced by ordinary linear regression of PM10 regressed on PM2.5. PM2.5 was an input was an input to equation 5-2.....	30
Figure 5-18. PM10 daily annual mean concentration map for 2003 produced by ordinary linear regression of PM10 regressed on AOT and PM2.5. AOT and PM2.5 were inputs to equation 5-3.....	31
Figure 5-19. Regression line between PM10.....	31
Figure 5-20. Regression diagnostic plot of PM10 and AOT.....	31
Figure 5-21. Variograms model of residual between PM10 and AOT (distance in km).....	32
Figure 5-22. PM10 daily annual mean concentration map for 2003 produced by RK of PM10 regressed on AOT .....	32
Figure 5-23. Regression line between PM10 and PM2.5. There is poor correlation as depicted by regression line .....	33
Figure 5-24. Regression diagnostic plot of PM10 and PM2.5. Residuals shows high correlation though deviates from normal distribution (see residual vs fitted and Normal Q-Q) .....	33
Figure 5-25. Exponential variograms model of residual between PM10 and PM2.5 (distance in km) .....	33
Figure 5-26. PM10 daily annual mean concentration map for 2003 produced by RK of PM10 regressed on PM2.5 .....	34
Figure 5-27. Diagnostic plot of PM10 regressed on both covariates (AOT and PM2.5).....	34
Figure 5-28. Exponential variograms model of residuals between PM10 regressed on PM2.5 and AOT (distance in km).....	35
Figure 5-29. PM10 daily annual mean concentration map for 2003 produced by RK of PM10 regressed on AOT and PM2.5.....	35
Figure 5-30. Hole effect model variograms (left) and computed model parameters (right) of PM10 daily annual mean concentration for the year 2003 .....	36
Figure 5-31. PM10 daily annual mean concentration predicted maps using hole effect model. Predictions presented in (A) were produced by OK and predictions presented in (B) were produced by UK using PM10 available observations. Both methods used model presented in figure 5-30.....	36
Figure 5-32. Hole effect model fitted to residuals of PM10 regressed on AOT and its corresponding RK map (right).....	37
Figure 5-33. Hole effect model fitted to residuals of PM10 regressed on PM2.5 and its corresponding RK map (right).....	37
Figure 5-34. Hole effect model fitted to residuals of PM10 regressed on AOT and PM2.5 (Left) and is its corresponding RK map (right).....	37
Figure 5-35. Cross variograms model between PM10 and AOT .....	38
Figure 5-36. PM10 daily annual mean concentration map for 2003 produced by cokriging of PM10 with AOT. (A) is the cokriging predictions and (B) is the cokriging variance. ....	39
Figure 5-37. Cross variograms model between PM10 and PM2.5.....	40
Figure 5-38. PM10 daily annual mean concentration map for 2003 produced by cokriging of PM10 with PM2.5.....	40
Figure 5-39. Cross variograms model between PM10 with AOT and PM2.5. ....	41
Figure 5-40. PM10 daily annual mean concentration map for 2003 produced by cokriging of PM10 with AOT and PM2.5.....	42
Figure 5-41. PM10 daily annual mean concentration for 2003 produced by RK of PM10 regressed to coarser PM2.5 at spatial resolution of 30 km. ....	43

## LIST OF TABLES

---

Table 1-1. Research objectives with specific research questions .....	3
Table 3-1. Number of stations per measurement techniques per country for the year 2006. ....	10
Table 3-2. Summary of background stations used for the year 2003.....	11
Table 5-1. Summary statistics of PM10 daily annual mean for 2006. ....	21
Table 5-2. Computed exponential model parameters of PM10 daily annual mean concentration for 2006	23
Table 5-3. Descriptive summary statistics for PM10 annual daily mean concentration for 2003 .....	24
Table 5-4. Summary statistics of PM2.5 data and its corresponding base-10 logarithmic transformed data. .....	25
Table 5-5. Computed exponential model parameters for PM10 daily annual mean concentration for the year 2003. ....	27
Table 5-6. Ordinary linear regression model results for (A) PM10 regressed on AOT, (B) PM10 regressed on PM2.5 and (C) PM10 regressed on both AOT and PM2.5 .....	29
Table 5-7. Residual model parameters of PM10 regressed on AOT (range in km).....	32
Table 5-8. Residual model parameters of PM10 regressed on PM2.5 (range in km) .....	33
Table 5-9. Residual model parameters of PM10 regressed on PM2.5 and AOT(range in km) .....	35
Table 5-10. Cross variograms model parameters between PM10 and AOT .....	38
Table 5-11. Cross variograms model parameters between PM10 and PM2.5. ....	39
Table 5-12. Cross variograms model parameters of PM10 with AOT and PM2.5. ....	41
Table 5-13. Regression model between PM10 and coarser resolution PM2.5 at 30 km square grid. ....	42
Table 5-14: RK model and predicted map when PM10 regressed on coarser PM2.5 at 30 km grid. ....	43
Table 5-15: Cokriging of PM10 daily annual mean concentration with coarser PM2.5 at 30 km square grid for 2003.....	44
Table 5-16. Accuracy assessment for results of PM10 predictions for 2003 when employing exponential model. Table 5-16 (a) AOT and PM2.5 used were at 10 km square grid and table 5-16 (b) PM2.5 used was at 30 km square grid. The observed mean equals 1.407.....	45
Table 5-17. Accuracy assessment for results of PM10 predictions for 2003 when employing hole effect model. AOT and PM2.5 were at 10 km square grid. The observed mean equals 1.407 .....	45
Table 5-18. Accuracy assessment of universal block kriging at different block sizes.....	46
Table 5-19. Model performance comparison between ordinary linear regression and RK. The observed mean equals 1.407.....	46



# 1. INTRODUCTION

## 1.1. Motivation and problem statement

Air pollution is a major problem for human health and a particular concern is respiratory illness (Zhang et al., 2010). People are affected through inhaling when exposed to polluted environment (indoor or outdoor) and have caused thousands of death due to cancer and lung diseases (Fischer et al., 2004; Stedman, 2004). Detailed explanations about individual pollutants' sources and health effects are found in Dickey (2000).

Many studies are concerned on spatial distribution of particulate matter (PM<sub>10</sub>) concentrations because it is one of the principal indicators of air quality and is believed to have more effect to human health (Emili et al., 2010; Schaap et al., 2009a; van de Kasstele, 2006). "PM<sub>10</sub>" is composed of solid and liquid particles sourcing from sea salt, volcanic ashes, dust from wind bowl, industries emissions, traffic emission, forest burnings etc having a diameter less than 10  $\mu\text{gm}^{-3}$  (Emili et al., 2010).

Due to problems associated with air pollution to human health and ecosystem, there is significant importance to understand the spatial distribution of air pollution at any given point in time and accurate mapping of its concentration. Air pollution concentration maps are generated from various data sources; in situ measurements, model outputs and remotely sensed images. These three sources measures air pollution concentration directly and indirectly at different spatial and temporal scales (Emili et al., 2010; van de Kasstele et al., 2006).

In situ measurements are considered to be accurate and precise in measuring air pollution as they make direct measurements (Cinzia Mazzetti and Todini, 2002; van de Kasstele, 2006). However, measurements from this source are sparsely located thus fail to capture pollution concentration at every area of interest due to their scarcity. Also being sparsely located limits prediction accuracy of air pollution maps using insitu data due to high spatial uncertainties (Bayraktar and Turalioglu, 2005; Beelen et al., 2009; Diem and Comrie, 2002; van de Kasstele and Stein, 2006; van de Kasstele et al., 2006). However, their scarcity is due to cost involved in handling them (Bayraktar and Turalioglu, 2005; van de Kasstele, 2006). For example, in the Netherlands, background stations were reduced from 73 to 32 in 1980s hence increased spatial uncertainties (van de Kasstele and Stein, 2006). Therefore interpolation techniques have been used for mapping pollution concentration at unmonitored locations (Beelen et al., 2009; Emili et al., 2010; van de Kasstele and Stein, 2006).

Apart from in situ measurements, there exist other data sources for mapping air pollution. For example air pollution maps are also produced from model outputs. For example PM<sub>2.5</sub> modelled by Chemical Transport Model (CTM) LOTOS-EUROS. Concentration maps are simulated by these models basing on knowledge of chemical and physical processes (Schaap et al., 2009b; van de Kasstele, 2006). However, model outputs have some limitations; e.g. Models requires detailed information of pollution source distributions, height of the source, meteorological condition e.g. Boundary Height Layer (BHL), Relative Humidity (RH) etc, terrain surface, emission etc (Beelen et al., 2009). In addition to that; models tends to under estimate pollutants concentration; for example LOTOS-EUROS model tends to underestimate PM<sub>2.5</sub> (Denby et al., 2008; van de Kasstele et al., 2006). Moreover model output maps are also available at coarser resolution grid of 0.5° by 0.25°, approximately 35 km by 25 km in Europe (Schaap et al.,

2009b). Furthermore, models are always subject to uncertainty due to uncertainties from inputs and the final predicted map will, therefore, be inaccurate (van de Kasstele et al., 2006).

Remotely sensed data has emerged as another important source for mapping air pollution. This does not measure PM10 directly but products derived from remote sensed data have shown to have correlation with air pollutants and has been useful information in prediction air pollution (Emili et al., 2010). The commonly remote sensing derived product correlated with PM10 concentration is Aerosols Optical Thickness (AOT) (Emili et al., 2010). The spatial coverage and temporal resolution of remotely sensed data makes this source important when mapping large area (Emili et al., 2010). The downside of it on the other hand is that, annual mean AOT is not fully representative of the year because its retrieval relies on cloud and snow free conditions and needs correct estimation of surface reflectance (Emili et al., 2010).

Incorporating data from other sources with insitu measurements has shown to be successful in increasing prediction accuracy of air pollution maps significantly (Singh et al., 2011; van de Kasstele and Stein, 2006; van de Kasstele et al., 2006). van de Kasstele & Stein (2006) used Kriging with External Drift (KED) to predict concentration of NO<sub>x</sub> in which the Operational Priority Substances (OPS) model outputs were used as covariate. Their approach aimed in improving the quality of air pollution maps by merging data from different sources and incorporated uncertainty of input data. Generally inclusion of dispersion model outputs improved prediction accuracy.

van de Kasstele et al. (2006) used linear modelling to standardize and predict PM10 concentration observed by in situ measurements over Western Europe. They used two secondary information; PM2.5 from dispersion models and AOT from MODIS. In their approach, PM2.5 was downscaled by bilinear interpolation to the MODIS grid and monitoring station locations for data matching. Their methods improved the prediction accuracy significantly. However, the issue of change of support was not addressed.

Cokriging is one among kriging techniques which is used to predict data at unsampled area using limited sampled data by the help of densely correlated variable known as covariate (Webster and Oliver, 2008). It differs to other kriging techniques explained so far in that not only variograms of primary variable is estimated but also the variograms of secondary data is required too. Finally, cross variograms model is built from the variograms of primary data and secondary data and used in prediction of primary variable at unsampled location using collocated values of secondary variables. It has been used in various research; in image integration for example, and has shown valuable contribution in increasing prediction accuracy. In addition, it has ability to account for different supports and to incorporate ancillary data in the process (Atkinson et al., 2008; Pardo Iguzquiza et al., 2006).

Most studies have not covered the effect of spatial scale in integrating dataset taking into account change of support. In this research, geostatistics will be used to analyse and predict PM10 concentration at background levels by integrating 3 datasets obtained at different spatial scale.

## **1.2. Research objectives**

This section provides research orientation in which objectives and research questions are addressed. The research will be achieved by answering these questions. Innovations and related work will be put in context as well.

**1.2.1. Overall research objectives**

To develop and apply geostatistical techniques to integrate in situ measurements, remote sensed data and air quality model output to provide accurate air pollution maps taking into account of different spatial scale

**1.2.2. Specific objectives**

- i. To develop and apply geostatistical methods to integrate in situ data, model output and remotely sensing data to model and map air quality.
- ii. To predict concentrations of pollutants in between in situ stations using remotely sensed data and model output.

**1.3. Research questions**

Objective no	Research questions
1	1.1 What is the spatial distribution in the data? 1.2 How should the 3 sources be integrated? 1.3 How to model different data sources taking into consideration different spatial supports?
2	2.1. Which kriging methodology is most accurate in predicting at unsampled location? 2.2. How can predictions be validated?

Table 1-1. Research objectives with specific research questions

**1.4. Innovation**

The novelty of this research aims at developing geostatistical approach for integrating data of different spatial scale. More, is to integrate 3 rather than 2 variables by cokriging.

**1.5. Thesis structure**

This thesis comprises of 7 chapters. Chapter 1 enlightens the rationale of the study in which the motivation, problem and objectives and research questions of this study are addressed. Chapter 2 provides literature review and some related works. Chapter 3 is about study area and data description. Chapter 4 explains methodologies adopted on this study. Chapter 5 provides results obtained. Discussion of results and analysis is presented in chapter 6. Chapter 7 concludes and provides recommendation for further studies



## 2. GEOSTATISTICAL METHODS

### 2.1. Introduction

Geostatistical methods are a collection of statistical techniques which interpolates locations that are not sampled using limited available data. Methods comprise three steps; estimation of sample variograms, modelling of sample variograms and kriging. Goovaerts (1999) defines kriging as a family of generalized least squares regression algorithms. Kriging represents interpolation techniques based on regionalized variables and accounts for variation in the phenomena (Beelen et al., 2009). Variations in the phenomena comprises three components (i) broad scale trend (drift) (ii) local spatially structured variation and (iii) non spatial random variation and therefore various techniques of kriging exists to model these variations (Beelen et al., 2009).

In this chapter; a brief explanation on some geostatistical methods and their application in air pollution mapping will be put into context. Some related works which applied these methods in air pollution mapping and in other fields will be highlighted under respective sections. Section 2.2 is about Ordinary Kriging (OK) and Universal Kriging (UK). Section 2.3 is about kriging methods which employ use of ancillary data during kriging. These methods are Regression Kriging (RK) and Cokriging (CK). Under this section linear regression is outlined. Section 2.4 explains the concept of change of support in prediction. Block Kriging (BK) is addressed.

### 2.2. Kriging of target variable only

Ordinary kriging and universal kriging predict the values of primary variable at unsampled locations based on availability of primary variable observations. Ordinary kriging is the most commonly used type of kriging which assumes constant but unknown mean which interpolates values at unsampled locations by weighting the available observations (Denby et al., 2008). The method takes into account only local variation of the variable of interest (Beelen et al., 2009). Armstrong (1984) describes OK as a method for estimating stationary phenomena and suitable in mining.

Universal kriging is the method which is applicable to random field with varying mean whereby drift is modelled as a function of coordinates (Hengl et al., 2007). It accounts for long range variation of the phenomena (Beelen et al., 2009).

These methods has been applied before in air pollution mapping and showed to produce better results. Beelen et al. (2009) conducted an assessment of UK, OK and RK in prediction of air pollution across Europe and found that UK gives more accurate maps than OK and RK. He worked with rural and urban background stations but they were modelled separately and the final map was obtained by combining (stamping) urban maps onto rural maps.

### 2.3. Kriging the target variable using ancillary information

RK and CK are kriging techniques which makes use of ancillary data in prediction of primary variable. Applicability of these methods in air pollution analysis is explained in this section. Ordinary linear regression is explained in this section in order to avoid confusion with regression kriging.

### 2.3.1. Ordinary linear regression

Ordinary linear regression is a method used to establish a mathematical relationship between the primary variable and secondary information (Goovaerts, 1999; Hengl et al., 2007). It is based on associating data at collocation and finding a function that relate the variables under consideration. During prediction, the equation/function formulated is used to predict primary variable at unsampled location taking advantage of availability of secondary information i.e. prediction of primary variable using secondary variable as input to the function. General formula for linear regression is presented in equation 2-1

$$f(x) = \beta_0 + \beta_1x_1 + \dots + \beta_nx_n + \varepsilon \quad (2-1)$$

Where;

$f(x)$  is the map of PM10 produced (response)

$x_i$  are the predictors value at a particular location (PM2.5 and AOT)

$\beta_0$  intercept.

$\beta_i$  are the model coefficients (weight)

$\varepsilon$  is the error.

However linear regression has limitation that predicting a value of primary variable at location ( $s_o$ ) is a computed using secondary variable at location ( $s_o$ ) without taking into account of neighbouring secondary values at location ( $s_i$ ). This means, linear regression does not consider spatial dependence within data (Goovaerts, 1999). Goovaerts (1999) generated annual erosivity map by linear model by associating limited daily read rain gauge stations (36 stations) and digital elevation model. For clarity, using established relationship between erosivity and elevation, values of erosivity was computed from elevation at each point.

Emili et al. (2010) used simple linear regression and multi-linear regression relationship to investigate the capability of satellite imagery to predict ground PM10 concentrations and studied the effect of spatial and temporal resolution in prediction. They used two datasets; geostationary Spinning Enhanced Visible and InfraRed Imager (SEVIRI) having coarse spatial resolution (25 km) but high temporal resolution (15 min) and MODIS having 10 km spatial resolution while gives two measurement per day. Using simple linear regression and multi-linear regression relationship between PM10 and Aerosols Optical Thickness (AOT), they found out SEVIRI had high correlation 0.7 while MODIS had 0.6 with regard to 24 h, however with regard to hourly time series observation both sensors showed low correlation with PM10 0.42 and 0.46 respectively reason behind assumed to be pixel to point comparison. They concluded that frequency of observations plays important role in PM10 while high spatial resolution does not generally improve PM10 estimation. Importantly, estimation of AOT depends on estimation of surface reflectance and cloud and snow free conditions

### 2.3.2. Regression kriging (RK)

Regression Kriging (RK) is in principle an extension to linear regression. But it accounts for spatial dependence between observations which is modelled by variograms (Goovaerts, 1999). In RK, prediction is done by modelling a relationship between primary variable and secondary information found in co location and then apply the model to predict values at unsampled location using the values of secondary variables. It usually performed into two steps, prediction of drift and residual differently and then adding them together (Hengl et al., 2007). Similar method was used by Denby et al. (2008) after linear regression for assessing PM10 exceedances on the European scale and provided better results compared to OK of observations. As part of RK; van de Kastele & Stein (2006) used KED to predict concentration of NOx in which the operational priority substances (OPS) model outputs were used as covariate. Their approach aimed at improving the quality of air pollution maps by merging data from different sources and intended

to incorporate uncertainty of input data. Generally inclusion of dispersion model outputs improved prediction accuracy.

Bourennane et al (2000) made a comparison study between ordinary linear regression and KED for soil mapping whereby digital elevation model was used as covariate. He found that KED results were better for 38% as compared to ordinary linear regression.

### **2.3.3. Cokriging (CK)**

Cokriging (CK) is one among kriging techniques which is used to predict data at unsampled area using limited primary variable sampled data by the help of highly correlated and more densely sampled covariate (Olea, 1991; Stein and Corsten, 1991; Webster and Oliver, 2008). Goovaerts (1999) defined cokriging as an estimate that is a linear combination of neighboring primary and secondary data. The most significant feature of CK relies on its mathematical concept. As opposed to other kriging methods, CK requires establishment of variograms of each data set involved and modelling cross variograms, a process which is termed as coregionalization. (Atkinson et al., 1992; Webster and Oliver, 2008)

Goovaerts (1999) used cokriging in mapping of rainfall erosivity where elevation was used as secondary information. Elevation in his case study was a data which is found everywhere in the study area hence being ideal covariate. He indicated that cokriging always gives better prediction results compared to other kriging techniques but it is more demanding in calculation as two autocovariance functions and cross variance function needs to be inferred.

In a very recent research; Singh et al. (2011) used cokriging to construct air pollution maps in the Milan Italy. In his approach he predicted daily mean PM<sub>10</sub> concentration using PM<sub>10</sub> simulated by deterministic model as a covariate.

## **2.4. Change of support**

Data integration normally uses data from different sources. There are several challenges pertaining to data integration, one among them having data at different support i.e. different spatial or temporal resolution. There exist several classical methods that are used to put data in the same support before integration. In this section block kriging and downscaling cokriging “geostatistical techniques” are put into context. Mathematical details of these techniques is found in Webster and Oliver (2008) and Atkinson et al. (1992).

Block kriging is one of kriging techniques used to facilitate change of support of the measurements (Wenxia et al., 2008). The term originates from mining whereby data collected at point support are normally aggregated to area units/blocks (Webster and Oliver, 2008). It can be used in combination with standard kriging or multivariate kriging methods to aggregate or disaggregate predictions into different spatial support.

Wenxia et al. (2008) used block kriging to interpolate airborne laser scanning point clouds to generate dense point cloud. They indicated that the technique provides change of support as data change from point support to area (block) support. Cinzia Mazzetti & Todini (2002) used block kriging for regularizing rain gauge data for the purpose of integrating with images. In principle, block kriging is an unbiased predictor which uses the value of the block to represent grid value.

Downscaling cokriging (DSCK) is the process of increasing the spatial resolution of coarse resolution image using information obtained from secondary data. According to Atkinson et al. (2008) and Pardo Iguzquiza et al. (2006); DSCK takes into account correlation and cross correlation of images, it accounts

for different supports and explicitly takes into account the point spread function of the sensor. In addition, ancillary data can be incorporated in the process. Finally, they concluded by saying; the success of cokriging depends on the estimation of point support covariance and cross covariance.

The method has been used in various research; in remote sensing for example, and has shown valuable contribution in increasing spatial resolution and prediction accuracy. In addition, it has ability to account for different supports and to incorporate ancillary data in the process (Atkinson et al., 2008; Pardo Iguzquiza et al., 2006). Downscaling cokriging which is in the field of remote sensing is also referred to super resolution mapping is becoming an important operation where finer resolution image is produced from coarse input image by superimposing coarser image to another image of the same variable acquired under different condition. According to Atkinson (2008) super resolution mapping (downscaling) refers to interpolation procedure where unsampled points are predicted at finer spatial resolution.

Pardo Iguzquiza et al. (2006) used downscaling cokriging for image sharpening. They successful increased spatial resolution of a coarser resolution band using spatial resolution of another finer resolution band. In their case, the targeted spatial resolution was equal to spatial resolution of one of inputs. Landsat Enhanced Thematic Mapper Plus was used in that project.

Atkinson et al. (2008) developed work done by Pardo Iguzquiza et al. (2006). The coarser resolution images were downscaled by cokriging method in super resolution mode. Meaning, the predicted image had finer spatial resolution than any input images used in prediction. In order to verify applicability of the method, they worked with degraded image and used original image for validation. Landsat Enhanced Thematic Mapper Plus was used in their project.

In this research block kriging was employed to examine the effect of change of support in prediction.

### 3. STUDY AREA AND DATA DESCRIPTION

#### 3.1. Introduction

The study area and datasets used in this study namely insitu measurement, model outputs and satellite imagery are explained in this section.

#### 3.2. Study area

The study area covers a total area of 2,505,074 km<sup>2</sup> and lies in between longitude 5.90 W to 15.919 E and latitude of 42.351 to 54.978 N consisting Germany, Netherlands, France, Austria, Belgium, Switzerland, Check Republic, North Italy, South Great Britain, Slovenia and Luxembourg (Figure 3-1). The choice of the study area is due to availability of different data sources for mapping air pollution. Also, the area have large network of monitoring stations and the region occupys many industries which makes the area suitable for study (van de Kasstele, 2006). Also there exists deterministic model called LOTOS-EURO which provides air pollution concentration maps across Europe.



Figure 3-1. Study area : Source (Google Earth)

### 3.3. Data description

Three dataset have been used in this study. Section 3.3.1 provides description of insitu measurements. Section 3.3.2 describes model outputs and section 3.3.3 gives brief explanation of AOT derived from MODIS satellite.

#### 3.3.1. In situ measurements (PM10)

In situ data are available through airbase database (European-Topic-Centre-on-Air-and-Climate-Change, 2011). Data are available in two formats CSV and XML. CSV has been prepared per country and contains 3 sub files; stations, statistics and measurement configurations. Stations contain spatial attributes of each monitoring station in longitude and latitude, altitude, station European code, local name etc. Statistics file contains information about air pollution including statistic name, statistic percentage, statistic value, statistic number, statistic year, and measurement European group code and statistic average groups. Measurement configurations file provides information about techniques used in measuring each air pollution component, calibration frequency and methods, sampling time, measurement start date etc.

#### Measuring techniques

Different countries use different techniques and practices in measuring insitu measurements (PM10). Also, other measurement techniques apart from gravimetry are subjected to artefacts and therefore calibrations are usually applied to observed data (van de Kassteele et al., 2006). For example beta absorption techniques is mostly used by Germany and Italy, oscillating microbalance is used mostly by Germany, Austria, Great Britain and Belgium, beta ray attenuation commonly used by the Netherlands, France and Czech Republic and tapered element oscillating microbalance is being used by Germany, Slovenia, Switzerland, Italy, Austria, Great Britain and Belgium. van de Kassteele (2006) reported that observations made by other instruments rather than gravimetry are subjected to artifacts therefore practices like calibration, sampling height of measurements, corrections applied to observation are not uniform for all countries.

#### PM10 daily annual mean concentrations for 2006

Daily annual mean concentration of PM10 for 2006 was used to explore the effect of combining data from different countries using different measuring techniques. Data were downloaded from Airbase and classified into two groups. First group combined data from all countries under study area without considering measurement technique. This group had 746 measurements. The second group comprised homogeneous data i.e. measured by one technique (beta ray attenuation). Six countries were found using this technique and consisted 237 measurements. Table 3-1 summaries numbers of stations per measurement techniques a country possess.

Technique	DE	SI	SWI	IT	AT	CZ	GB	FR	BE	NL
Beta absorption	30		3	43						
Beta ray attenuation	116			3	4	47	1	38	4	24
Gravimetry	9		9	17	8	28	3			
Oscillating microbalance				8				179		
Tapered element oscillating microbalance	28	7	3	1	32		47		16	
Nephelometry	2			6						
Chromatography	1									
Concuctimetry				1						
Unknown	23		1	4						
	<b>209</b>	<b>7</b>	<b>16</b>	<b>83</b>	<b>44</b>	<b>75</b>	<b>51</b>	<b>217</b>	<b>20</b>	<b>24</b>

Table 3-1. Number of stations per measurement techniques per country for the year 2006.

**PM10 daily annual mean concentrations for 2003**

PM10 daily annual mean concentrations maps were produced based on data for the year 2003. This was due to availability of secondary data for 2003. Total of 607 background measurement stations were involved and are summarized in Table 3-2 and their distribution on Figure 3-2. Locations of air pollution monitoring stations across Europe for the year 2003. These 607 measurements stations were obtained after data cleaning according to defined criteria. The criteria among others were statistic year=2003, pollutant=PM10, statistic value=mean, statistic average group=daily etc. Therefore 3 files were downloaded for each country. Data cleaning was carried out to obtain targeted component PM10, area of interest, station type, statistic year and statistic average group for each table and they were linked together using primary key. From these tables hourly, 3 hour, 8 hour, daily, weekly and 2 weeks mean values from continuous observation are usually calculated for the user.

Background station type	Number of stations
Rural	147
Sub rural	194
Urban	266

Table 3-2. Summary of background stations used for the year 2003

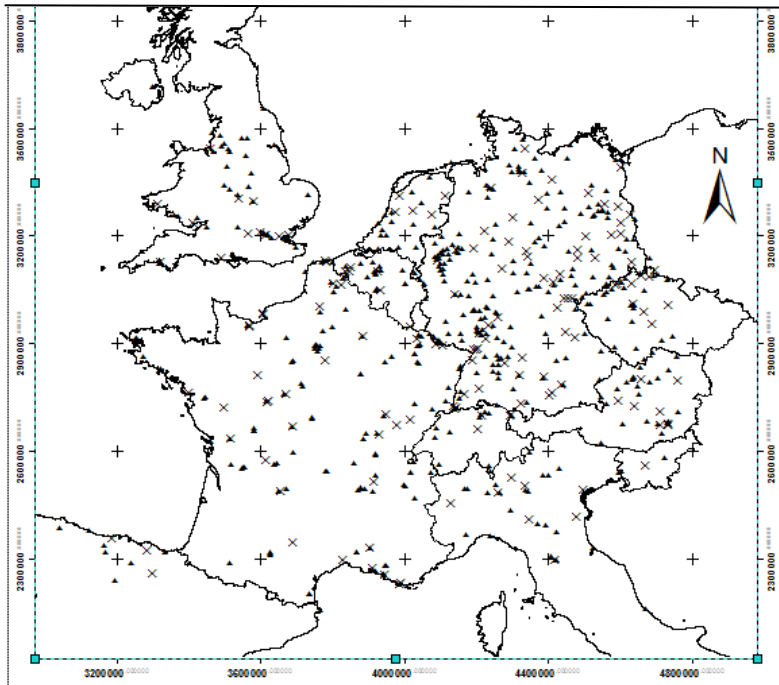


Figure 3-2. Locations of air pollution monitoring stations across Europe for the year 2003

Stations shown are background stations which observe PM10 concentrations across in the study area. Geometric symbol triangles and crosses present stations used in prediction and for accuracy assessment respectively.

**3.3.2. Satellite image data (AOT)**

Aerosols Optical Thickness (AOT) is an aerosol parameter which quantifies the attenuation of aerosol with electromagnetic radiation in the atmospheric column at a given wavelength (Emili et al., 2010; van de

Kasstele et al., 2006). According to Hutchison et al. (2005) and van de Kasstele et al. (2006) annual averages of AOT is correlated to ground measurement concentration hence making them significant secondary information in studying air pollution.

AOT daily annual averages for 2003 were used in this study. They were provided by van de Kasstele and shown in Figure 3-3. AOT daily annual averages derived from MODIS projected to LAEA 1989 at spatial resolution of 10 km by 10 km square grid.. They were derived from MODERate resolution Imaging Spectroradiometer (MODIS) at a spatial resolution of  $0.1^\circ$  by  $0.1^\circ$  grids approximately 10 km square grid in Europe.

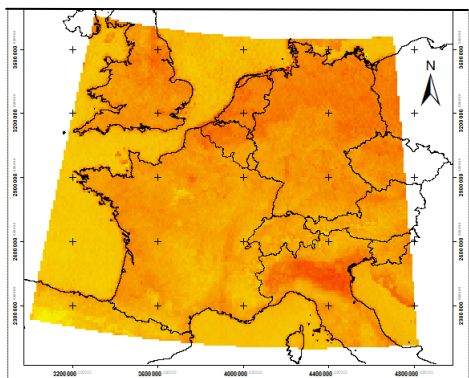


Figure 3-3. AOT daily annual averages derived from MODIS projected to LAEA 1989 at spatial resolution of 10 km by 10 km square grid.

### 3.3.3. Model outputs (PM<sub>2.5</sub>)

PM<sub>2.5</sub> from LOTOS-EUROS, the deterministic model were used in this study. The model calculates air quality concentration basing on chemical, empirical and physical process. The model calculates concentration and deposition takings into account height of emission source, transport, dispersion, wet and dry deposition, wind direction and deposition. It also predicts air pollutants at fine temporal resolution but relatively low spatial resolution compared to AOT derived from MODIS. Figure 3-4 (left) is the resulting model outputs gridded at  $0.5^\circ$  (longitude) by  $0.25^\circ$  (latitude) in geographical coordinates system (Denby et al., 2008; Schaap et al., 2009b; van de Kasstele, 2006) projected at spatial resolution of 30 km by 30 km. Figure 3-4 (right) presents PM<sub>2.5</sub> downscaled by bilinear interpolation to AOT grid i.e. spatial resolution of  $0.1^\circ$  by  $0.1^\circ$  by van de Kasstele et al. (2006) and projected at spatial resolution of 10 km by 10 km.

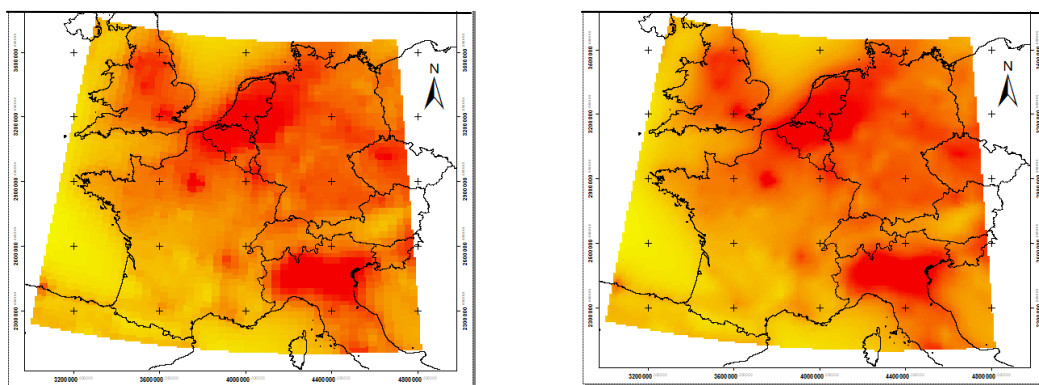


Figure 3-4. Monthly annual averages PM<sub>2.5</sub> modelled by LOTOS-EUROS for 2003 projected to LAEA 1989 coordinates system at 30 km by 30 km square grid (left) and to 10 km by 10 km square grid (right).

Figure 3-4 left is the PM<sub>2.5</sub> at coarser resolution 0.5° by 0.25° projected at spatial resolution of 30 km by 30 km square grid. On the right is PM<sub>2.5</sub> downscaled by bilinear interpolation to 0.1° by 0.1° followed by projection to 10 km by 10 km square grid.



## 4. METHODOLOGY

### 4.1. Data preprocessing

Data pre processing in this study is referred to applying appropriate algorithm to derive AOT from MODIS and calculation of annual mean PM<sub>2.5</sub> concentration from model outputs at a spatial resolution of 0.5° by 0.25°. PM<sub>2.5</sub> annual mean concentrations were calculated by averaging the monthly concentrations. These processes were done by van de Kasstele et al. (2006). Furthermore, PM<sub>2.5</sub> concentrations were downscaled by bilinear interpolation to 0.1° by 0.1° square grid (MODIS grid) so that they have the same support as AOT.

### 4.2. Data projection

PM<sub>10</sub>, PM<sub>2.5</sub> and AOT dataset had geographical coordinate system which is not suitable in prediction due to distance differences in North-South and East-West directions. Hence, they were projected to European conventional Terrestrial Reference System Lambert Azimuth Equal Area 1989 (ETRS LAEA 1989). Downscaled PM<sub>2.5</sub> by bilinear interpolation and AOT were projected to LAEA 1989 in ARCGIS at spatial resolution of 10 km square grid. Also the coarser PM<sub>2.5</sub> was projected at spatial resolution of 30 km square grid corresponding to its original dataset. According to Annon et al. (2001); ETRS LAEA 1989 is the best projection to be used for statistical mapping in the Europe. The projection has been used before for statistical mapping of air pollution by Denby et al. (2008). There is distortion in distance which is critical in statistical mapping but in comparison with the extent covered, the reference is suitable for statistical mapping (Annon et al., 2001).

### 4.3. Data exploration

Prior to data exploration, dataset were imported to R software by gdal package. PM<sub>10</sub> was projected in R using gdal package. Quantitative and descriptive data analyses were used to understand nature of data on hand. Combinations of summary statistics, histogram, normal probability plots and bubble plots were employed during data exploration. This procedure was important for sound decision making in data transformation.

### 4.4. Country by country data exploration for 2006

Country by country data exploration was conducted to explore the effect of combining data from different countries measured by different techniques. PM<sub>10</sub> measurements for 2006 were used for this analysis. As usual; histograms, normal probability plots and descriptive summary statistics were used to explore data of each country. To understand the impact, the following category of data exploration were achieved

- i) Exploring PM<sub>10</sub> spatial structure of PM<sub>10</sub> from different countries measured by different techniques.
- ii) Exploring spatial structure of PM<sub>10</sub> from different countries measured by a common measurement technique (beta ray attenuation).
- iii) Individual country data exploration for (i) and (ii)

### 4.5. Subsetting in situ measurements

Before start of modelling; the in-situ data for 2003 were divided into two groups; one for prediction containing 455 stations (pm10.extra) and the other for accuracy assessment containing 152 stations (pm10.valid). The procedure for sub setting data was in a way that one data was picked after every 4 rows

in data series. Despite being a systematic way of subsetting the dataset, still there is good representative of data as shown in Figure 3-2 in which stations with geometric symbol triangle were used prediction and those with cross were used for accuracy assessment.

#### 4.6. Modelling

The process involved estimation and fitting of appropriate model to variograms.

##### 4.6.1. Empirical variograms

The power of geostatistical methods lies on its ability to model spatial variations in the phenomena. Methods use knowledge of underlying spatial relationship in the data. The underlying spatial relationship is normally modelled by means of variograms (Bayraktar and Turalioglu, 2005). “Variograms” is described as a half semivariance plotted as a function of distance between point pairs. Equation 4-1 was used to calculate sample empirical variograms; i.e. half difference square of attribute of a random field separated by distance  $h$  on space.

$$\gamma^*(h) = \frac{1}{2N(h)} \sum_{i=1}^{N(h)} [z(x_i) - z(x_i + h)]^2 \quad (4-1)$$

$\gamma^*$  is the estimated semivariogram from observations;  $z(x_i)$  is the observed attribute value at location  $x_i$ ,  $z(x_i+h)$  is observed attribute value at location  $x_i+h$ ,  $h$  is the separation distance between two points.

PM10, PM2.5 and AOT empirical variograms were calculated in R using `gstat` package. It has default function to calculate variograms whereby cut off is normally 1/3 of the maximum distance of the study area and width is usually cut off divided by 15, where 15 is the number of variograms formed by default. Hence changing cut off and width provided an opportunity to explore and understand spatial structure in data e.g. spatial behaviour at longer distances.

##### 4.6.2. Modelling the variograms

Fitting a model to experimental variograms was done in R using `gstat` package. First, model parameters (nugget, range and sill) were estimated by eye from plotted variograms. These estimates were used as initial values by model to calculate model parameters which best fit variograms with minimum variance using least squares algorithms. This process enabled calculation of model parameters which are the range, nugget and sill. The intention has to be paid on giving more weight to points which are near to prediction location than those far apart. This can be achieved by having large range for exponential models (Webster and Oliver, 2008).

##### 4.6.3. Selection of variograms model

Different models are usually fitted to empirical variograms. The commonly used models are exponential, spherical and Gaussian model functions, each of them combined with nugget model. The choice depends on knowledge of underlying sample process or by experimenting all of them and choosing one which provides minimum error. In this research, the choice of model relied on the second approach. The variograms of the same cut off and width were fitted with exponential model, spherical model and Gaussian model. Standard kriging was done and Mean Error (ME), Sum Square Error (SSE) and Root Mean Square Error (RMSE) were calculated for each model. These statistical error measures were used to determine the model function to be used.

##### 4.6.4. Modelling the hole effect.

Empirical variograms of PM10 concentrations showed clear deep hole effect at 400 km and 800 km. It was dropping after reaching partial sill then rises. This may be an indication of periodicity or repeated pattern in the phenomena. An alternative model that could fit better this phenomena was the hole effect model. The cut off of 1000 km and width of 60 km were maintained in order to compare two model functions applied in prediction (exponential and hole effect models).

## 4.7. Prediction

Different kriging methods were used to predict air pollution concentration at unsampled locations. PM10 daily annual mean concentration observations from 455 measurements stations were used in kriging. Methods applied were ordinary kriging (OK) and universal kriging (UK) ordinary linear regression, regression kriging (RK) and cokriging (CK).

### 4.7.1. Kriging of PM10 only

Ordinary kriging and universal kriging were used in kriging of PM10 daily annual mean concentration observations only. While OK considers local variations, UK considers long range variations whereas coordinates were used as covariates.

### 4.7.2. Universal block kriging

The block size of 2 km, 5 km, 10 km, 20 km and 30 km were used in UK of PM10 daily annual mean concentration observations. This was achieved by adding block size in universal kriging code. A reason for doing block kriging is to know its efficiency in prediction of points to area units compared to punctual kriging.

### 4.7.3. Ordinary linear regression

The relationship between PM10 daily annual mean concentration observations and secondary information were established using linear model function found in R software. The linear system of equation was established between known corresponding values of PM10 and that of secondary information found on co locations. This was achieved by overlaying PM10 data with secondary data (Figure 4-1). This system of equations was used to calculate unknown parameters  $\beta_0$ ,  $\beta_1$ ,  $\beta_2$  and  $\epsilon$  as presented in equation 2-1. The computed parameters are then used in computing PM10 at unsampled location using values of secondary information at that location (Goovaerts, 1999)

### 4.7.4. Regression kriging (RK)

Regression kriging is an extension of linear regression applicable when residuals of the linear model are normal distributed (Denby et al., 2008). Creating concentration map by regression kriging was done using R in two steps; ordinary linear regression (regressed map) and kriging of residuals (kriged residual map)(Hengl et al., 2004). Then kriged residuals map output was added to regressed map output to produce air pollution concentration maps (Hengl et al., 2004). Two models were fitted to residual variograms, exponential and hole effect maps. These models were all used in predictions to evaluate their performances. The general methodology adopted for ordinary linear regression and regression kriging is presented in Figure 4-2

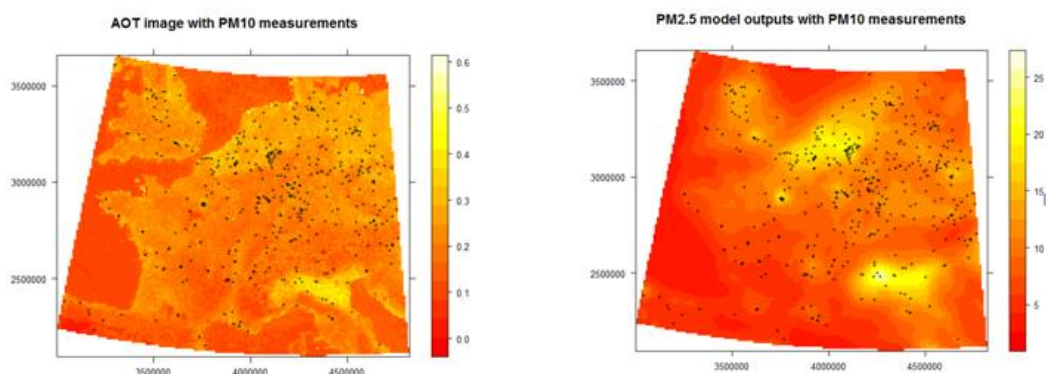


Figure 4-1. Overlay of PM10 daily annual mean concentration observations with secondary information for 2003; AOT overlaid with PM10 (left) and PM2.5 overlaid with PM10 (right)

Refer Figure 4-1 left is the AOT image at spatial resolution of 10 km square grid overlaid with PM10. On the right are the PM2.5 model outputs at 10 km spatial resolution overlaid with PM10. PM2.5 was downscaled by bilinear interpolation to match AOT grid. All data were projected using LAEA 1989 projection.

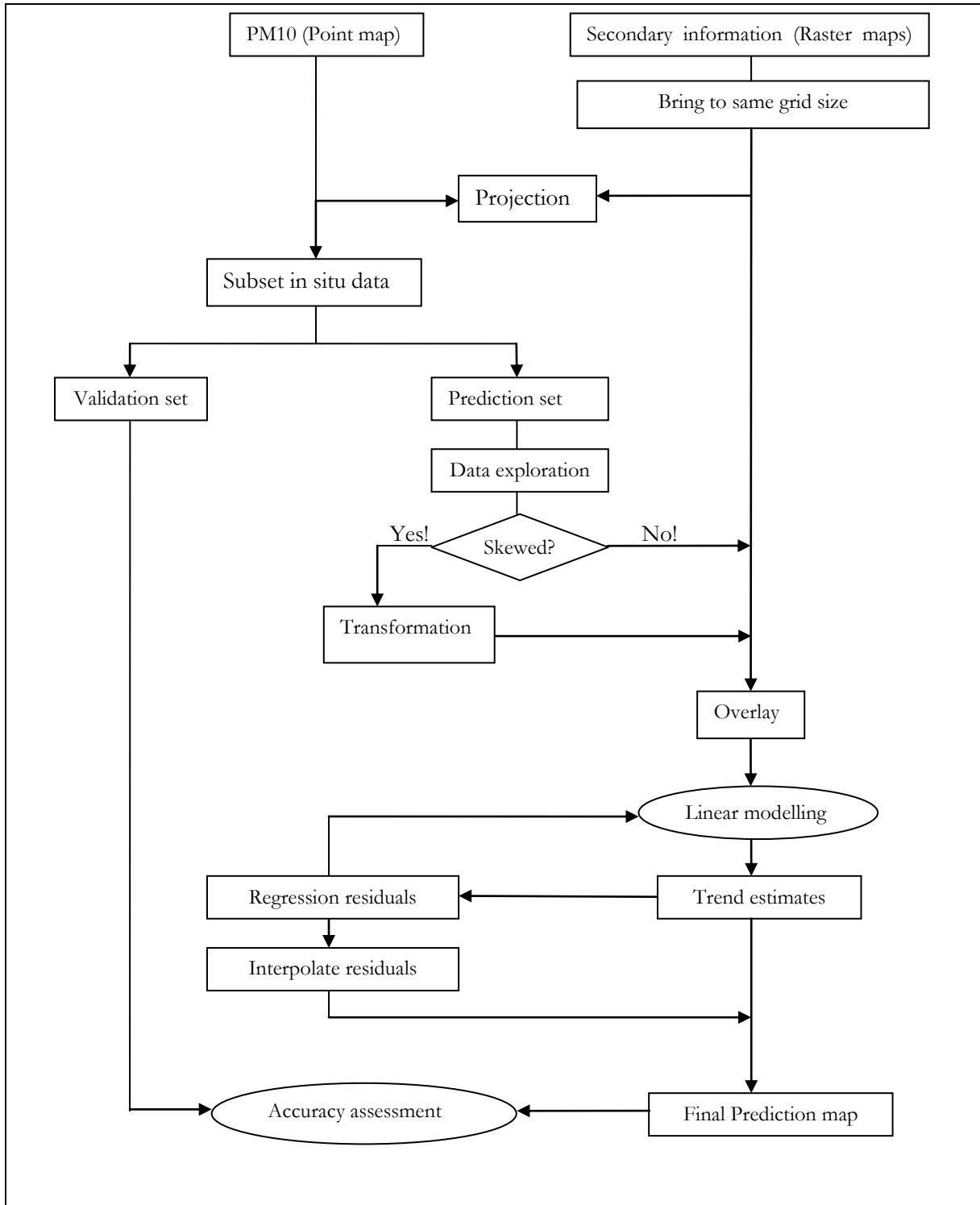


Figure 4-2. Methodology for linear regression and regression kriging (Adopted from (Hengl et al., 2004))

Geographical coordinates were projected to LAEA 1989 coordinate system. Downscaling by bilinear interpolation and resampling process were used to bring secondary data into same support.

**4.7.5. Cokriging (CK)**

This process takes into account the spatial structure of covariate. The process involved three steps, (i) modelling spatial structure of primary and secondary dataset, (ii) modelling of coregionalization and (iii) prediction.

**Modelling spatial structure of each data set**

Apart from variograms model of PM10 concentrations, variograms model for PM2.5 and AOT were established. The variograms of each data set were estimated at co located points. To achieve this dataset were overlaid. Coincident data points were used to estimate and model variograms.

**Model of co regionalization**

This is a process of forming cross variograms and fitting model to it which is then used in prediction by cokriging method. Estimated variograms of PM10, AOT and PM2.5 were used as an input for this task. linear model of coregionalization (LMC) was used to fit a model to the resulting cross variograms while ensuring they lead to a positive definite cokriging system (Webster and Oliver, 2008). The LMC enforces the range of both models to be the same while allowing nugget and partial sill to vary.

**Cokriging prediction**

Three maps were produced by cokriging predictions; between PM10 and AOT; PM10 and PM2.5; PM10 and (AOT and PM2.5). General methodology used for kriging is presented in Figure 4-3.

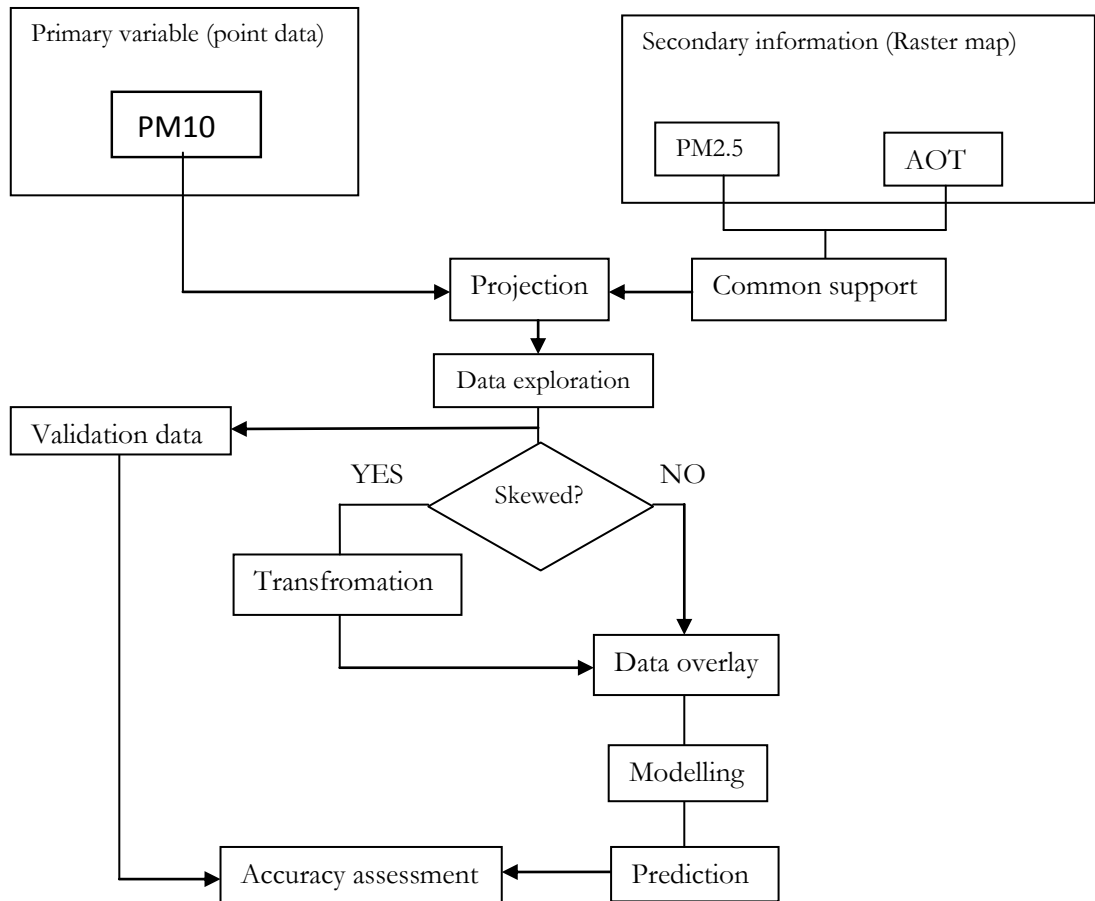


Figure 4-3. General methodology for kriging

#### 4.8. Uncertainty assessment

Accuracy assessment is the process of counter checking the results of a model. Precision of prediction is often reliable when assessed by independent data set. Validation dataset (pm10.extra) contained 152 stations whose PM10 concentration is known and they compared with predicted value at validation point (Bourennane et al., 2000). Equations 4-2, 4-3, 4-4 presents Mean Error (ME), Sum of Square Error (SSE), Root Mean Square Error (RMSE) respectively which were used to evaluate models used in this study.

$$ME = \frac{1}{N} \sum_{i=1}^N z^*(x_i) - z(x_i) \quad (4-2)$$

$$SSE = \sum_{i=1}^N (z^*(x_i) - z(x_i))^2 \quad (4-3)$$

$$RMSE = \left[ \frac{1}{N} \sum_{i=1}^N (z^*(x_i) - z(x_i))^2 \right]^{0.5} \quad (4-4)$$

$z^*(x_i)$  is the estimated value at location  $x_i$  and  $z(x_i)$  is the observed value at location  $x_i$

## 5. RESULTS

### 5.1. Country by country data analysis for 2006

Daily annual mean PM10 concentrations for 2006 were explored to understand the effect of combining data from different countries measured by different techniques. The results of exploration for two groups of data as described in section 4.4 are presented. It is important to know that PM10 data for 2006 was not used in kriging but only for mentioned reason.

Measurement technique	Raw data					Log 10 transformation				
	min	median	mean	max	std	min	median	mean	max	std
All tech.	10.45	24.17	25.87	67.00	8.55	1.02	1.38	1.39	1.83	0.13
Beta ray tech	11.15	24.74	26.10	64.19	8.63	1.05	1.39	1.40	1.81	0.13

Table 5-1. Summary statistics of PM10 daily annual mean for 2006.

Table 5-1 revealed that the summary statistics for combined data from different countries measured by all techniques “All tech” is almost similar to summary statistics for combined data from different countries measured by beta ray absorption techniques.

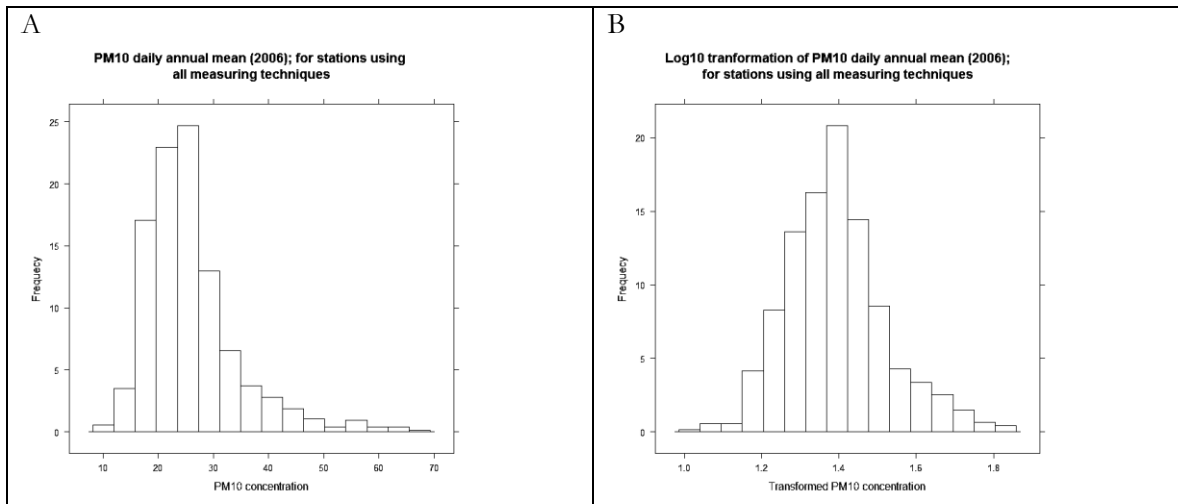


Figure 5-1. Histograms for combined PM10 daily annual mean concentration measured by all techniques. A-raw data, B-log 10

Figure 5-1 presents histograms of daily annual mean concentration of PM10 for the year 2006 for combined data from different countries measured by different techniques. (A) is histogram of raw data and it can be seen to be positively skewed and (B) is histogram of transformed data to base 10 logarithmic scale showing to be normally distributed.

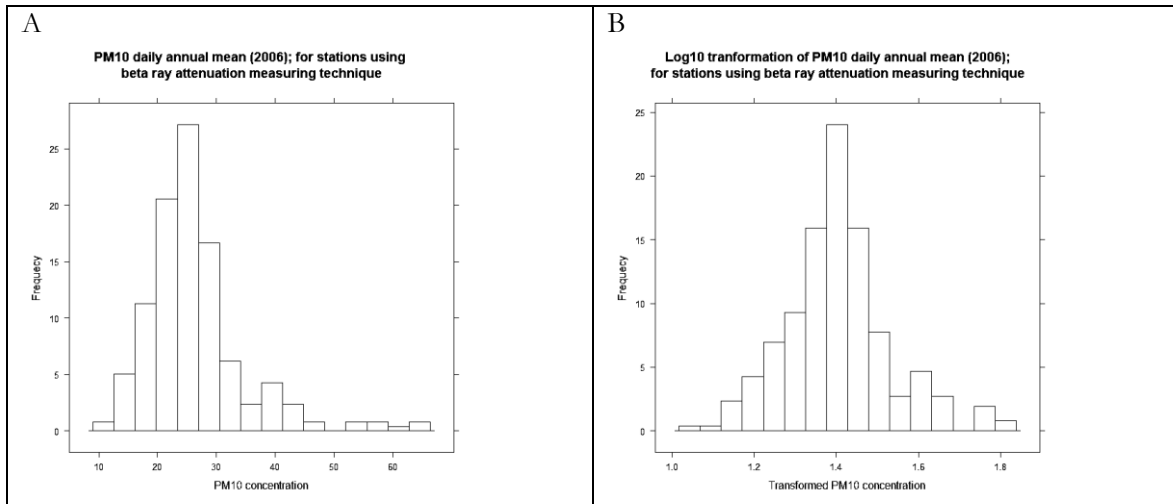


Figure 5-2. Histograms of combined PM10 daily annual mean concentration measured by beta ray technique for the year 2006

Figure 5-2 present histograms for combined PM10 daily annual mean concentration for 2006 measured by beta ray attenuation technique in different countries. Figure 5-2 (A) is the histogram of raw data which positively skewed and Figure 5-2 (B) is the base 10 logarithmic transformed data histogram showing to be normally distributed.

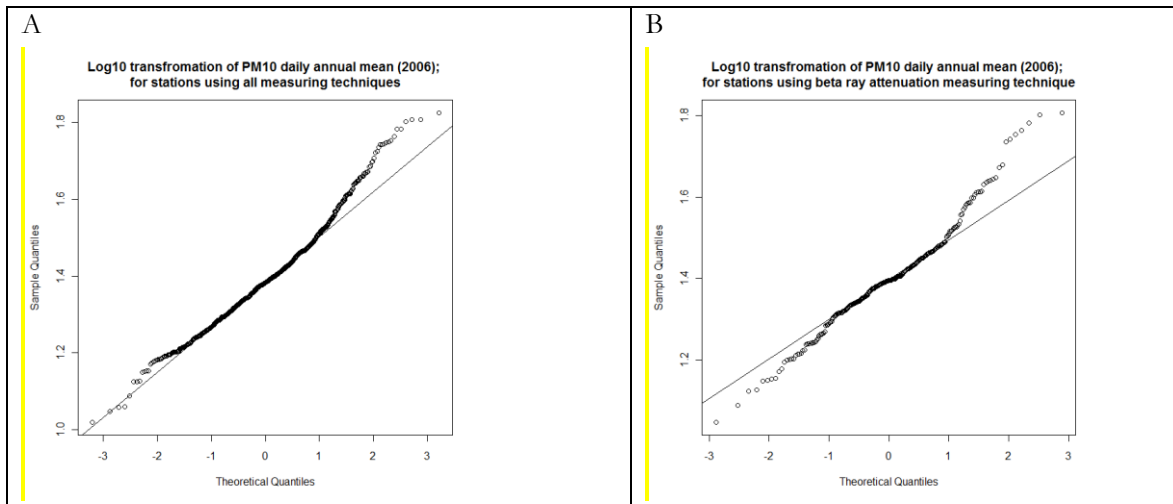


Figure 5-3. Log10 normal probability plots of PM10 daily annual mean concentration for 2006. (A) combined PM10 data measured by all techniques and (B) combined PM10 data measured by beta ray attenuation technique for the year 2006.

From Figure 5-3 it can be seen that data measured by different techniques tends to be closer to normal distribution than those measured by beta ray attenuation techniques.

The spatial structures between these two groups of data were also explored. Due to skewedness in dataset, base 10 logarithmic scale was applied during estimation of empirical variograms. Cut off and bin width were maintained for comparison purposes between two structure. Figure 5-4 (A) presents estimated empirical variograms model for combined data measured by different technique. Figure 5-4 (B) is the estimated empirical variograms model for combined data measured by beta ray attenuation. There is small difference in range and total sill between two structures (Table 5-2), but the spatial structure is relatively similar.

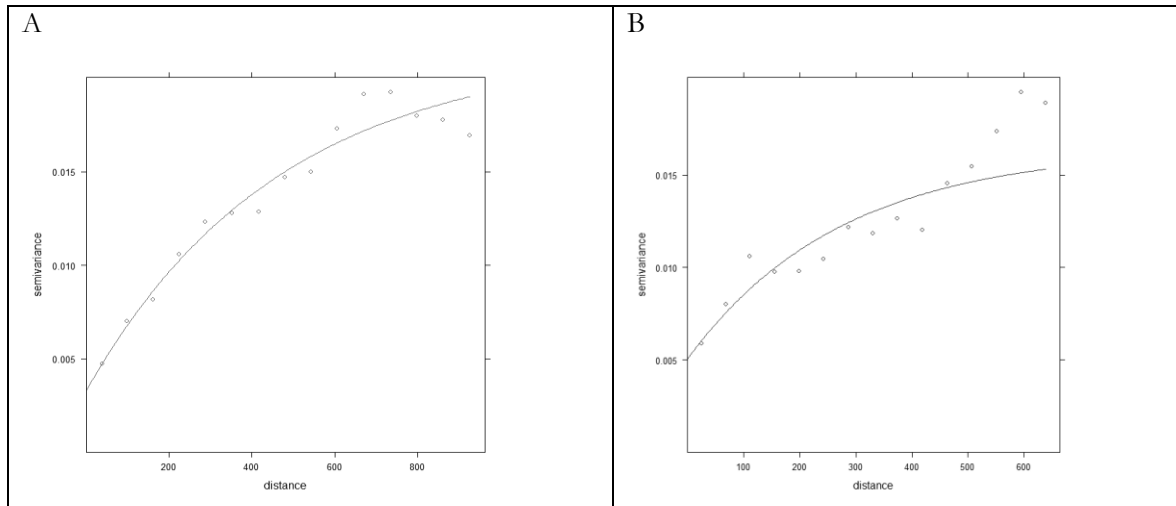


Figure 5-4. Variograms models for PM10 concentration for the year 2006: A-for combined PM10 data measured by all techniques and B-for data measured by beta ray technique.

	Model	psill	range	cutoff	width
Case1	Nug	0.003	0.00	850	50
	Exp	0.019	434.489		
Case2	Nug	0.005	0.00		
	Exp	0.012	273.693		

Table 5-2. Computed exponential model parameters of PM10 daily annual mean concentration for 2006

From Table 5-2, case1 are computed model parameters for combined PM10 daily annual mean concentration measured using all techniques and case2 are the model parameters for combined PM10 daily annual mean concentration measured by beta ray attenuation technique for the year 2006.

**Observations from country to country data exploration for the year 2006**

In general combining data measured by different techniques gave almost the same structure with those measured by beta ray attenuation techniques. Consider Table 5-1, it is clear that two groups have almost similar statistics. Figure 5-1 (A) and Figure 5-2 (A) shows the histograms of raw data and Figure 5-1 (B) and Figure 5-2 (B) base-10 logarithm transformed data to be almost similar. Figure 5-3 shows normal probability plot of base-10 logarithmic scale transformation between two groups of data to be similar. The spatial structure presented in Figure 5-4 (A and B) also shows small difference in structure between two groups but not significant different.

Further investigation was done on spatial structure in data for individual countries (Appendix A and B). However, due to low number of stations and other factors that have not been identified, it was difficult to have reliable spatial structure for some countries e.g. The Netherlands. Following this exploration it was decided to use data measured by all measuring techniques for this study without considering standardization (Denby et al., 2008).

**5.2. Data exploration for 2003**

PM10 daily annual mean concentration for 2003 was the target variable in this study. The selection of the year was due to availability of secondary data for the year 2003 i.e. AOT and PM2.5. Data exploration results for PM10, AOT and PM2.5 for 2003 are presented in this section. It is important to understand that from this section and rest of sections described below are associated with data for the year 2003.

**5.2.1. PM10 daily annual mean concentration for 2003**

Descriptive data analysis results are shown in Figure 5-5 and Figure 5-6 where; Figure 5-5 (a) is the histogram of the raw data showing to be slightly positively skewed. Figure 5-5 (b) is histogram of log10 transformed data showing to be normally distributed, Figure 5-5 (c) is the histogram of natural logarithm transformed data also showing to be normally distributed. Figure 5-6 (a), (b) and (c) are normal probability plots of the raw data, log10 and natural logarithm transformed data respectively.

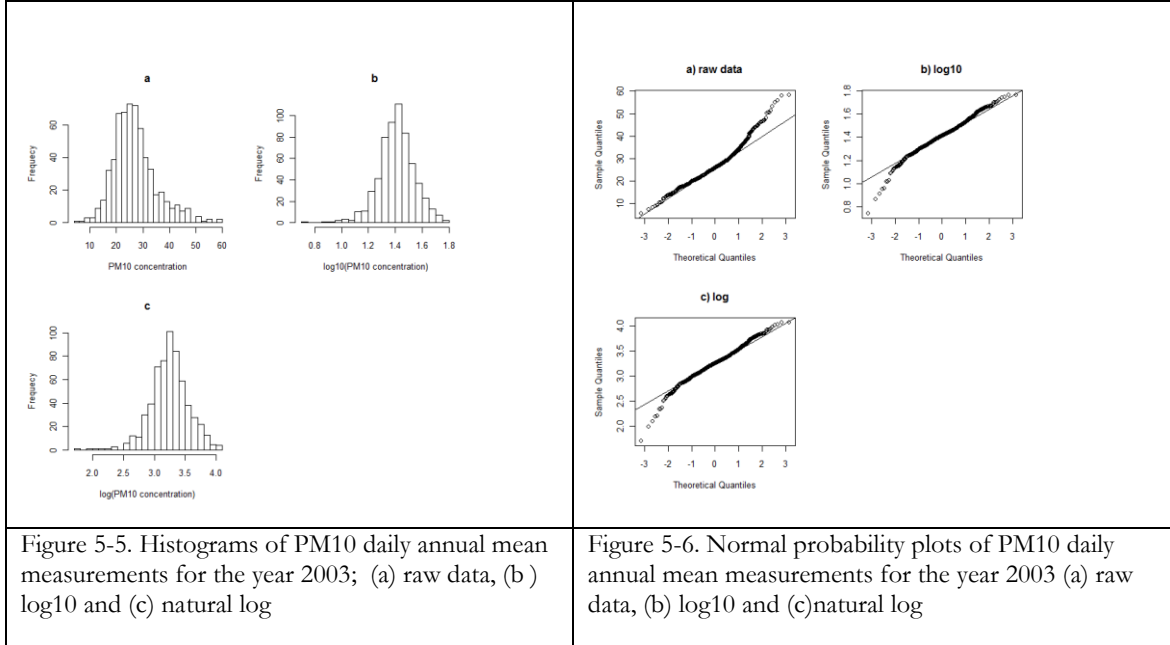


Figure 5-5. Histograms of PM10 daily annual mean measurements for the year 2003; (a) raw data, (b) log10 and (c) natural log

Figure 5-6. Normal probability plots of PM10 daily annual mean measurements for the year 2003 (a) raw data, (b) log10 and (c) natural log

	Summary statistics					
	Min.	1st Qu.	Median	Mean	3rd Qu.	Max.
a) Raw data	5.501	21.370	25.820	26.830	30.750	58.350
b) log10	0.740	1.330	1.412	1.409	1.488	1.766
c) Natural logarithm	1.705	3.062	3.251	3.244	3.426	4.067

Table 5-3. Descriptive summary statistics for PM10 annual daily mean concentration for 2003

It is difficult to make decision on whether data transformation should be done or not using normal probability plots. The distribution of raw data and transformed data deviate from normally distribution (refer Figure 5-6 (a), (b) and (c)). Histogram of raw data Figure 5-5 (a) shows the distribution being slightly positively skewed. The skewedness is also shown by descriptive summary statistics Table 5-3(a) in which minimum, mean, median, maximum and inter-quartile values are shown. It can be seen that log10 transformation has almost similar mean and mode than raw data and natural logarithmic scaled data.

Therefore PM10 data used in this study were transformed by base-10 logarithmic transformations. The in situ measurements skewness were also found by Denby et al. (2008) and Beelen et al. (2009). They transformed their data to base-10 and natural logarithmic scales transformation respectively.

**5.2.2. PM2.5 monthly annual mean averages for 2003**

PM2.5 used as covariate in this study was obtained by downscaling original model outputs PM2.5 at 0.5° by 0.25° to 0.1° by 0.1° by bilinear interpolation. The product was then projected to LAEA 1989 at 10 km square grid using ARCGIS.

PM2.5 monthly annual mean concentration was found to be positively skewed as shown in Figure 5-7 (A). Summary statistics of raw data and base-10 logarithmic transformed data are presented in Table 5-4. It is

difficult to use summary statistics in this case to know whether data are skewed or not. Data were transformed to base-10 logarithmic scale and it was found to be normally distributed as shown in Figure 5-7 (B). This was important for cokriging since it requires estimation of covariates variograms (Webster and Oliver, 2008).

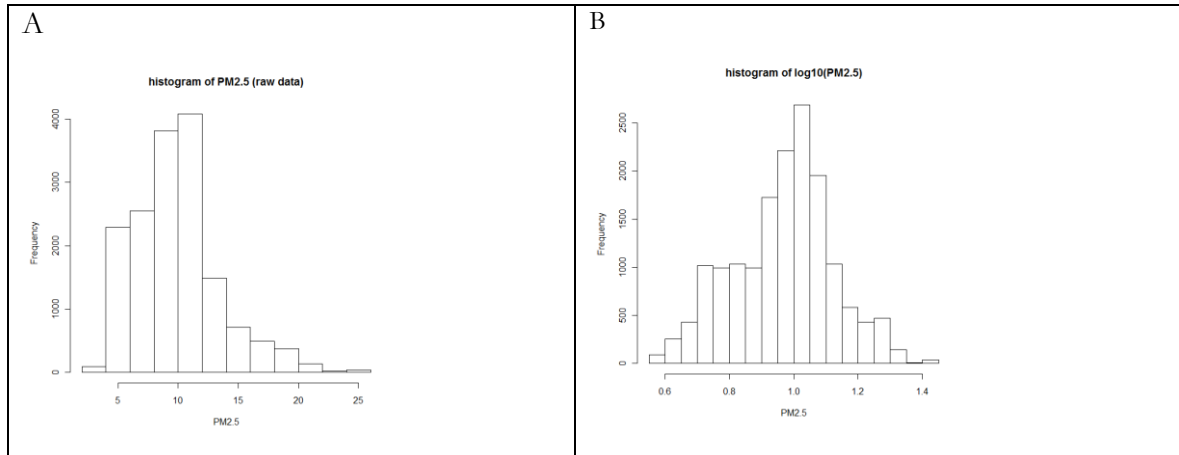


Figure 5-7. Histograms of PM2.5 monthly annual mean concentration averages for 2003. (A) is the PM2.5 raw data histogram which is positively skewed. (B) is the histogram of base-10 logarithm transformed PM2.5 showed to be normally distributed.

Raw data						Base 10 logarithm transformation					
Min	1st Qu	Median	Mean	3rd Qu.	Max.	Min	1st Qu	Median	3rd Qu	Max	Min
3.66	7.28	9.57	9.86	11.49	25.82	0.56	0.86	0.98	0.97	1.06	1.41

Table 5-4. Summary statistics of PM2.5 data and its corresponding base-10 logarithmic transformed data.

From summary statistics (Table 5-4), it is hard to know whether PM2.5 is normally distributed or not. Histogram in Figure 5-7 (A) has been more informative in describing distribution of PM2.5 than summary statistics

### 5.2.3. AOT daily annual averages for 2003

AOT was found normally distributed as shown by the histogram of raw values presented in Figure 5-8

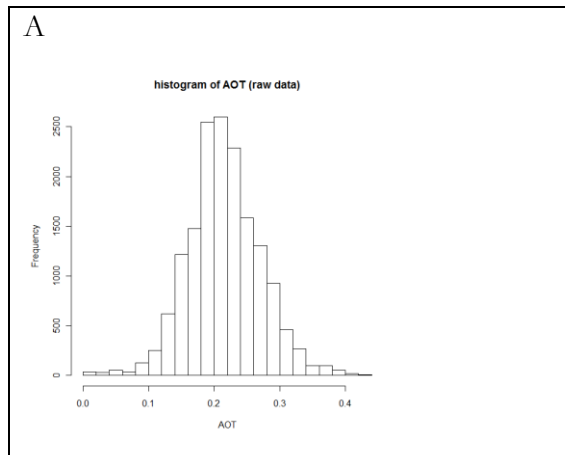


Figure 5-8. Histogram of AOT daily annual averages for 2003.

**5.3. Spatial data analysis**

The PM10 monitoring stations extend from 2000 km to 3750 km north and 3000 km to 5000 km east (Figure 3-2). Figure 5-9 presents bubble plot which show that daily annual averages of PM10 in the study area for 2003 ranging from 5.5  $\mu\text{gm}^{-3}$  to 58.35  $\mu\text{gm}^{-3}$

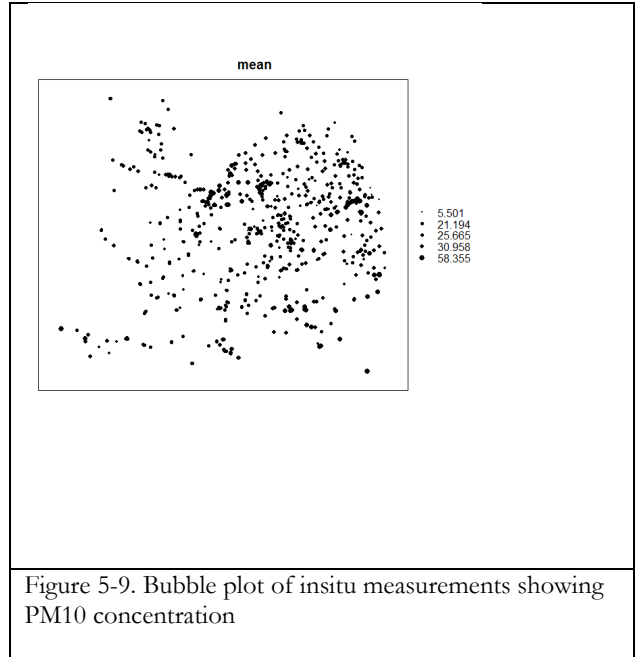


Figure 5-9. Bubble plot of insitu measurements showing PM10 concentration

“mean” as used here refers to PM10 daily annual mean concentration for 2003.

**5.4. Variogram models**

**5.4.1. Selection of variograms model**

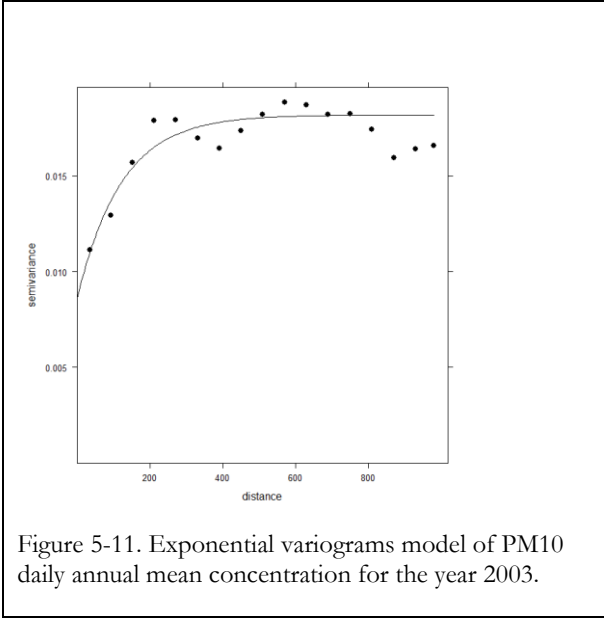
Figure 5-10 shows three model functions fitted to experimental variograms. These models were fitted on estimated variograms of the same cutoff and width. Then, they were applied in kriging. Accuracy assessment was done using independent validation dataset. The resulting errors are also shown in Figure 5-10. Exponential model had lower RMSE as compared to spherical and Gaussian models. Thus it was selected to be used in prediction.

Model	Exponential model	Spherical model	Gaussian model
ME	0.009	0.009	0.009
SSE	1.417	1.490	1.569
RMSE	0.096	0.099	0.102

Figure 5-10. Selecting variograms model for PM10 concentration for 2003

**5.4.2. Exponential variograms model of PM10 daily annual mean concentration for the year 2003**

Different cut off and widths were experimented to explore the spatial structure of PM10 daily annual mean concentration at longer and shorter distances. The number of point pairs forming variograms was investigated. Cut off 1000 km and width of 60 km were finally selected for modelling. Exponential model fitted to empirical variograms is shown in Figure 5-11. Computed model parameters are shown in Table 5-5. The model was used in OK, UK and in universal block kriging of PM10. Also it was used in calculation of cross variograms for cokriging with other secondary information.



Model	parameters	
	psill	range
Nug	0.0086	0.0000
Exp	0.0096	121.9784

Table 5-5. Computed exponential model parameters for PM10 daily annual mean concentration for the year 2003.

**5.5. Kriging of PM10 only**

In total 455 out of 607 measurements stations were used in kriging. Maps created by different kriging techniques are presented in this section. Measurements were kriged by ordinary kriging and universal kriging. Figure 5-12 and Figure 5-13 presents resulting PM10 concentration maps (left) and kriging variance (right) produced by ordinary kriging and universal kriging of measurements only respectively.

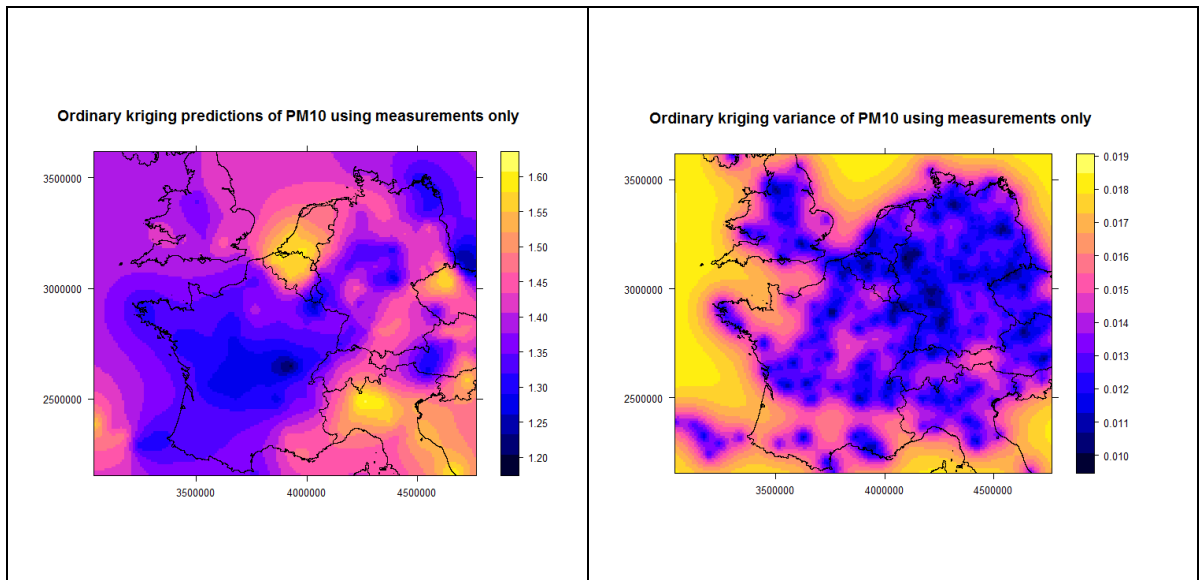


Figure 5-12. PM10 daily annual mean concentrations map for the year 2003 produced by OK of in situ measurements.

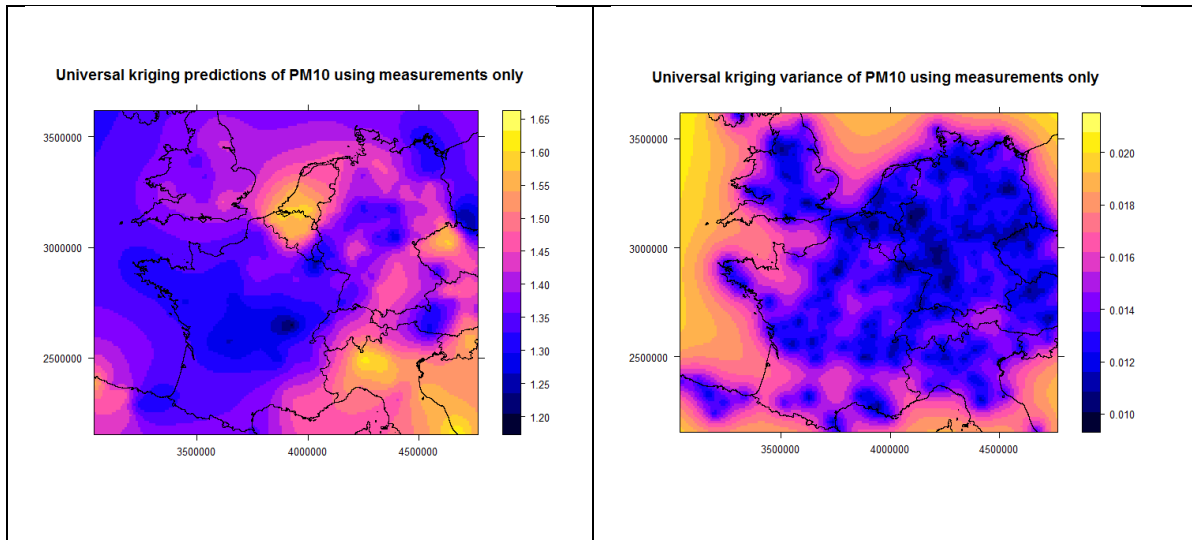


Figure 5-13. PM10 daily annual mean concentrations map for the year 2003 produced by UK of in situ measurements.

### 5.6. Universal block kriging

Universal block kriging was applied at block sizes of 2 km, 5 km, 10 km, 20 km and 30 km. Figure 5-14 and Figure 5-15 presents block kriged predictions of PM10 measurements at block size of 10 km by 10 km and 30 km by 30 km respectively. Block kriged predictions at block size of 2 km, 5 km and 20 km are not presented here.

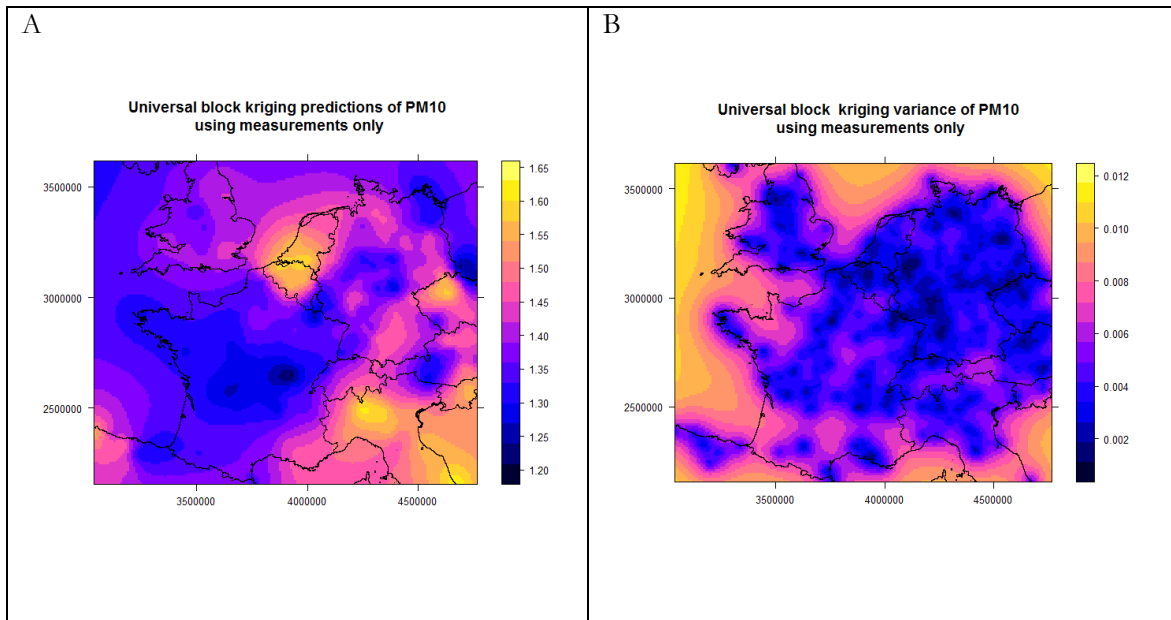


Figure 5-14. PM10 daily annual mean concentrations map for the year 2003 produced by universal block kriging of in situ measurements at the block size of 10 km by 10 km. (A) is the prediction map at area support (B) is the kriging variance

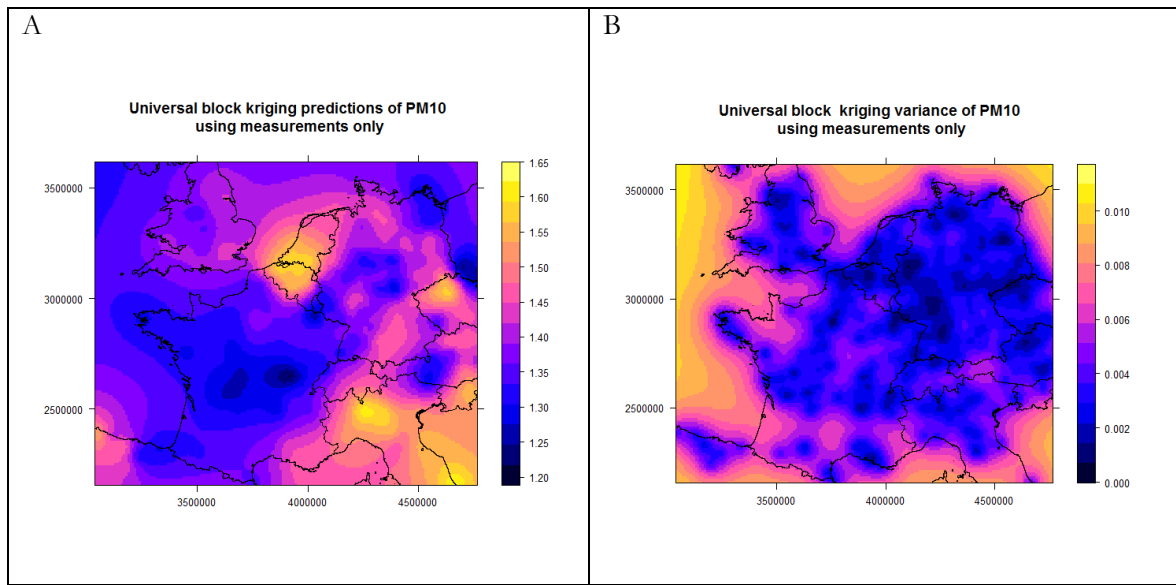


Figure 5-15. PM10 daily annual mean concentrations map for the year 2003 produced by universal block kriging of in situ measurements at the block size of 30 km by 30 km. (A) is the prediction map at area support (B) is the kriging variance

## 5.7. Kriging of PM10 using ancillary data

### 5.7.1. Ordinary linear regression

Three models were established using ordinary linear modelling. Table 5-6 presents the summary of the linear model between PM10 and secondary data. Three models were found significant having p-value < 0.01. However, R<sup>2</sup> was small meaning only 0.16 to 0.20 of variability in PM10 was explained by secondary data.

N=455	model coefficient	Standard error (SE)	t value	Pr(>  t )	Residual standard error (RSE)	R <sup>2</sup> model	r
A)							
intercept	1.148	0.028	41.05	<2e-16			
AOT	1.047	0.111	9.46	<2e-16	0.122	0.163	0.40
B)							
intercept	1.234	0.019	65.879	<2e-16			
PM2.5	0.015	0.002	9.686	<2e-16	0.121	0.170	0.41
C)							
intercept	1.142	0.027	41.846	<2e-16			
AOT	0.626	0.137	4.553	< 6.80e-06			
PM2.5	0.009	0.002	4.950	< 1.05e-06	0.118	0.204	0.45

Table 5-6. Ordinary linear regression model results for (A) PM10 regressed on AOT, (B) PM10 regressed on PM2.5 and (C) PM10 regressed on both AOT and PM2.5

From Table 5-6, predictors were AOT and PM2.5. Coincident number of observation (N) between PM10 and secondary data were 455. The deterministic model coefficient (R<sup>2</sup>) increased when PM10 regressed on both covariates.

### Mathematical relation between PM10 and secondary data

From linear model parameters presented in Table 5-6, mathematical relationship between PM10 and secondary data were established as presented by equations 5-1, 5-2 and 5-3.

$$PM_{10} = 1.148 + 1.047 AOT \tag{5-1}$$

$$PM_{10} = 1.234 + 1.015 PM_{2.5} \tag{5-2}$$

$$PM_{10} = 1.142 + 0.551 AOT + 0.011 PM_{2.5} \tag{5-3}$$

**Maps by ordinary linear regression model**

Relationship between PM10 and secondary data modelled by equations 5-1, 5-2 and 5-3 were used to produce maps presented in Figure 5-16, Figure 5-17 and Figure 5-18 respectively.

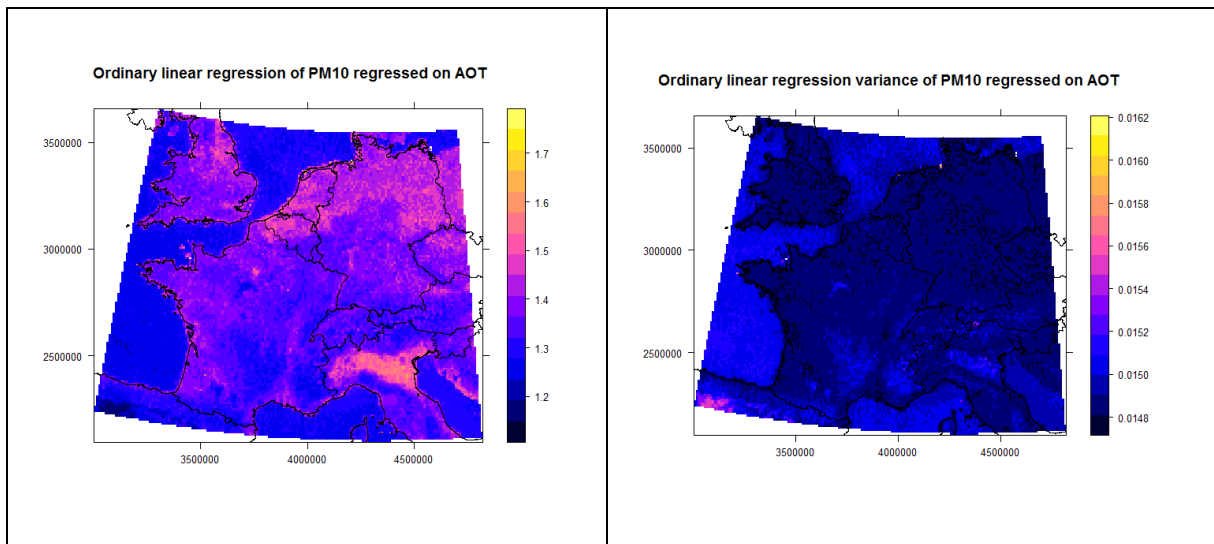


Figure 5-16. PM10 daily annual mean concentration map for 2003 produced by ordinary linear regression of PM10 regressed on AOT. AOT was an input to equation 5-1.

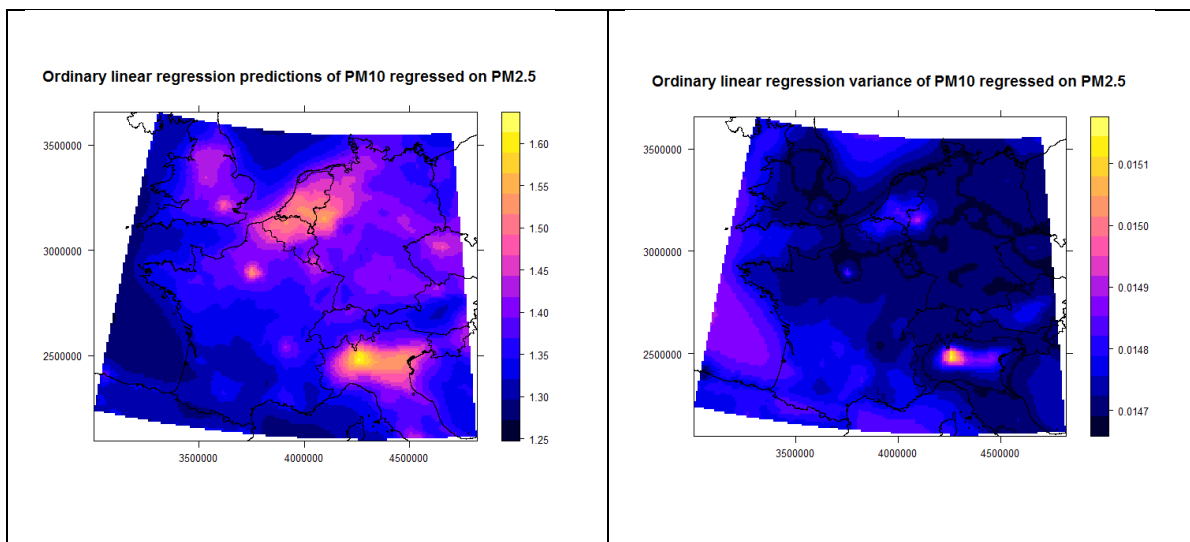


Figure 5-17. PM10 daily annual mean concentration map for 2003 produced by ordinary linear regression of PM10 regressed on PM2.5. PM2.5 was an input was an input to equation 5-2.

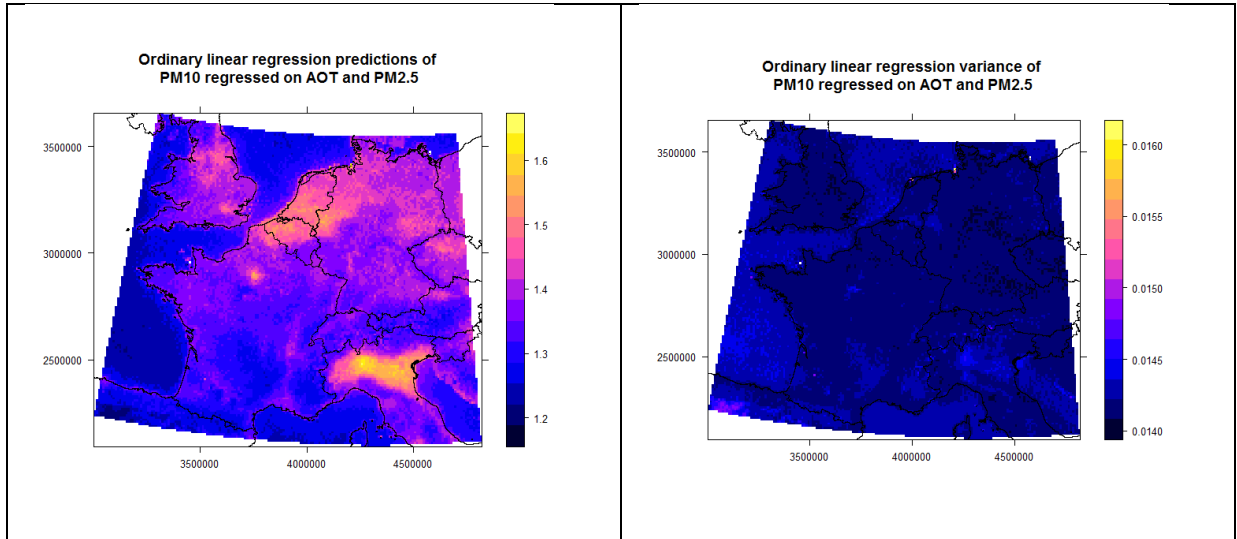


Figure 5-18. PM10 daily annual mean concentration map for 2003 produced by ordinary linear regression of PM10 regressed on AOT and PM2.5. AOT and PM2.5 were inputs to equation 5-3.

**5.7.2. Regression kriging using exponential model**

**Regression kriging of PM10 on AOT**

Refer to summary of the linear model between PM10 and AOT presented in Table 5-6, the deterministic model coefficient ( $R^2$ ) between PM10 and AOT was found to be 0.16 i.e. only 0.16 of variability in measurements is being explained by AOT. Figure 5-19 shows the scatter plot describing relationship between PM10 and AOT. The diagnostic plots presented in Figure 5-20 shows residuals are normally distributed.

Residual modelling was done in R software to be used in RK. Figure 5-21 shows exponential variograms model of residuals showing hole effect. Computed residual model parameters used for kriging of residuals are presented in Table 5-7. Figure 5-22 is the PM10 concentrations map created by RK between PM10 as response and AOT as explanatory variable.

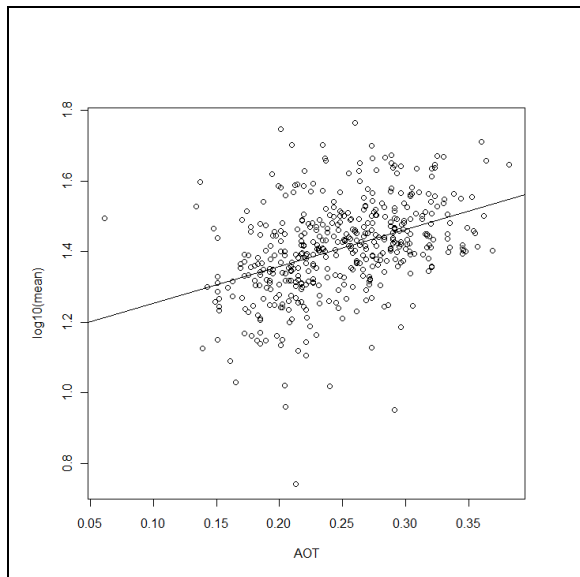


Figure 5-19. Regression line between PM10 and AOT

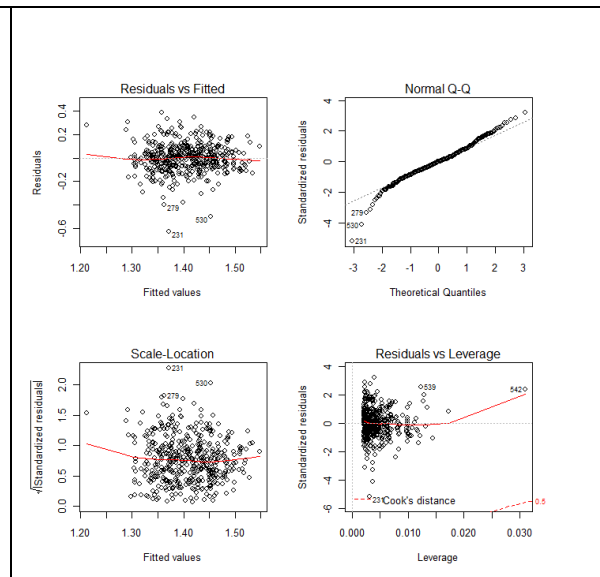
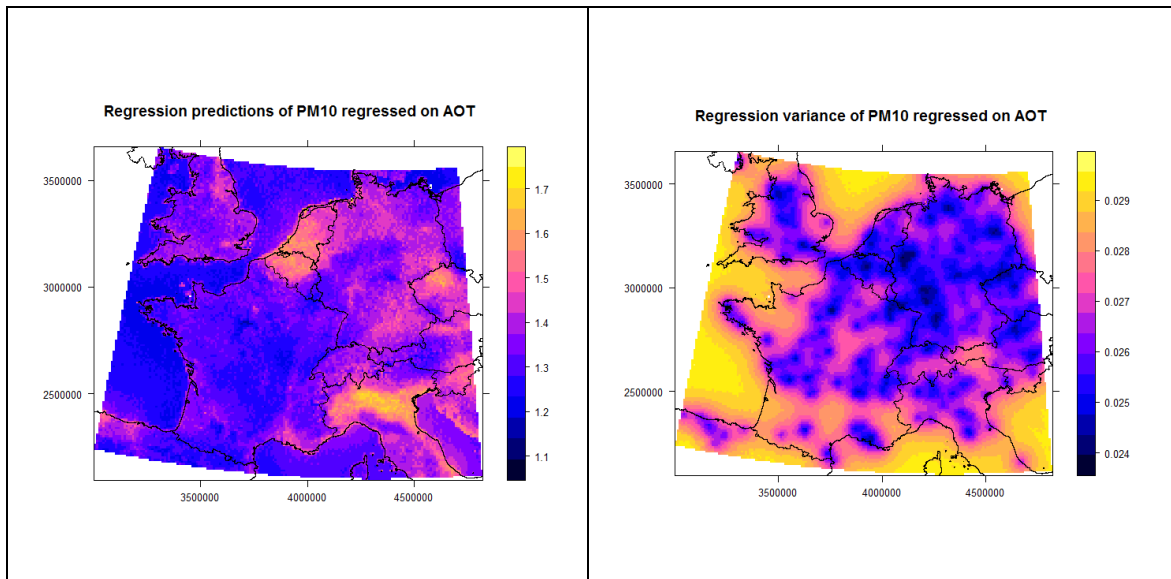
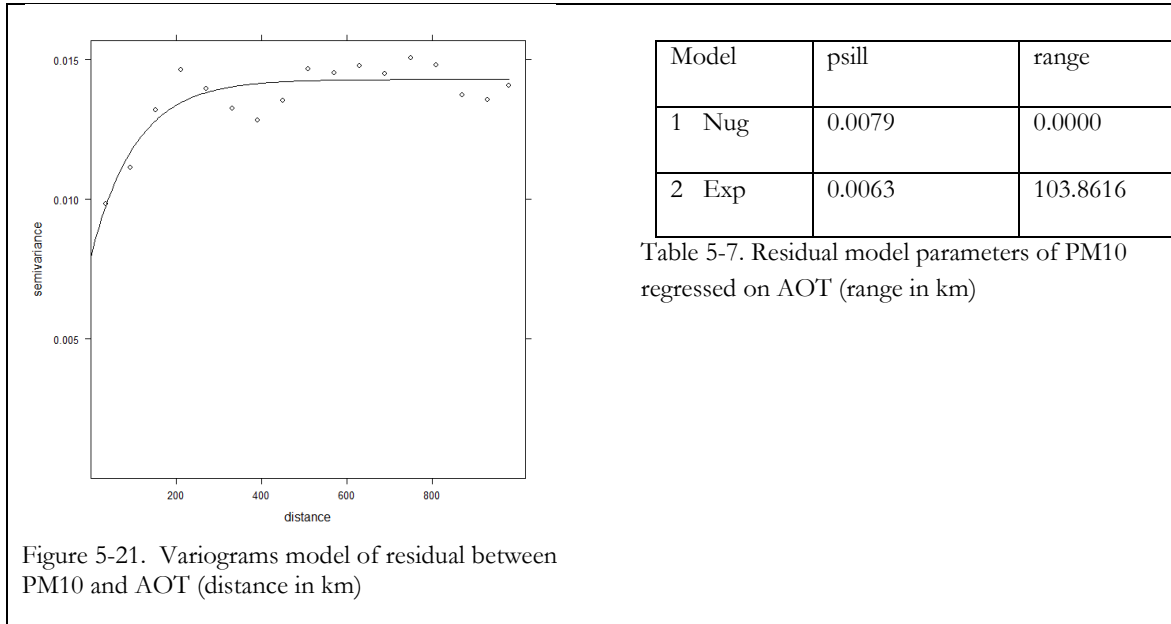


Figure 5-20. Regression diagnostic plot of PM10 and AOT



**Regression kriging of PM10 on PM2.5**

Refer to linear model between PM10 and PM2.5 summarized in Table 5-6, the  $R^2$  between PM10 and PM2.5 was found to be 0.17. This means that; only 0.17of variability in PM10 is being explained by PM2.5. The scatter plot presented in Figure 5-23 describes the relation between variables along regression line. Figure 5-24 presents the diagnostic plots between PM10 and PM2.5 from which residuals are shown to be normally distributed.

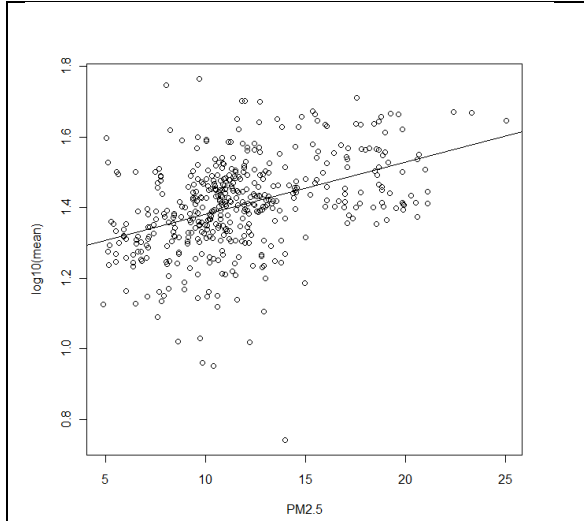


Figure 5-23. Regression line between PM10 and PM2.5. There is poor correlation as depicted by regression line

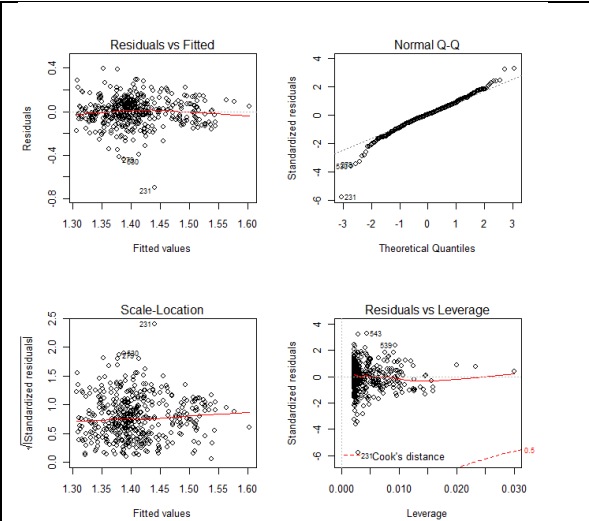


Figure 5-24. Regression diagnostic plot of PM10 and PM2.5. Residuals shows high correlation though deviates from normal distribution (see residual vs fitted and normal probability plot)

Residual modelling was done in R software and was used in RK to produce map presented in Figure 5-26(left). Figure 5-25 show the variograms model of residuals showing hole effect at 400 km and computed residual model parameters used in RK are presented in Table 5-8

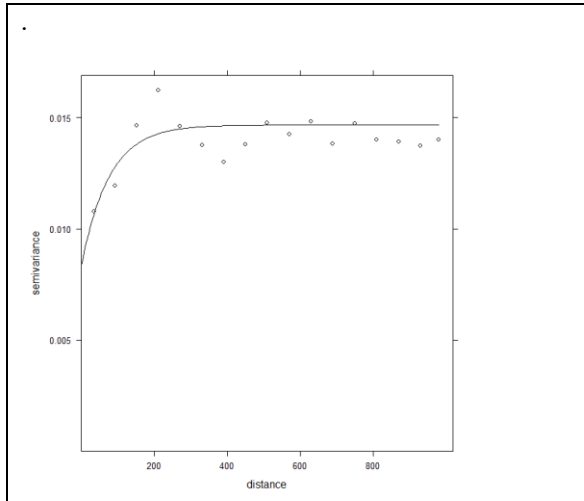


Figure 5-25. Exponential variograms model of residual between PM10 and PM2.5 (distance in km)

model	psill	range
1 Nug	0.008	0.000
2 Exp	0.006	75.946

Table 5-8. Residual model parameters of PM10 regressed on PM2.5 (range in km)

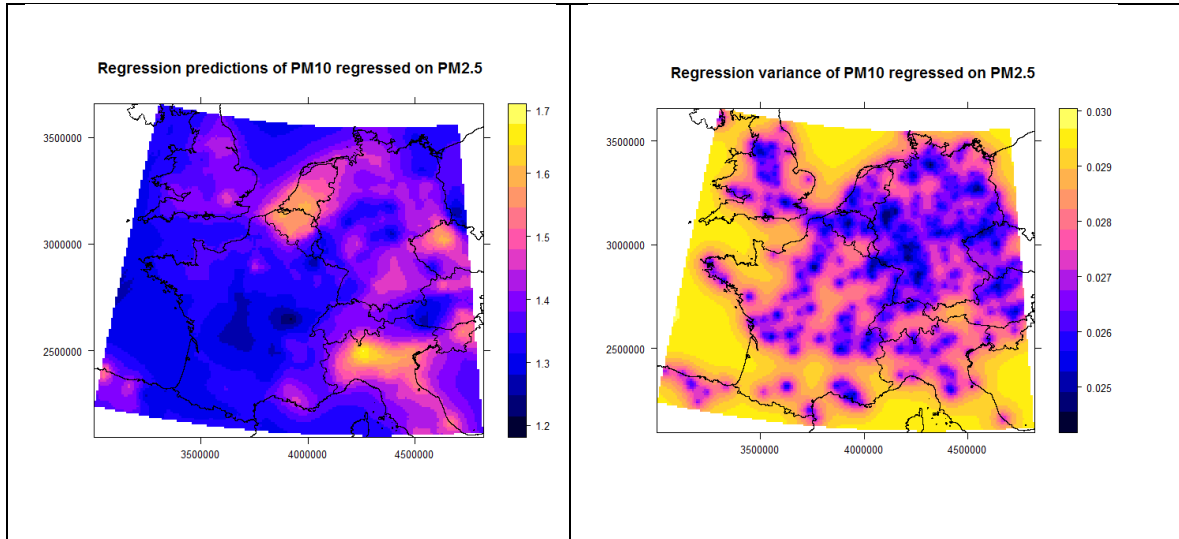


Figure 5-26. PM10 daily annual mean concentration map for 2003 produced by RK of PM10 regressed on PM2.5

**Regression kriging of PM10 on AOT and PM2.5**

The regression model of PM10 regressed on AOT and PM2.5 resulted to  $R^2$  of 0.2 (refer to Table 5-6). This means that 20% of variability in measurements was explained by secondary information. The diagnostic plots of regression model residual are normally distributed (Figure 5-27).

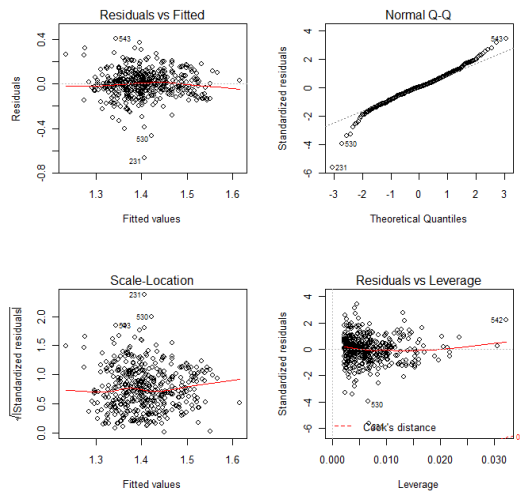
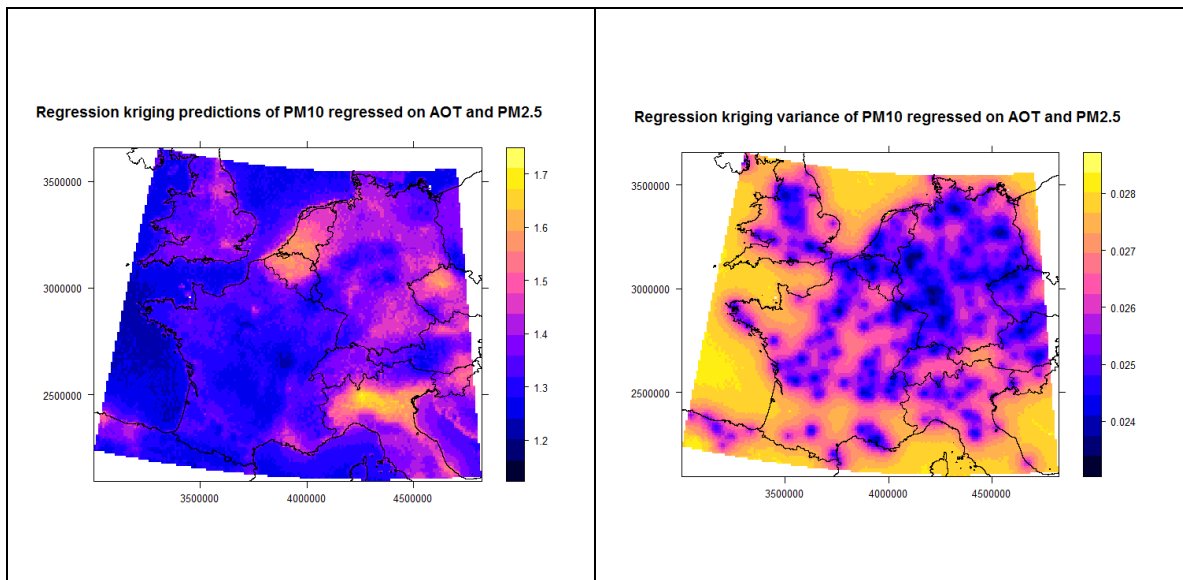
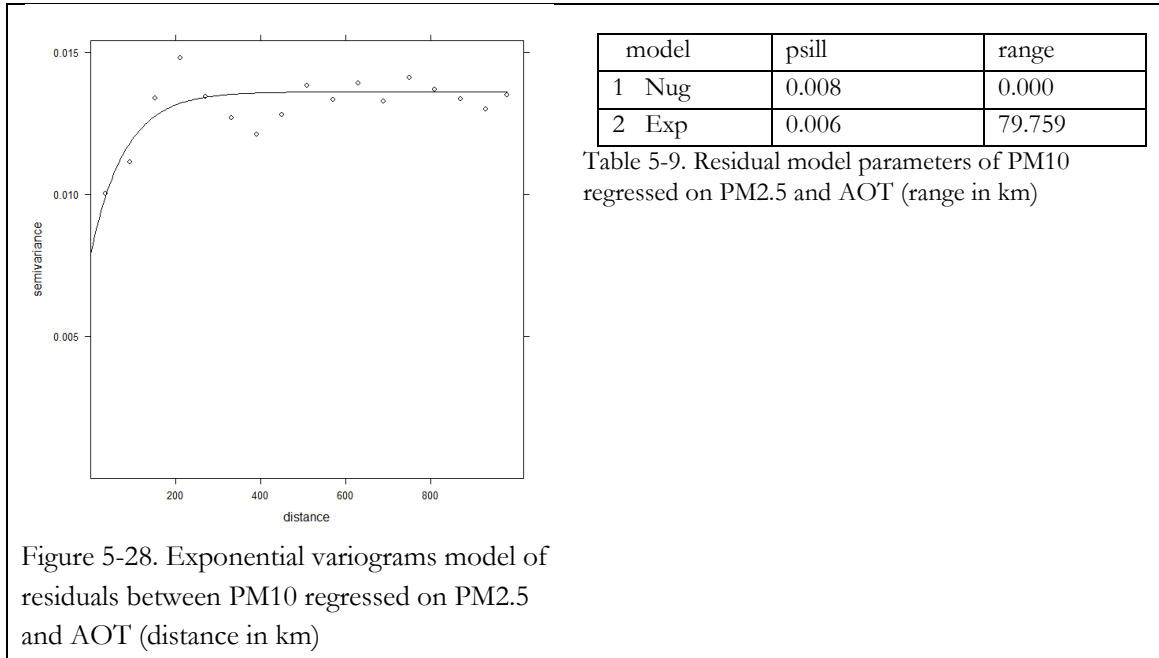


Figure 5-27. Diagnostic plot of PM10 regressed on both covariates (AOT and PM2.5).

Figure 5-28 show the variograms model of residuals showing hole effect at 400 km. Computed residual model parameters are presented in Table 5-9. Figure 5-29 (left) is the PM10 concentrations map produced by RK of PM10 regressed on AOT and PM2.5.



### 5.7.3. Kriging using hole effect model

#### Measurement only

The hole effect model was fitted to empirical variograms of PM10 daily annual mean concentration for the year 2003 due to hole effect at 400 km and 800 km. Figure 5-30 shows the hole effect model and its computed model parameters for PM10 concentrations. The model was then used to predict two maps shown in Figure 5-31 by ordinary kriging (A) and universal kriging (B).

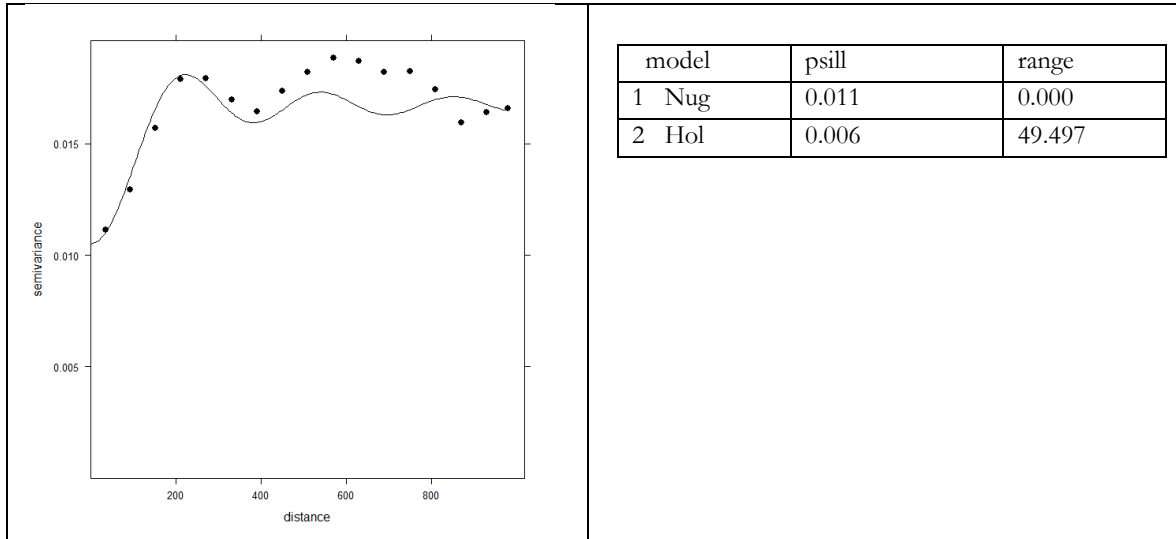


Figure 5-30. Hole effect model variograms (left) and computed model parameters (right) of PM10 daily annual mean concentration for the year 2003

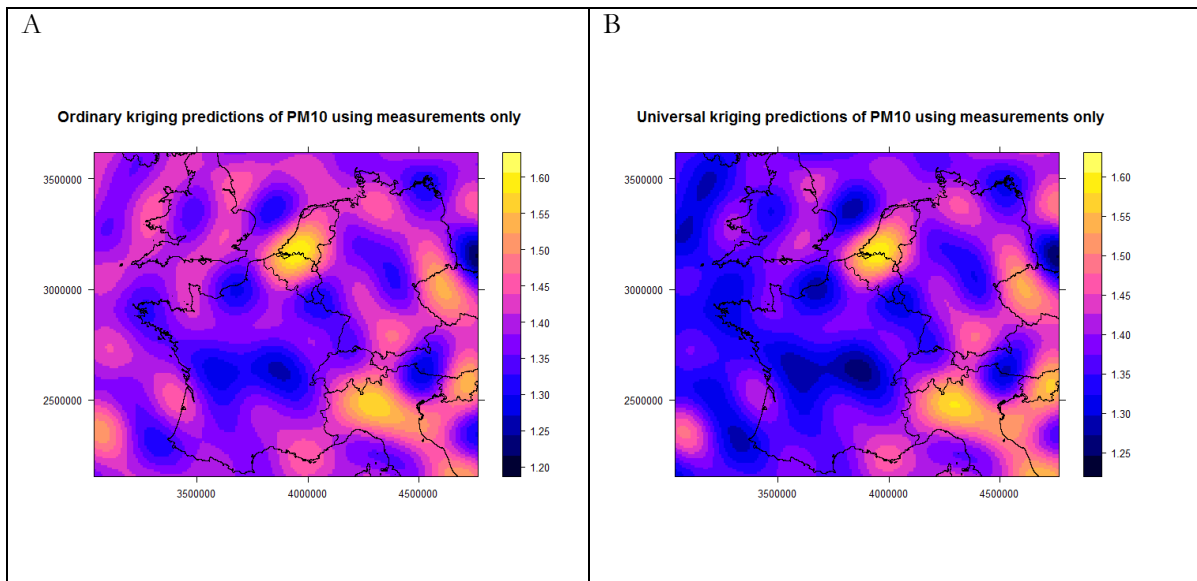


Figure 5-31. PM10 daily annual mean concentration predicted maps using hole effect model. Predictions presented in (A) were produced by OK and predictions presented in (B) were produced by UK using PM10 available observations. Both methods used model presented in figure 5-30

**RK using hole effect model**

Variograms of residuals showed hole effect. Therefore hole effect model was fitted to variograms of residuals of PM10 regressed to AOT, PM2.5 and both covariates. Then these models were used in RK of PM10 and secondary data. Figure 5-32, Figure 5-33 and Figure 5-34 presents hole effect models and corresponding RK maps of PM10 regressed on AOT, PM10 regressed on PM2.5 and PM10 regressed on AOT and PM2.5 respectively. The hole effect model fitted better estimated empirical variograms at shorter distances up to 400 km compared to exponential model.

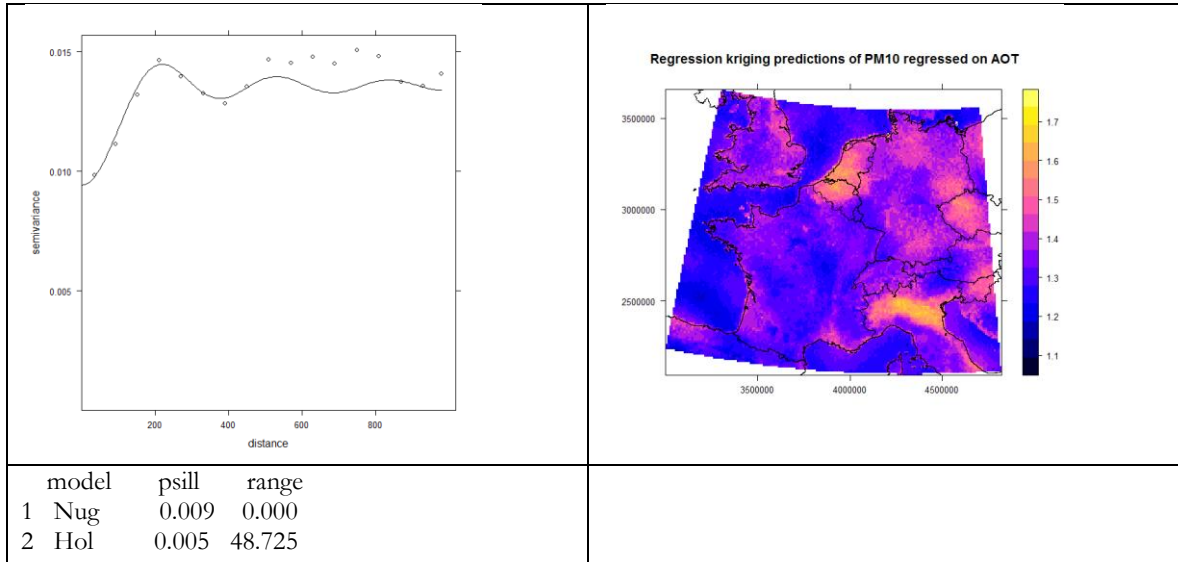


Figure 5-32. Hole effect model fitted to residuals of PM10 regressed on AOT and its corresponding RK map (right)

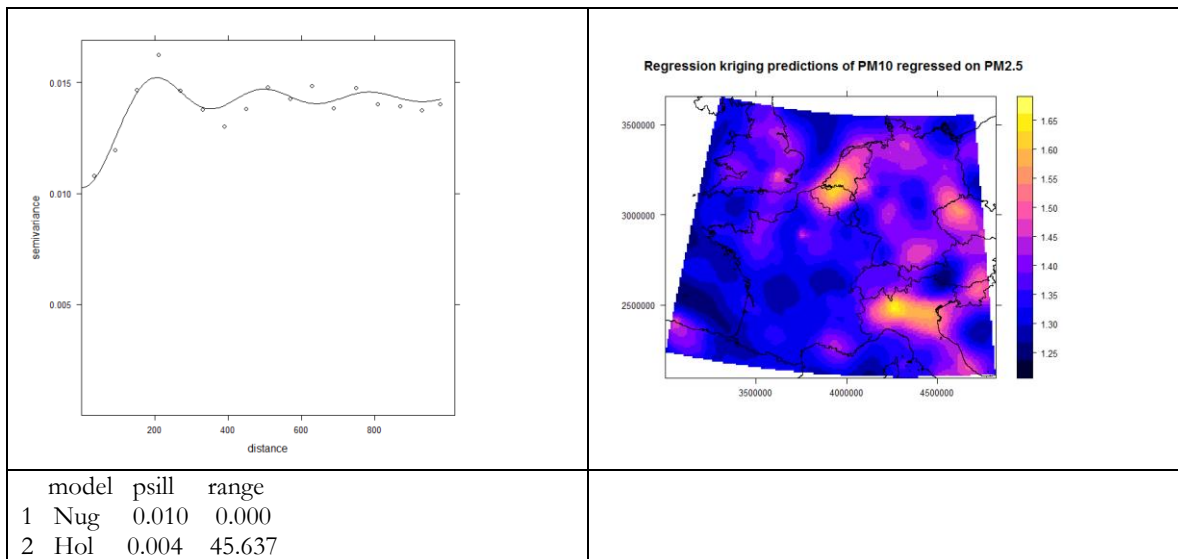


Figure 5-33. Hole effect model fitted to residuals of PM10 regressed on PM2.5 and its corresponding RK map (right)

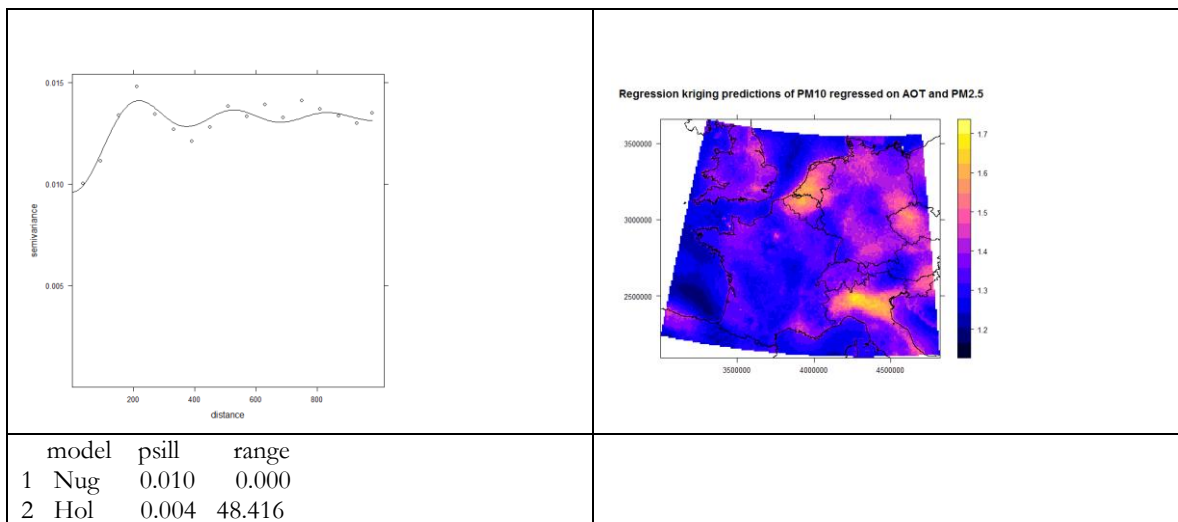


Figure 5-34. Hole effect model fitted to residuals of PM10 regressed on AOT and PM2.5 (Left) and its corresponding RK map (right)

**5.7.4. Cokriging (CK)**

Table 5-10, Table 5-11 and Table 5-12 shows the cross variograms model parameters between PM10 and AOT, PM10 and PM2.5 and PM10 with AOT and PM2.5 respectively. Figure 5-35, Figure 5-37 and Figure 5-39 show the cross variograms models for PM10 and AOT, PM10 and PM2.5 and PM10 with AOT and PM1.5 respectively. Kriging predictions produced by three cokriging models are presented in Figure 5-36, Figure 5-38 and Figure 5-40 on left and their corresponding cokriging variance on the right.

**PM10 cokriged with AOT**

Table 5-10 show the cross variograms model parameters between PM10 and AOT. Figure 5-35 show the cross variograms models for PM10 and AOT. Cokriging predictions produced by this model is presented in Figure 5-36.

<pre>(g &lt;- gstat(g, id = "PM10", model = m , fill.all=T))</pre>				<pre>(g &lt;- fit.lmc(v.cross, g))</pre>			
data:				data:			
PM10 : formula = log10(mean)~1 ; data dim = 455 x 1				PM10 : formula = log10(mean)~1 ; data dim = 455 x 1			
AOT : formula = AOT~1 ; data dim = 455 x 3				AOT : formula = AOT~1 ; data dim = 455 x 3			
variograms:				variograms:			
	model	psill	range		model	psill	range
PM10[1]	Nug	0.0086	0.0	PM10[1]	Nug	0.0076	0.0
PM10[2]	Exp	0.0096	121978.4	PM10[2]	Exp	0.0109	121978.4
AOT[1]	Nug	0.0086	0.0	AOT[1]	Nug	0.0005	0.0
AOT[2]	Exp	0.0096	121978.4	AOT[2]	Exp	0.0020	121978.4
PM10.AOT[1]	Nug	0.0086	0.0	PM10.AOT[1]	Nug	0.0004	0.0
PM10.AOT[2]	Exp	0.0096	121978.4	PM10.AOT[2]	Exp	0.0027	121978.4

Table 5-10. Cross variograms model parameters between PM10 and AOT

“Mean” as defined when building variograms object represents PM10 daily annual mean concentration. Base 10 logarithm transformation of PM10 (mean) was applied due to skewedness of raw data.

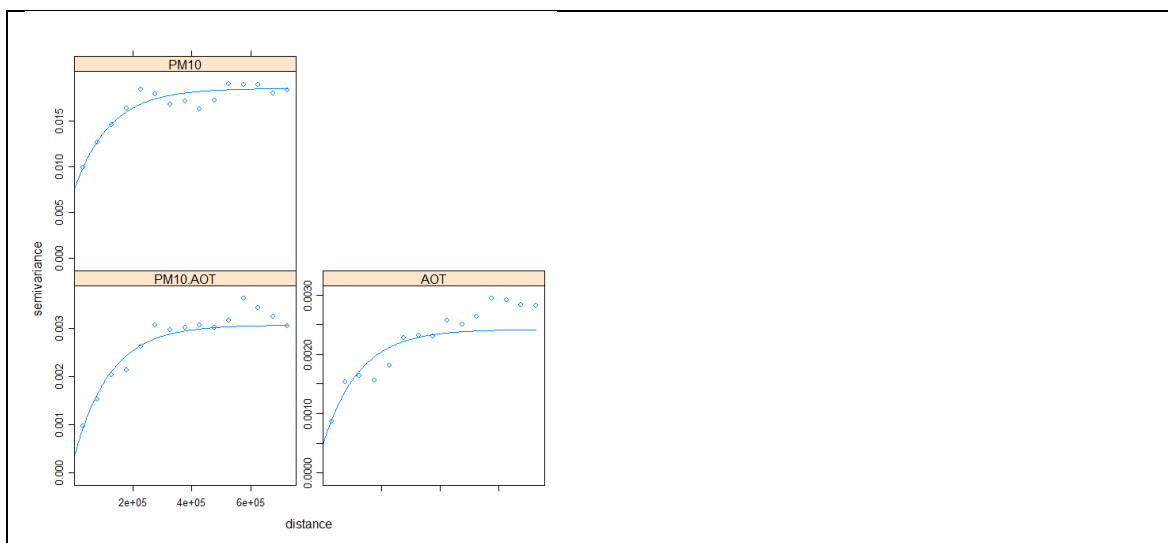


Figure 5-35. Cross variograms model between PM10 and AOT

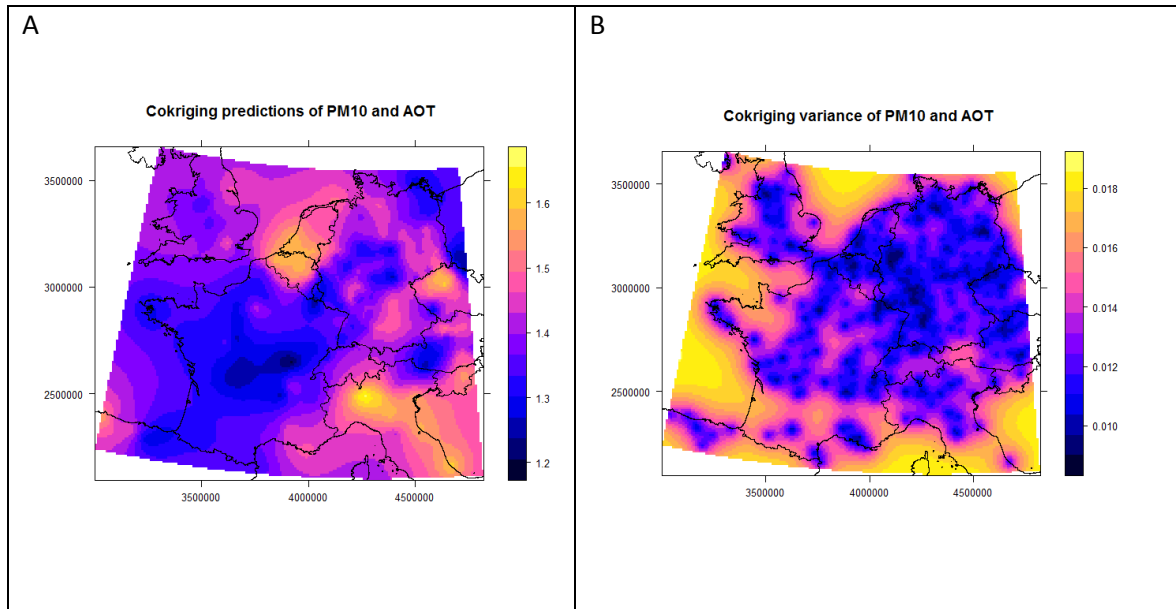


Figure 5-36. PM10 daily annual mean concentration map for 2003 produced by cokriging of PM10 with AOT. (A) is the cokriging predictions and (B) is the cokriging variance.

### PM10 cokriged with PM2.5

Table 5-11 shows the cross variograms model parameters between PM10 and PM2.5. Figure 5-37 show the cross variograms models PM10 and PM2.5. Cokriging predictions produced by this model are presented in Figure 5-38 on left and their corresponding cokriging variance on the right.

<pre>&gt; (g &lt;- gstat(g, id = "PM10", model =m , fill.all=T)) data: PM10 : formula = log10(mean)~1 ; data dim = 455 x 1 PM25 : formula = log10(PM2.5)~x + y ; data dim = 455 x 3 variograms:</pre> <table border="1"> <thead> <tr> <th></th> <th>model</th> <th>psill</th> <th>range</th> </tr> </thead> <tbody> <tr> <td>PM10[1]</td> <td>Nug</td> <td>0.0086</td> <td>0.0</td> </tr> <tr> <td>PM10[2]</td> <td>Exp</td> <td>0.0096</td> <td>121978.4</td> </tr> <tr> <td>PM25[1]</td> <td>Nug</td> <td>0.0086</td> <td>0.0</td> </tr> <tr> <td>PM25[2]</td> <td>Exp</td> <td>0.0096</td> <td>121978.4</td> </tr> <tr> <td>PM10.PM25[1]</td> <td>Nug</td> <td>0.0086</td> <td>0.0</td> </tr> <tr> <td>PM10.PM25[2]</td> <td>Exp</td> <td>0.0096</td> <td>121978.4</td> </tr> </tbody> </table>		model	psill	range	PM10[1]	Nug	0.0086	0.0	PM10[2]	Exp	0.0096	121978.4	PM25[1]	Nug	0.0086	0.0	PM25[2]	Exp	0.0096	121978.4	PM10.PM25[1]	Nug	0.0086	0.0	PM10.PM25[2]	Exp	0.0096	121978.4	<pre>&gt; (g &lt;- fit.lmc(v.cross, g)) data: PM10 : formula = log10(mean)~1 ; data dim = 455 x 1 PM25 : formula = log10(PM2.5)~x + y ; data dim = 455 x 3 variograms:</pre> <table border="1"> <thead> <tr> <th></th> <th>model</th> <th>psill</th> <th>range</th> </tr> </thead> <tbody> <tr> <td>PM10[1]</td> <td>Nug</td> <td>0.0076</td> <td>0.0</td> </tr> <tr> <td>PM10[2]</td> <td>Exp</td> <td>0.0109</td> <td>121978.4</td> </tr> <tr> <td>PM25[1]</td> <td>Nug</td> <td>0.0002</td> <td>0.0</td> </tr> <tr> <td>PM25[2]</td> <td>Exp</td> <td>0.0112</td> <td>121978.4</td> </tr> <tr> <td>PM10.PM25[1]</td> <td>Nug</td> <td>-0.0011</td> <td>0.0</td> </tr> <tr> <td>PM10.PM25[2]</td> <td>Exp</td> <td>0.0072</td> <td>121978.4</td> </tr> </tbody> </table>		model	psill	range	PM10[1]	Nug	0.0076	0.0	PM10[2]	Exp	0.0109	121978.4	PM25[1]	Nug	0.0002	0.0	PM25[2]	Exp	0.0112	121978.4	PM10.PM25[1]	Nug	-0.0011	0.0	PM10.PM25[2]	Exp	0.0072	121978.4
	model	psill	range																																																						
PM10[1]	Nug	0.0086	0.0																																																						
PM10[2]	Exp	0.0096	121978.4																																																						
PM25[1]	Nug	0.0086	0.0																																																						
PM25[2]	Exp	0.0096	121978.4																																																						
PM10.PM25[1]	Nug	0.0086	0.0																																																						
PM10.PM25[2]	Exp	0.0096	121978.4																																																						
	model	psill	range																																																						
PM10[1]	Nug	0.0076	0.0																																																						
PM10[2]	Exp	0.0109	121978.4																																																						
PM25[1]	Nug	0.0002	0.0																																																						
PM25[2]	Exp	0.0112	121978.4																																																						
PM10.PM25[1]	Nug	-0.0011	0.0																																																						
PM10.PM25[2]	Exp	0.0072	121978.4																																																						

Table 5-11. Cross variograms model parameters between PM10 and PM2.5.

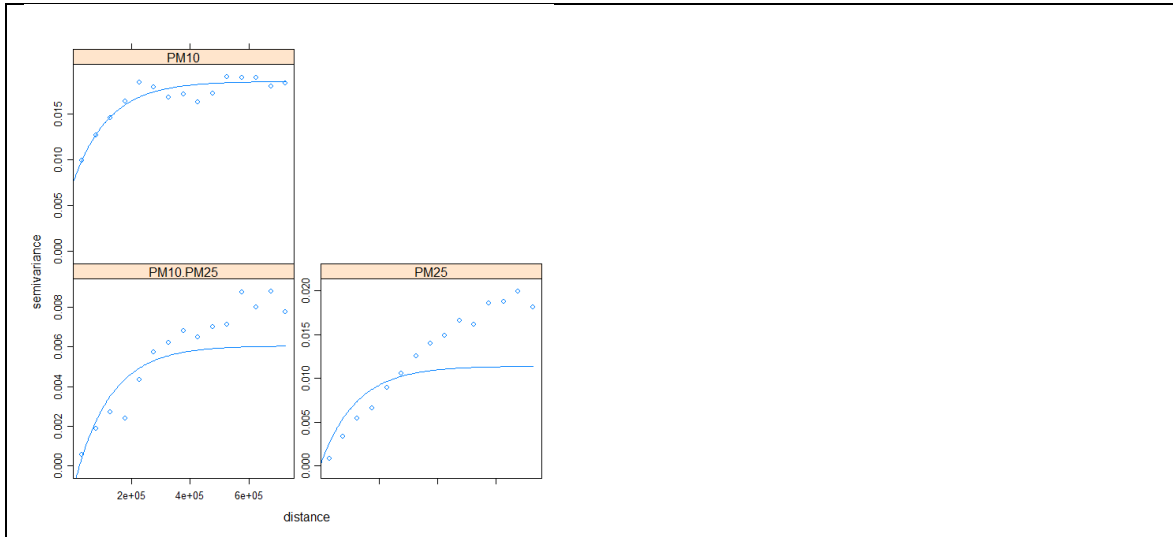


Figure 5-37. Cross variograms model between PM10 and PM2.5

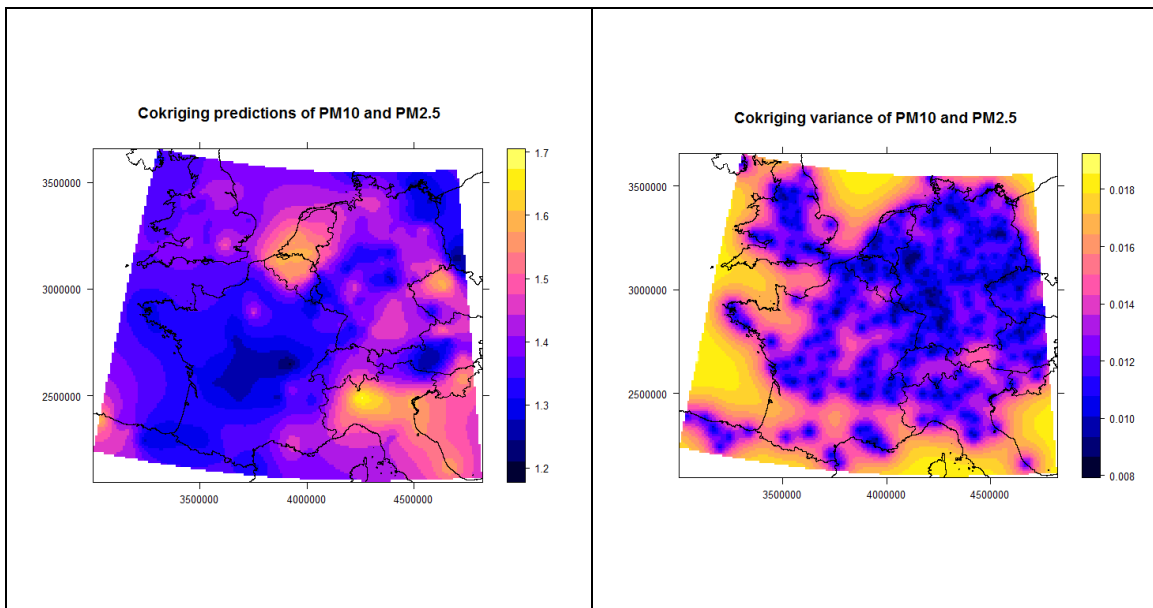


Figure 5-38. PM10 daily annual mean concentration map for 2003 produced by cokriging of PM10 with PM2.5.

**PM10 cokriged with AOT and PM2.5**

Table 5-12 shows the cross variograms model parameters between PM10 with AOT and PM2.5. Figure 5-39 show the cross variograms model between PM10 with AOT and PM2.5. Cokriging predictions produced by this model are presented in Figure 5-40 on the left and their corresponding kriging variance on the right.

<pre>(g &lt;- gstat(g, id = "PM10", model =mm , fill.all=T)) data: PM10 : formula = log10(mean)~1 ; data dim = 455 x 1 AOT : formula = AOT~1 ; data dim = 455 x 3 PM25 : formula = log10(PM2.5)~x + y ; data dim = 455 x 3 variograms:</pre>				<pre>(g &lt;- fit.lmc(v.cross, g)) data: PM10 : formula = log10(mean)~1 ; data dim = 455 x 1 AOT : formula = AOT~1 ; data dim = 455 x 3 PM25 : formula = log10(PM2.5)~x + y ; data dim = 455 x 3 variograms:</pre>			
	model	psill	range		model	psill	range
PM10[1]	Nug	0.0086	0.0	PM10[1]	Nug	0.0076	0.0
PM10[2]	Exp	0.0096	121978.4	PM10[2]	Exp	0.0109	121978.4
AOT[1]	Nug	0.0086	0.0	AOT[1]	Nug	0.0005	0.0
AOT[2]	Exp	0.0096	121978.4	AOT[2]	Exp	0.0020	121978.4
PM25[1]	Nug	0.0086	0.0	PM25[1]	Nug	0.0002	0.0
PM25[2]	Exp	0.0096	121978.4	PM25[2]	Exp	0.0112	121978.4
PM10.AOT[1]	Nug	0.0086	0.0	PM10.AOT[1]	Nug	0.0004	0.0
PM10.AOT[2]	Exp	0.0096	121978.4	PM10.AOT[2]	Exp	0.0027	121978.4
PM10.PM25[1]	Nug	0.0086	0.0	PM10.PM25[1]	Nug	-0.0011	0.0
PM10.PM25[2]	Exp	0.0096	121978.4	PM10.PM25[2]	Exp	0.0072	121978.4
AOT.PM25[1]	Nug	0.0086	0.0	AOT.PM25[1]	Nug	-0.0002	0.0
AOT.PM25[2]	Exp	0.0096	121978.4	AOT.PM25[2]	Exp	0.0031	121978.4

Table 5-12. Cross variograms model parameters of PM10 with AOT and PM2.5.

It was important to calculate PM2.5 variograms with trend using coordinates because it provided relatively similar structure with other variables used in estimation of cross variograms.

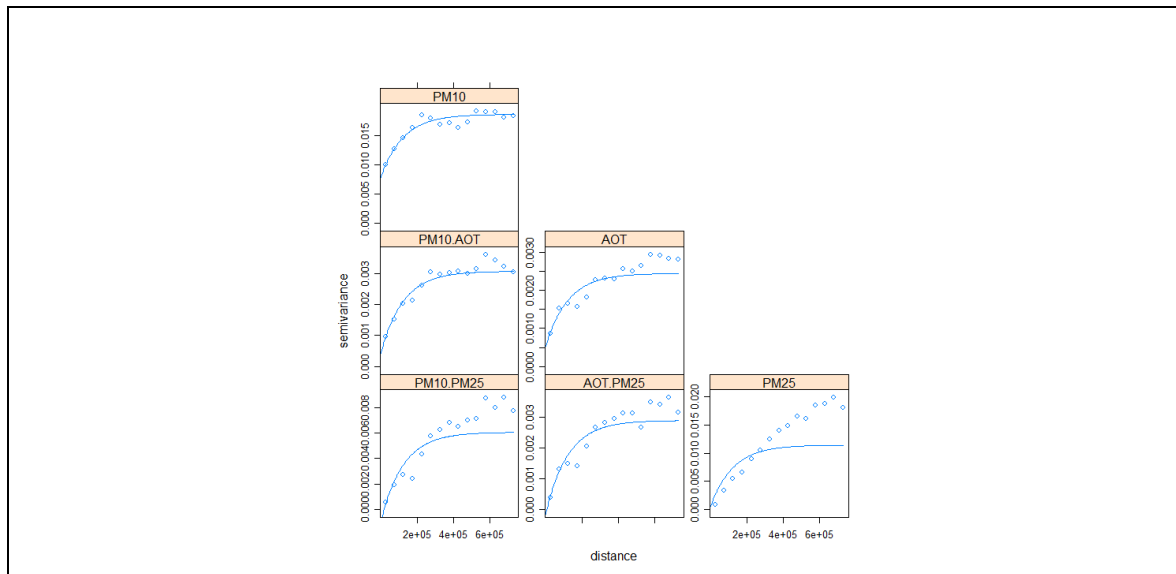


Figure 5-39. Cross variograms model between PM10 with AOT and PM2.5.

Collocated pixels with PM10 stations values were used in estimation of individual variograms models and hence cross variograms

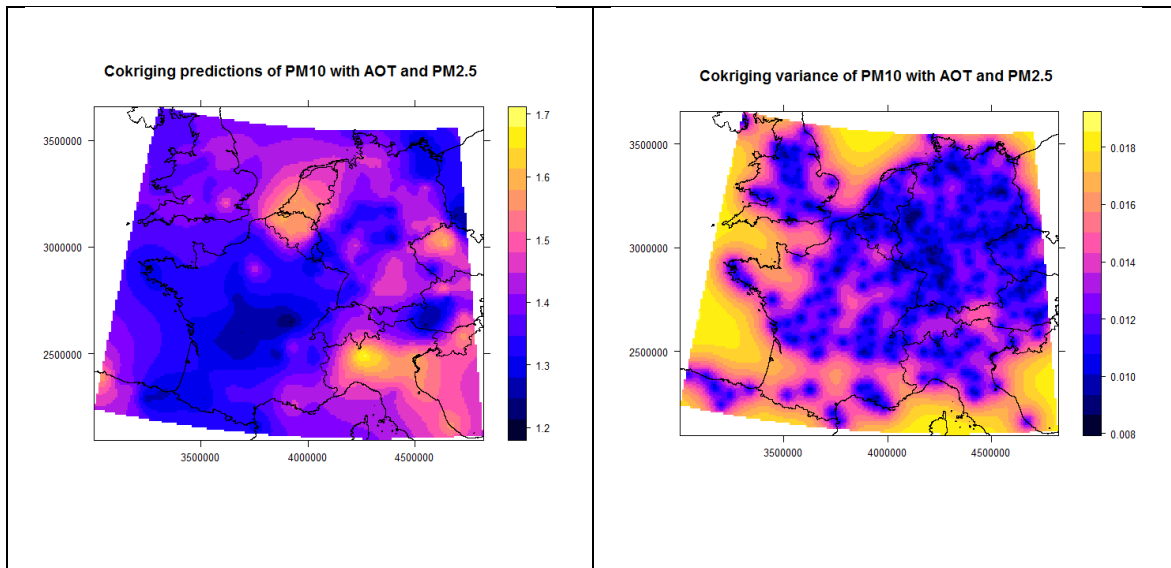


Figure 5-40. PM10 daily annual mean concentration map for 2003 produced by cokriging of PM10 with AOT and PM2.5

## 5.8. Using coarse model outputs

### 5.8.1. RK of PM10 regressed on coarser PM2.5

The linear model results between PM10 and coarser PM2.5 is presented in Table 5-13. The model was significant but  $R^2$  was small (0.16). Table 5-14 (A) shows the scatter plot between variables. The model residuals were normally distributed as presented by diagnostic plot in Table 5-14 (B). Variograms model of residuals and the calculated residual model parameters are shown in Table 5-14 (C and D) respectively. The model was applied in RK to predict map shown in Figure 5-41.

```
Call:
lm(formula = log10(mean) ~ PM2.5, data = as.data.frame(pm10.extraproj))

Residuals:
    Min       1Q   Median       3Q      Max
-0.70524 -0.06468  0.00327  0.07368  0.39854

Coefficients:
            Estimate Std. Error t value Pr(>|t|)
(Intercept)  1.244118   0.018157  68.522  <2e-16 ***
PM2.5         0.013841   0.001465   9.448  <2e-16 ***
---
Signif. codes:  0 '***' 0.001 '**' 0.01 '*' 0.05 '.' 0.1 ' ' 1

Residual standard error: 0.1216 on 453 degrees of freedom
Multiple R-squared:  0.1646,    Adjusted R-squared:  0.1628
F-statistic: 89.26 on 1 and 453 DF,  p-value: < 2.2e-16
```

Table 5-13. Regression model between PM10 and coarser resolution PM2.5 at 30 km square grid.

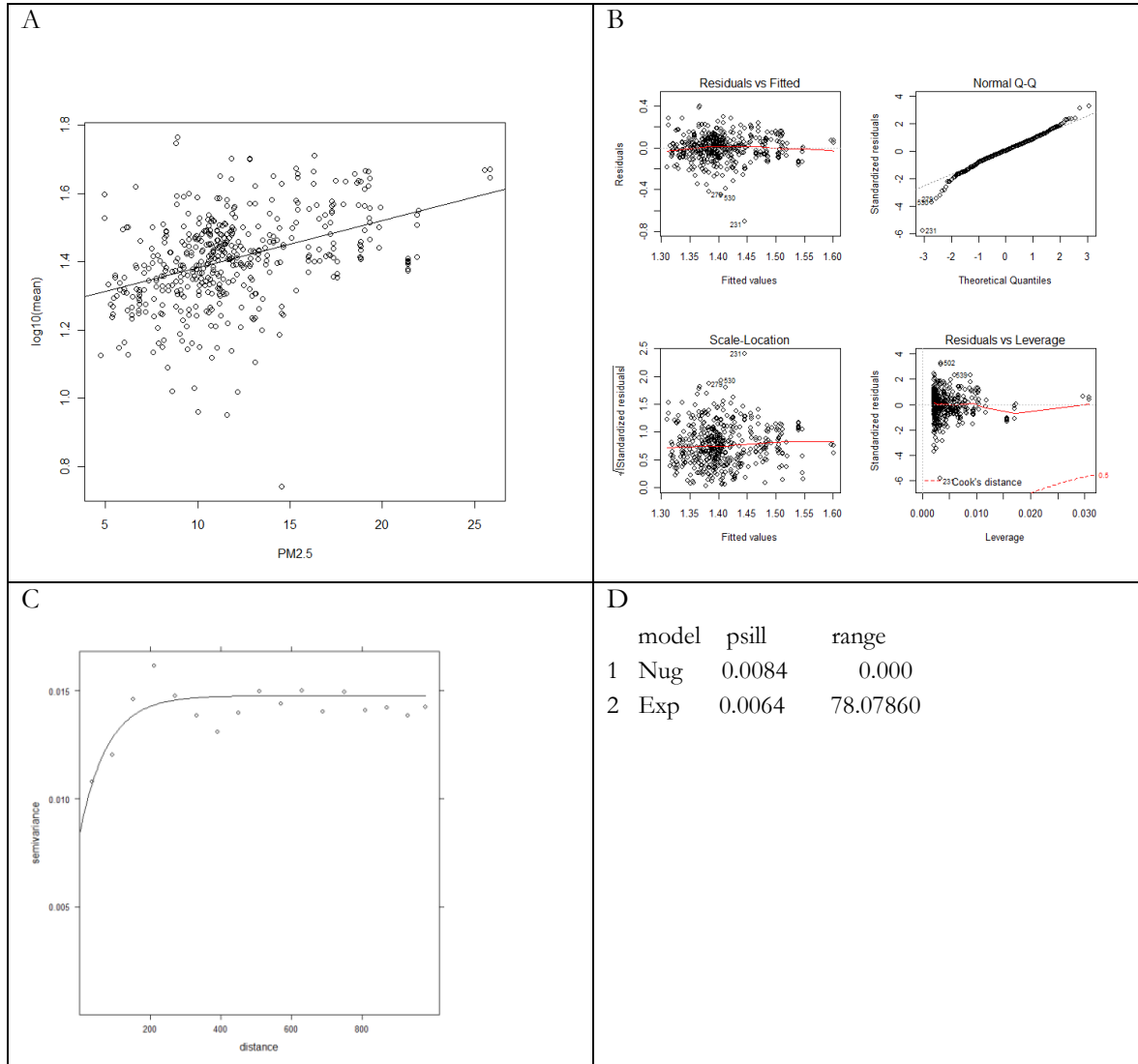


Table 5-14: RK model and predicted map when PM10 regressed on coarser PM2.5 at 30 km grid.

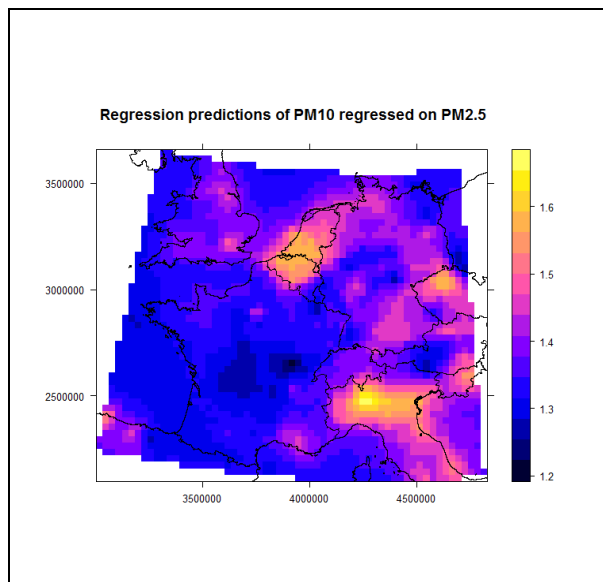


Figure 5-41. PM10 daily annual mean concentration for 2003 produced by RK of PM10 regressed to coarser PM2.5 at spatial resolution of 30 km.

**5.8.2. Cokriging of PM10 with coarser PM2.5**

Using PM2.5 at 30 km square grid, modelling and cokriging between PM10 and PM2.5 was performed. Table 5-15 (A) presents cross variograms model between PM10 and coarser PM2.5. Table 5-15 (B) presents the cross variograms model parameters which then were used to produce cokriged map between PM10 and coarser PM2.5 presented in Table 5-15 (C). Table 5-15 (D) presents the model performance at validation points.

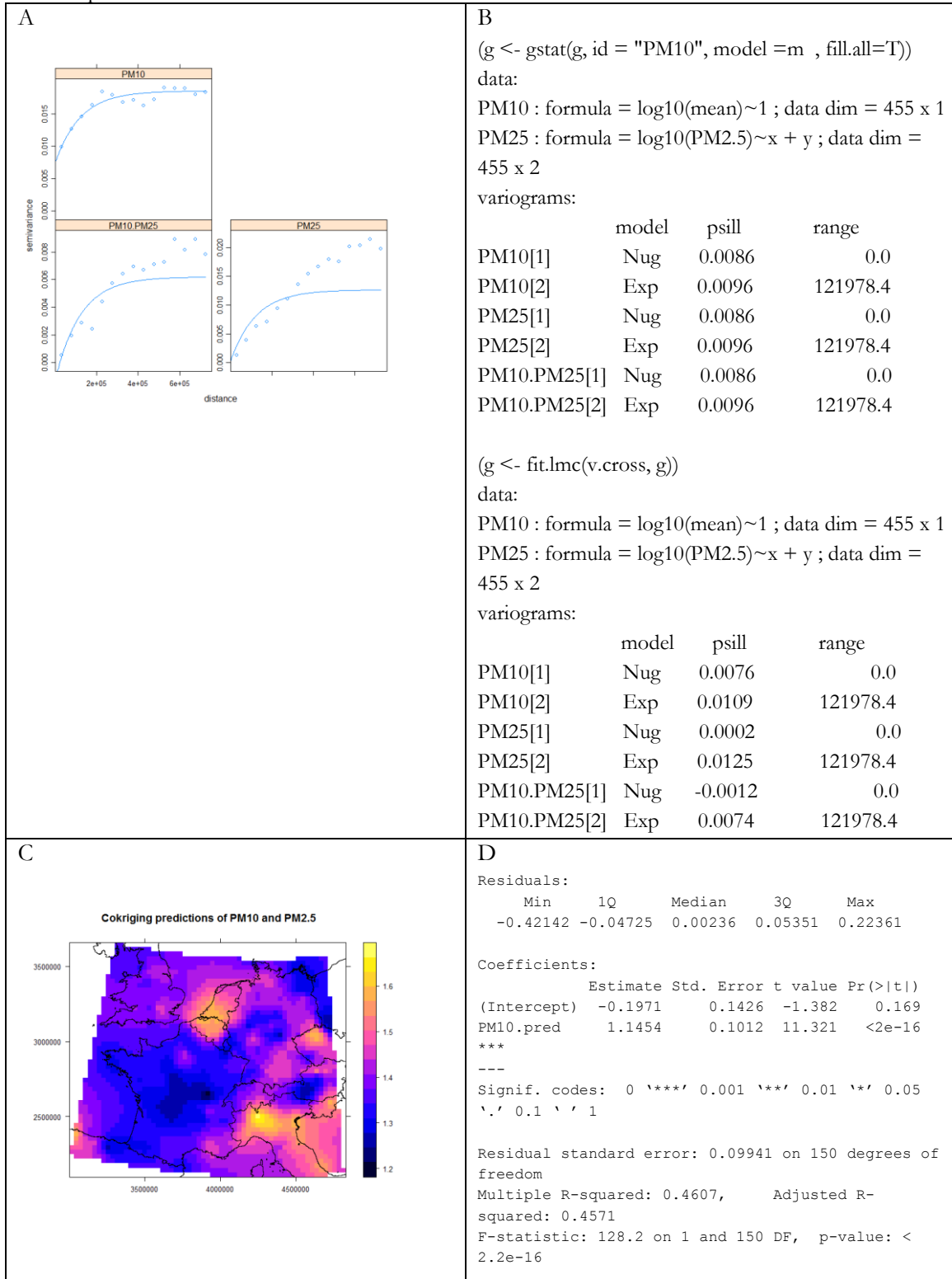


Table 5-15: Cokriging of PM10 daily annual mean concentration with coarser PM2.5 at 30 km square grid for 2003

**5.9. Accuracy assessment**

This section presents error measure indicators for each kriging method used. Table 5-16 presents accuracy assessment of different kriging methods that used “exponential model” in prediction. Table 5-17 presents accuracy assessment of kriging methods when “hole effect model” was used in prediction. Table 5-18 presents accuracy assessment for universal blocking at different sizes. Table 5-19 gives comparison between ordinary linear regression and RK. These results are based on independent dataset (152 measurement stations). Thus it was the comparison between predicted values and known values at these stations. ME, SSE and RMSE were calculated using observed values and predicted values at validation points.

**5.9.1. Prediction using exponential model**

a)

	Modelled mean	ME	SSE	RMSE	R	Secondary variable
OK	1.406	0.009	1.425	0.097	0.72	-
UK	1.406	0.009	1.417	0.096	0.72	coordinates
RK						
	1.409	0.006	1.390	0.096	0.71	AOT
	1.405	0.010	1.449	0.098	0.71	PM2.5
	1.407	0.008	1.398	0.096	0.72	AOT+PM2.5
CK						
	1.407	0.007	1.421	0.097	0.71	AOT
	1.405	0.009	1.496	0.099	0.69	PM2.5
	1.406	0.009	1.500	0.099	0.68	AOT+PM2.5

b)

	Modelled mean	ME	SSE	RMSE	R	Secondary variable
RK	1.404	0.010	1.512	0.100	0.69	PM2.5
CK	1.405	0.010	1.547	0.101	0.67	PM.25

Table 5-16. Accuracy assessment for results of PM10 predictions for 2003 when employing exponential model. Table 5-16 (a) AOT and PM2.5 used were at 10 km square grid and table 5-16 (b) PM2.5 used was at 30 km square grid. The observed mean equals 1.407.

PM2.5 used in table (a) was obtained by downscaling PM2.5 at 0.5° by 0.25° to 0.1° by 0.1° by bilinear interpolation to match AOT derived from MODIS, then projected at 10 km square grid. PM2.5 used in table (b) was obtained by projecting PM2.5 at 0.5° by 0.25° to 30 km square grid. Resulting RMSE and R were better for CK and RK of PM10 with resampled PM2.5 than with coarser PM2.5. However differences were small but are noticeable.

**5.9.2. Prediction using hole effect model**

	Modelled mean	ME	SSE	RMSE	R	Secondary variable
OK	1.406	0.008	1.741	0.107	0.63	-
UK	1.406	0.009	1.703	0.106	0.63	coordinates
RK	1.410	0.004	1.692	0.105	0.62	AOT
	1.405	0.010	1.707	0.106	0.63	PM2.5
	1.407	0.007	1.682	0.105	0.63	AOT+PM2.5

Table 5-17. Accuracy assessment for results of PM10 predictions for 2003 when employing hole effect model. AOT and PM2.5 were at 10 km square grid. The observed mean equals 1.407

From Table 5-17, Small RMSE equals to 0.105 was found for RK of PM10 regressed to AOT and PM10 regressed to both covariates. But the correlation between predicted values and observed values was better

for RK of PM10 regressed to both covariates (0.63) compared to RK of PM10 regressed to AOT (0.62). Also considering modelled mean, It can be concluded that for hole effect model, RK of PM10 regressed to both covariates gave relatively better results than other methods.

**5.9.3. Block kriging**

Table 5-18 presents results of uncertainty assessment when different block sizes were applied. The trend is clear, the uncertainties increases as the block size increases

	Block sizes in km				
	2	5	10	20	30
ME	0.009	0.009	0.009	0.0099	0.009
SSE	1.417	1.418	1.419	1.426	1.436
RMSE	0.0966	0.0966	0.0966	0.0968	0.0972

Table 5-18. Accuracy assessment of universal block kriging at different block sizes

Change of support from point to area has shown that as the block size increases, the uncertainties increases. SSE is more sensitive to change of support than RMSE. There is no change of RMSE from point to block size of 10 km while SSE has been changing (Table 5-18).

**5.9.4. Ordinary linear regression and RK**

	Ordinary linear regression			Regression kriging		
	Meas. & AOT	Meas. & PM2.5	Meas. & AOT+PM2.5	Meas. & AOT	Meas. & PM2.5	Meas. & AOT+PM2.5
R	0.364	0.358	0.401	0.712	0.708	0.715
SSE	2.390	2.432	2.326	1.390	1.449	1.398
ME	0.005	0.015	0.011	0.006	0.010	0.008
RMSE	0.125	0.126	0.124	0.096	0.098	0.096
Modelled mean	1.410	1.399	1.404	1.409	1.405	1.407

Table 5-19. Model performance comparison between ordinary linear regression and RK. The observed mean equals 1.407.

From Table 5-19 it is clearly shown that RK performed better than ordinary linear regression. The difference in results is due to difference in mechanism of methods. RK considers of spatial structure in the data modelled by variograms while ordinary linear regression does not. Hence these results indicates importance of understanding spatial structure in data (Goovaerts, 2000).





## 6. DISCUSSION

This chapter discusses in details the results obtained in this study. Discussion is based on data exploration, performance of various kriging methods used and model functions applied.

Investigating spatial distribution in data, two groups of data were explored. Combined PM10 concentration from different countries measured by different techniques and combined PM10 concentration by beta ray absorption technique. Both descriptive and quantitative data analysis were performed and were helpful to see the effect of combining data from different countries. Histogram showed both data are skewed Figure 5-1 and Figure 5-2. Although summary statistics for raw data between two groups were slightly different; base-10 logarithm transformed data showed similar statistics for both groups (Table 5-1). Spatial structures for two groups are presented in Figure 5-4 and model parameters in Table 5-2. Despite of small difference on nuggets, partial sill and range between two groups; the general spatial structures of two groups are relatively similar. However, it was not possible to get reliable spatial structure for some countries due to small number of observations and other factors not explored. Basing in exploration results it was decided to use combined data from different countries measured by different techniques in this study.

Data exploration showed that PM10 daily annual mean concentration for 2003 ranged from  $5.5 \mu\text{gm}^{-3}$  to  $58.35 \mu\text{gm}^{-3}$ . PM2.5 monthly annual averages for 2003 ranged from  $2.521 \mu\text{gm}^{-3}$  to  $25.815 \mu\text{gm}^{-3}$ . The AOT values ranged from 0.0 to 0.449. When explored using quantitative and descriptive statistics AOT was normally distributed while PM10 and PM2.5 were positively skewed. They were transformed using base-10 logarithm transformation. Skewedness in PM10 and PM2.5 was also found by van de Kassteele et al. (2006) and were transformed by base-10 logarithm and natural logarithm transformation respectively. Transformation of PM2.5 was important especially in cokriging because of a need to estimate variograms and cross variograms which usually require normally distributed data (Webster and Oliver, 2008).

Ordinary linear model results between observed PM10 concentration and covariates (AOT and PM2.5) are presented in Table 5-6. The model between PM10 and covariates was found significant ( $p\text{-value} \ll 0.01$ ) but deterministic model coefficient ( $R^2$ ) was small for both cases.  $R^2$  between PM10 and PM2.5 was found to be 0.17 and 0.16 for PM10 and AOT. On the other hand linear model of PM10 and both covariates (AOT and PM2.5) resulted at  $R^2$  of 0.204. Denby et al. (2008) obtained  $R^2$  of 0.21 between PM10 and PM2.5 for the year 2003 but only 127 rural background stations were used as opposed to this study whereby 607 urban, sub urban and rural background stations have been used. So inclusion of urban and suburban stations has increased uncertainties. Also according to scale of rural background, model outputs were capable to capitalize the local variation in PM10.

Preliminary linear model results suggested that incorporating these covariates in prediction of PM10 could improve accuracy of resulting maps. This was found true for predicted maps that used hole effect model (Table 5-17) but the trend was not clear for exponential model (Table 5-16). Accuracy assessment of results at validation points show that hole effect model gave results that reflected correlation between observed PM10 and secondary data. For example RK using hole effect model of PM10 regressed on both covariates (AOT and PM2.5) gave better results compared to PM10 regressed on individual covariates (Table 5-17). Furthermore, there were improvements in results when covariates were used compared to OK and UK of PM10 only though the difference was small to honour the use of covariates.

Though correlation (R) for PM10 regressed on PM2.5 was better (0.41) than for PM10 regressed on AOT (R=0.40), for exponential model RK of PM10 regressed to AOT after ordinary linear regression gave better results than using PM2.5. For example map produced by RK of PM10 regressed on AOT provided a lower RMSE value (0.096) as compared to PM10 regressed on PM2.5 (0.098). Both models R increased from 0.40 to 0.71 and 0.41 to 0.71 for RK of PM10 regressed on AOT and RK of PM10 regressed on PM2.5 respectively. Combining both covariates in RK of PM10 gave similar results but less biased to UK (Table 5-16(a)).

Table 5-16 (b) presents results of RK and CK when PM10 kriged using PM2.5 at 30 km spatial resolution as covariate. RK of PM10 regressed on PM2.5 downsampled by bilinear interpolation were better than RK of PM10 regressed to coarser PM2.5. But  $R^2$  for PM10 regressed to coarser PM2.5 (Table 5-13) and PM10 regressed to fine PM2.5 (Table 5-6) was relatively similar. On the other hand, the results for cokriging of PM10 with PM2.5 downsampled by bilinear interpolation was better than with coarser resolution. The results for RK were better than for CK. The results contradicts an assumption that cokriging always gives good results (Goovaerts, 1999). Poor performance of cokriging is due to low correlation and coarser spatial resolution of covariate (PM2.5). As observed by (Stein and Corsten, 1991) that CK performs well when target variable is high correlated with intensively sampled covariates. These conditions are not met for CK of PM10 and PM2.5 as correlation is low and there is an uncertainty in sampling of PM2.5 due to its spatial resolution. Even if PM2.5 downsampled by bilinear interpolation improved RK and CK of PM10 results compared to coarser resolution, a better downscaling techniques “Downscaling cokriging” is required which not only pixel size will be increased but also the detail in order to improved CK performance. Downscaling by bilinear interpolation neither account for spatial structure in data nor covariates on its downscaling process.

Both RK and CK were able to integrate three dataset at different support but not explicitly. It was required to put data into same support by applying resampling techniques and overlaying of measurements. Modelling was done using collocated values. RK was found to perform better than CK when three dataset were integrated. However, the contribution of ancillary data in prediction of PM10 by RK or CK was not valuable as optimal results were similar to results obtained by OK and UK. The performance of RK and CK as compared to OK and UK can be improved by adding more covariates. For example Emili, et al. (2010) found high correlation between PM10 and AOT from SEVIRI and MODIS to be higher to 24 h aggregated data. These improvements on 24 h aggregation was obtained at expense of including meteorological data i.e. Relative Humidity (RH) and Boundary Layer Height (BLH). Therefore considering model variables could improve results

Overall accuracy assessment has shown predicted results to have agreement with observation for 0.63 to 0.72 for the all kriging methods used (excluding ordinary linear regression). RK provided relatively good results compared to other methods, however it is slightly different from OK and UK. This contradicts the results by (Beelen et al., 2009) who obtained good results with UK in his methods comparison study in air pollution mapping across European union. These results agrees with results found by Denby et al. (2008) who used data for the year 2003 but only 127 rural background were considered.

Two model functions were used to fit estimated empirical variograms; exponential model and hole effect model. The use of two model function was due to hole effect emerged on the estimated variograms of PM10 concentration for 2003. Visually hole effect model fitted much better the empirical variograms specifically at shorter distance up to 400 km compared to exponential model. Assessment done at validation points show that prediction maps by kriging methods which used exponential model resulted at low RMSE and high correlation between observed and predicted PM10 values compared to hole effect

model. However results from hole effect model were less unbiased as compared to those of exponential model (compare the ME for Table 5-16 and Table 5-17)

Universal block kriging was performed at block size of 2 km, 5 km, 10 km, 20 km and 30 km. Accuracy assessment at validation points showed RMSE to be low for block size less or equal to 10 km. RMSE increased as block size greater than 10 km. The limitation of block kriging is that on accuracy assessment as observations are at point support while predicted values are at area support.



## 7. CONCLUSION AND RECOMMENDATIONS

### 7.1. Conclusions

The objectives of the study was to develop and apply geostatistical methods to integrate in situ data, model output and remotely sensing data to model and map air quality. Also it intended to predict concentrations of pollutants in between in situ stations using remotely sensed data and model output. To achieve these objectives five research questions were formulated (Table 1-1). From results obtained and discussion made, the research questions are addressed to conclude the findings.

#### **What is spatial distribution in the data?**

Employing both descriptive and quantitative data analysis e.g. histogram, summary statistics and variograms modelling, two groups of data were explored for 2006. Combined data from different countries measured by different techniques and combined data from different countries measured by beta ray attenuation techniques. It was found that two groups of data had relatively similar data behaviour. They are all positively skewed, having almost the same summary statistics when transformed to base-10 logarithmic scale (Table 5-1) and the nugget and partial sill were relatively similar. Data measured by all techniques showed more variability having slightly long range compared to data measured by beta ray attenuation. Therefore despite of small difference on nuggets, partial sill and range between two groups; the general spatial structures of two groups were found are relatively similar.

#### **How should 3 data sources be integrated?**

Two approaches were used to integrate 3 data sources. RK after ordinary linear regression was applied. Linear model residuals were analysed and variograms of residuals estimated. Two maps residual map and ordinary linear regression map were added to give PM10 daily annual mean concentration map. Second approach was cokriging. This involved estimation of individual variograms of each dataset using values at collocation. These variograms were used to calculate cross variograms using LMC. This model was used in prediction to produce PM10 daily annual mean concentration map. RK gave better results than CK when 3 data sources were integrated. However the use of covariates gave disappointing results in general as methods gave almost similar results to kriging using independent measurement by UK and OK. This was due to low correlation between PM10 and covariates.

#### **How to model different data sources taking into consideration different spatial support**

In order to model dataset, first AOT and PM2.5 were put on the same spatial support. PM2.5 at 35 km by 25 km square grid were downscaled by bilinear interpolation to AOT spatial resolution of 10 km square grid. Overlay of secondary data with in situ measurements were made to obtain corresponding values of AOT and PM2.5 at collocated points with in situ measurements. The corresponding/collocated values were used in modelling i.e. either for linear modelling between PM10 and covariates or for estimation of empirical variograms for each dataset and cross variograms between dataset.

Downscaling by bilinear interpolation approach is a simple resampling technique in sense that grids are sub divided into finer grids but the information of resulting pixels remains almost similar to that of large pixel. This was observed when PM10 were regressed on coarser PM2.5 at 30 km square grid. The resulting  $R^2$  was almost similar to  $R^2$  obtained when PM10 were regressed on PM2.5 downscaled by bilinear

interpolation as shown in Table 5-6 and Table 5-13. Downscaling cokriging which use point variograms estimated from empirical variograms by deconvolution to downscale data would be appropriate techniques to downscale coarse covariates to finer grid.

#### **Which kriging methodology is more accurate in predicting at unsampled locations?**

Overall RK using exponential model gave accurate results. However use of covariates gave almost similar results obtained when predicting independent measurements using UK and OK. Therefore the value of covariates was not honoured in this study.

#### **How can predictions be validated?**

Predictions were assessed using independent dataset. Criteria used were the correlation coefficient (R) and RMSE between predicted values and observed values at validation points. Predictions were considered better if it provides higher R and lower RMSE value. Also ME was used to assess prediction results. This is an appropriate approach and has been used in various research (Beelen et al., 2009; Bourennane et al., 2000).

### **7.2. Recommendations**

Basing on the findings of this study, I would recommend application of downscaling cokriging to downscale PM<sub>2.5</sub> before being used as covariate. This could improve information to a targeted pixel size hence capitalize local scale variations.

## LIST OF APPENDICES

---

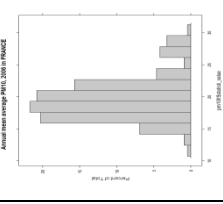
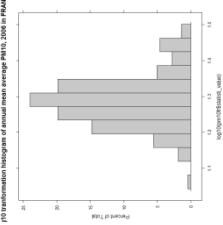
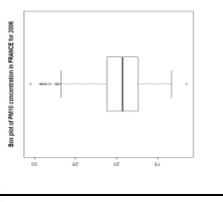
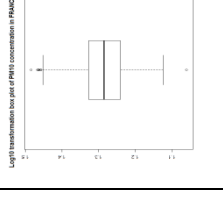
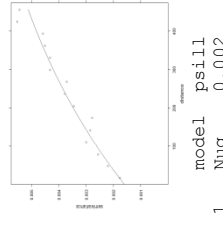
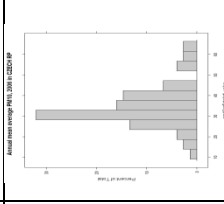
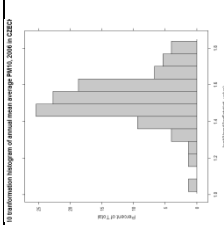
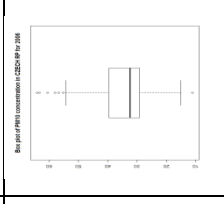
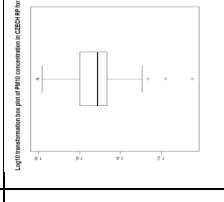
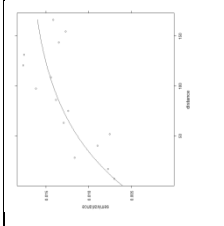
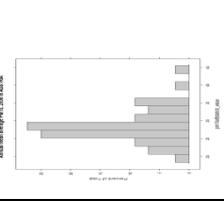
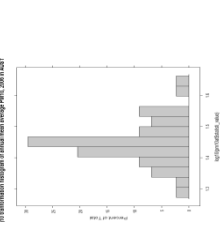
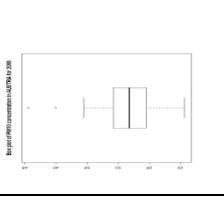
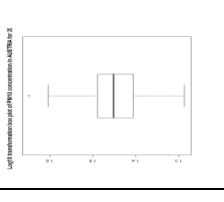
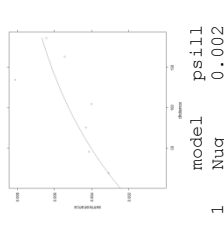
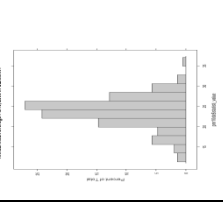
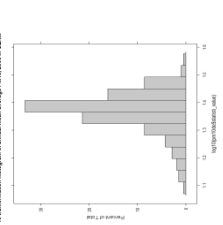
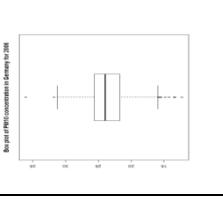
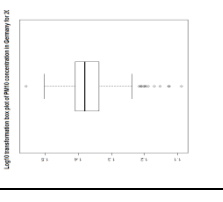
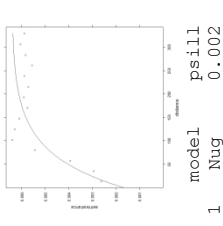
Appendix A. Country by country data exploration for combined PM10 concentration measured by different techniques for 2006.....	57
Appendix B: Country by country data exploration for combined PM10 concentration measured by beta ray absorption technique for the 2006. ....	59
Appendix C. Summary of linear model of PM10 regressed on AOT.....	62
Appendix D. Summary of linear model of PM10 regressed on PM2.5.....	62
Appendix E. Summary of linear model of PM10 regressed on AOT and PM2.5.....	63
Appendix F: Code for cokriging. ....	65



Appendix A. Country by country data exploration for combined PM10 concentration measured by different techniques for 2006

Individual country data exploration of PM10, daily annual mean averages, 2006. Data includes all measurement techniques											
FR	Min.	11.47	1st Qu.	17.39	Median	19.68	3rd Qu.	21.20	Max.	30.50	
	Log10	Min.	1.060	1st Qu.	1.240	Median	1.288	3rd Qu.	1.326	Max.	1.484
CZ	Min.	11.15	1st Qu.	29.24	Median	32.49	3rd Qu.	34.59	Max.	64.19	
	Log10	Min.	1.047	1st Qu.	1.466	Median	1.512	3rd Qu.	1.598	Max.	1.808
AT	Raw data	Min.	19.35	1st Qu.	25.51	Median	28.26	3rd Qu.	30.80	Max.	44.48
	Transformed	Min.	1.287	1st Qu.	1.407	Median	1.451	3rd Qu.	1.489	Max.	1.648
DE	Min.	12.27	1st Qu.	21.74	Median	24.00	3rd Qu.	25.63	Max.	36.12	
	Log10	Min.	1.089	1st Qu.	1.337	Median	1.380	3rd Qu.	1.367	Max.	1.558

 <p>Annual mean average PM10, 2006 in France</p>	 <p>PM10 transformation histogram of annual mean average PM10, 2006 in France</p>	 <p>Box plot of PM10 concentration in France for 2006</p>	 <p>Log10 transformation box plot of PM10 concentration in France for 2006</p>	 <p>model psill range 1 Nug 0.002 0.000 2 Exp 0.007 594.802</p>
 <p>Annual mean average PM10, 2006 in CZ</p>	 <p>PM10 transformation histogram of annual mean average PM10, 2006 in CZ</p>	 <p>Box plot of PM10 concentration in CZ for 2006</p>	 <p>Log10 transformation box plot of PM10 concentration in CZ for 2006</p>	 <p>model psill range 1 Nug 0.006 0.000 2 Exp 0.011 80.041</p>
 <p>Annual mean average PM10, 2006 in AT</p>	 <p>PM10 transformation histogram of annual mean average PM10, 2006 in AT</p>	 <p>Box plot of PM10 concentration in Austria for 2006</p>	 <p>Log10 transformation box plot of PM10 concentration in Austria for 2006</p>	 <p>model psill range 1 Nug 0.002 0.000 2 Exp 0.007 182.465</p>
 <p>Annual mean average PM10, 2006 in DE</p>	 <p>PM10 transformation histogram of annual mean average PM10, 2006 in DE</p>	 <p>Box plot of PM10 concentration in Germany for 2006</p>	 <p>Log10 transformation box plot of PM10 concentration in Germany for 2006</p>	 <p>model psill range 1 Nug 0.002 0.000 2 Exp 0.006 72.554</p>

GEOSTATISTICAL ANALYSIS OF AIR POLLUTION USING MODELS, IN SITU AND REMOTE SENSED DATA

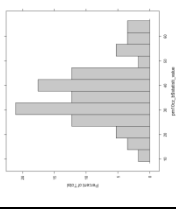
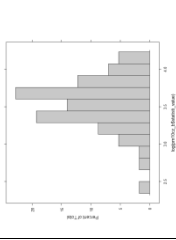
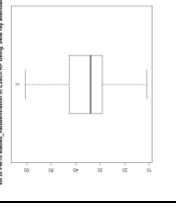
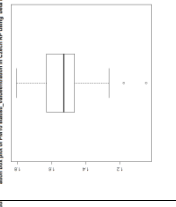
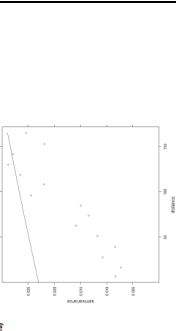
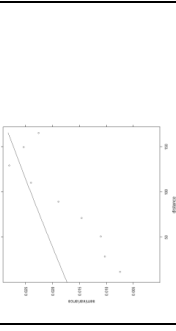
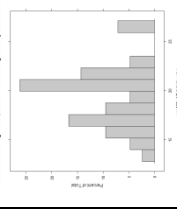
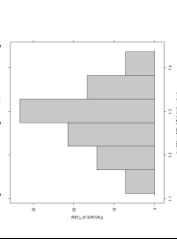
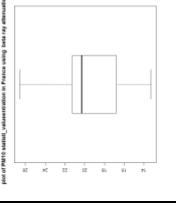
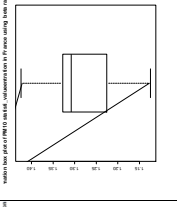
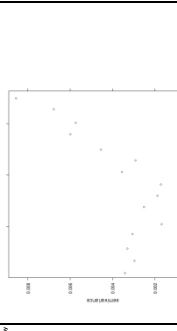
GB	<p>Min. 1st Qu. Median Mean 3rd Qu. Max.            11.46 21.71 23.55 23.50 25.80 34.27</p> <p>Log10            Min. 1st Qu. Median Mean 3rd Qu. Max.            1.059 1.337 1.372 1.366 1.412 1.535</p>					 <p>model psill range            1 Nug 0.003 0.000            2 Exp 0.001 108.980</p>
BE	<p>Min. 1st Qu. Median Mean 3rd Qu. Max.            18.63 31.70 33.08 31.93 35.05 38.14</p> <p>Log10            Min. 1st Qu. Median Mean 3rd Qu. Max.            1.270 1.501 1.520 1.498 1.545 1.581</p>					 <p>model psill range            1 Nug 0.000 0.000            2 Exp 0.005 37.816</p>
NL	<p>Min. 1st Qu. Median Mean 3rd Qu. Max.            24.01 25.39 27.31 28.09 30.16 33.66</p> <p>Log 10            Min. 1st Qu. Median Mean 3rd Qu. Max.            1.380 1.405 1.436 1.446 1.479 1.527</p>					 <p>Warning: singular model in variograms fit</p>
BE	<p>Min. 1st Qu. Median Mean 3rd Qu. Max.            18.63 31.70 33.08 31.93 35.05 38.14</p> <p>Log10            Min. 1st Qu. Median Mean 3rd Qu. Max.            1.270 1.501 1.520 1.498 1.545 1.581</p>					



GEOSTATISTICAL ANALYSIS OF AIR POLLUTION USING MODELS, IN SITU AND REMOTE SENSED DATA

NL	<p>Min. 1st Qu. Median Mean 3rd Qu. Max.            24.01 25.39 27.31 28.09 30.16 33.66</p> <p>Log10            Min. 1st Qu. Median Mean 3rd Qu. Max.            1.380 1.405 1.436 1.446 1.479 1.527</p>					
DE	<p>Min. 1st Qu. Median Mean 3rd Qu. Max.            12.27 21.69 24.15 23.61 25.85 36.12</p> <p>Log10            Min. 1st Qu. Median Mean 3rd Qu. Max.            1.089 1.336 1.383 1.366 1.412 1.558</p>					 <pre>           model psill range           1 Nug 0.004 0.000           2 Exp 0.003 61.448           Use of raw data         </pre>
AT	<p>Min. 1st Qu. Median Mean 3rd Qu. Max.            22.50 24.54 26.98 27.18 29.07 34.81</p> <p>Log10            Min. 1st Qu. Median Mean 3rd Qu. Max.            1.352 1.390 1.431 1.431 1.464 1.542</p>					 <pre>           model psill range           1 Nug 10.308 0.000           2 Exp 6.062 80.527         </pre>

GEOSTATISTICAL ANALYSIS OF AIR POLLUTION USING MODELS, IN SITU AND REMOTE SENSED DATA

CZ	<p>Min. 1st Qu. Median Mean 3rd Qu. Max.            11.15 29.25 33.93 36.24 42.78 64.19</p> <p>Log10            Min. 1st Qu. Median Mean 3rd Qu. Max.            1.047 1.466 1.531 1.535 1.631 1.808</p>					 <p>Warning: singular model in variogram fit</p> <pre> model          psill      range 1  Nug         0.023      0.000 2  Exp         0.041     1069.932     </pre> <p>Changing bin width</p>  <p>Warning: singular model in variogram fit</p> <pre> model          psill      range 1  Nug         0.017      0.000 2  Exp         0.108     1540.702     </pre>
FR	<p>Min. 1st Qu. Median Mean 3rd Qu. Max.            13.31 16.96 20.32 19.49 21.18 26.57</p> <p>Log10            Min. 1st Qu. Median Mean 3rd Qu. Max.            1.124 1.229 1.308 1.284 1.326 1.424</p>					 <p>Warning: singular model in variogram fit</p>

Appendix C. Summary of linear model of PM10 regressed on AOT

```
> lm.pm10.aot <- lm(log10(mean)~AOT, as.data.frame(pm10.extraproj))
> summary(lm.pm10.aot) Call:
lm(formula = log10(mean) ~ AOT, data =
as.data.frame(pm10.extraproj))

Residuals:
    Min       1Q   Median       3Q      Max
-0.630621 -0.069642  0.001308  0.070656  0.388864

Coefficients:
            Estimate Std. Error t value Pr(>|t|)
(Intercept)  1.14802    0.02796   41.05 <2e-16 ***
AOT          1.04730    0.11071    9.46 <2e-16 ***
---
Signif. codes:  0 '***' 0.001 '**' 0.01 '*' 0.05 '.' 0.1 ' ' 1

Residual standard error: 0.1216 on 453 degrees of freedom
Multiple R-squared:  0.165,    Adjusted R-squared:  0.1631
F-statistic: 89.49 on 1 and 453 DF,  p-value: < 2.2e-16
```

Appendix D. Summary of linear model of PM10 regressed on PM2.5

```
> lm.pm10.pm25 <- lm(log10(mean)~PM2.5, as.data.frame(pm10.extraproj))
> summary(lm.pm10.pm25) Call:
lm(formula = log10(mean) ~ PM2.5, data =
as.data.frame(pm10.extraproj))

Residuals:
    Min       1Q   Median       3Q      Max
-0.699673 -0.064400  0.004019  0.071859  0.395317

Coefficients:
            Estimate Std. Error t value Pr(>|t|)
(Intercept)  1.234083    0.018733   65.879 <2e-16 ***
PM2.5        0.014738    0.001522    9.686 <2e-16 ***
---
Signif. codes:  0 '***' 0.001 '**' 0.01 '*' 0.05 '.' 0.1 ' ' 1

Residual standard error: 0.1211 on 453 degrees of freedom
Multiple R-squared:  0.1716,    Adjusted R-squared:  0.1697
F-statistic: 93.81 on 1 and 453 DF,  p-value: < 2.2e-16
```

Appendix E. Summary of linear model of PM10 regressed on AOT and PM2.5

```

> summary(lm.meas.AOT.PM2.5)
Call:
lm(formula = log10(mean) ~ PM2.5 + AOT, data = as.data.frame(pm10.WGS84))

Call:
lm(formula = log10(mean) ~ AOT + PM2.5, data = as.data.frame(pm10.extraproj))

Residuals:
    Min       1Q   Median       3Q      Max
-0.66619 -0.06279  0.00329  0.06962  0.40435

Coefficients:
            Estimate Std. Error t value Pr(>|t|)
(Intercept)  1.142050   0.027292   41.846 < 2e-16 ***
AOT          0.625946   0.137476   4.553 6.80e-06 ***
PM2.5       0.009389   0.001897   4.950 1.05e-06 ***
---
Signif. codes:  0 '***' 0.001 '**' 0.01 '*' 0.05 '.' 0.1 ' ' 1

Residual standard error: 0.1185 on 452 degrees of freedom
Multiple R-squared: 0.2079,    Adjusted R-squared: 0.2044
F-statistic: 59.31 on 2 and 452 DF,  p-value: < 2.2e-16

```



Appendix F: Code for cokriging.

```

#CODES FOR COKRIGING
#libraries used
require(rgdal)
library(sp)
library(lattice)
trellis.par.set(sp.theme()) # plots the final predictions using blue-pink-yellow legend
#Reading model output
PM25= readGDAL("D:\\NEW_DATA\\pm10\\PM10_Jan\\pm25_ProjectRaster.img")# FROM arcgis
model.PM25=PM25
proj4string(model.PM25) <- CRS("+init=epsg:3035")
#Reading remotely sensed data
AOT= readGDAL("D:\\NEW_DATA\\pm10\\PM10_Jan\\aot_ProjectRaster.img") # FROM arcgis
modis.aot=AOT
proj4string(modis.aot) <- CRS("+init=epsg:3035")
#combine PM2.5 and AOT in one
combine_PM25.AOT=model.PM25
combine_PM25.AOT$AOT=modis.aot$band1
combine_PM25.AOT$PM2.5=model.PM25$band1
str(combine_PM25.AOT)
#Reading in situ data
pm10b=read.table("D:\\NEW_DATA\\pm10\\PM10_Jan\\PM10e.txt", header=T) #t
class(pm10b)#this is data.frame
pm10insitu=pm10b #copying
#Subsetting data for prediction (pm10.extra) and for validation (pm10.valid)
#pm10.extra data for prediction while pm10.valid is data for validation
pm10.valid <- pm10insitu[ seq(1, length(pm10insitu$mean), by=4),c("mean","x", "y")]
pm10.extra <- pm10insitu[setdiff(rownames(pm10insitu), rownames(pm10.valid)),c("mean","x",
"y")]
write.table(pm10.valid, file="D:\\NEW_DATA\\pm10\\PM10_Jan\\pm10valid_latlong.txt")
#Modeling spatial structure of the data
#Change data.frame to spatialpointdata
#spatialpointdata~x_km+y_km
coordinates(pm10insitu) <- ~x+y
coordinates(pm10.extra) <- ~x+y
coordinates(pm10.valid) <- ~x+y
proj4string(pm10insitu) <- CRS("+proj=longlat +datum=WGS84")
proj4string(pm10.extra)<-CRS("+proj=longlat +datum=WGS84")
proj4string(pm10.valid)<- CRS("+proj=longlat +datum=WGS84")
#Projecting coordinates ready for modeling and prediction
pm10.extraproj<-spTransform(pm10.extra, CRS("+init=epsg:3035"))
# Display of in situ data with secondary data
print(spplot(combine_PM25.AOT, scales=list(draw=T),
sp.layout=list("sp.points", pm10.extraproj, pch="+"),main="Overlay of PM2.5 and PM10"))
#Overlay
model.PM25.AOT.ov = overlay(combine_PM25.AOT, pm10.extraproj) # create grid-points overlay
str(model.PM25.AOT.ov@data)

#correlation
cor(log10(pm10.extra$mean),log10(model.PM25.AOT.ov$PM2.5))
plot(log10(pm10.extra$mean),log10(model.PM25.AOT.ov$PM2.5))
cor(log10(pm10.extra$mean),model.PM25.AOT.ov$AOT)
plot(log10(pm10.extra$mean),model.PM25.AOT.ov$AOT)
#EMPERICAL VARIOGRAM
require(gstat)
v.log1 = variogram(log10(mean)~1, data=pm10.extraproj, cutoff=1000000,width=60000)
v.log2 = variogram((AOT)~1, data=model.PM25.AOT.ov,cutoff=1000000,width=60000)
v.log3 = variogram(log10(PM2.5)~x+y, data=model.PM25.AOT.ov,cutoff=1000000,width=60000)
#scaling of distance for variogram plotting.
vb.sc1=v.log1
vb.sc1$dist=v.log1$dist/1000
vb.sc1
plot(vb.sc1)

```

```

vb.sc2=v.log2
vb.sc2$dist=v.log2$dist/1000
vb.sc2
plot(vb.sc2)
vb.sc3=v.log3
vb.sc3$dist=v.log3$dist/1000
vb.sc3
plot(vb.sc3)
#####
# Variogram modelling
#####
require(lattice)
v.log.exp1 = fit.variogram(vb.sc1, vgm(0.01, "Exp", 150, 0.005))
plot(vb.sc1, model=v.log.exp1, col="black")

v.log.exp2 = fit.variogram(vb.sc2, vgm(0.0, "Exp", 500, 15))
plot(vb.sc2, model=v.log.exp2, col="black")

v.log.exp3 = fit.variogram(vb.sc3, vgm(0.005, "Exp", 200, 0.015))
plot(vb.sc3, model=v.log.exp3, col="black")
# compare variogram structure to target variable
v.log.exp1$range[2]; v.log.exp2$range[2];v.log.exp3$range[2]
round(v.log.exp1$psill[1]/sum(v.log.exp1$psill),2)
round(v.log.exp2$psill[1]/sum(v.log.exp2$psill),2)
round(v.log.exp3$psill[1]/sum(v.log.exp3$psill),2)
#model cross variogram
(g <- gstat(NULL, id = "PM10", form = log10(mean)~ 1, data=pm10.extraproj))
(g <- gstat(g, id = "AOT", form = AOT~ 1, data=model.PM25.AOT.ov))
(g <- gstat(g, id = "PM25", form = log10(PM2.5)~x+y, data=model.PM25.AOT.ov))
v.cross <- variogram(g)
str(v.cross)
plot(v.cross)
#Fitting model of co regionalization
mm <- vgm( 0.009563601,"Exp", 121978.4, 0.008629772)
(g <- gstat(g, id = "PM10", model =mm , fill.all=T))
(g <- fit.lmc(v.cross, g))
#plot the cross variogram model
plot(variogram(g), model=g$model)
#cokriging prediction
k.c <- predict.gstat(g, combine_PM25.AOT)
#IMPORTING SHAPE FILES
nlboundary<- readOGR("D:\\EURO_0711\\SHP_FILES\\NL", "wce_bound2")
x11()
plot(nlboundary)
nlboundary@ proj4string
nlbound<-nlboundary
nlbound.ETRS<-spTransform(nlbound, CRS("+init=epsg:3035"))
#Plot cokriging predictions
library(sp)
library(lattice)
trellis.par.set(sp.theme())
spplot(k.c , "PM10.pred",do.log = TRUE,key.space=list(x=0.2,y=0.9,corner=c(0,1)),
scales=list(draw=T),
main="Cokriging predictions of PM10 with AOT and PM2.5",
more = TRUE,sp.layout = list("sp.lines", as(nlbound.ETRS, "SpatialLines")))
spplot(k.c , "PM10.var",do.log = TRUE,key.space=list(x=0.2,y=0.9,corner=c(0,1)),
scales=list(draw=T),
main="Cokriging variance of PM10 with AOT and PM2.5",
more = TRUE,sp.layout = list("sp.lines", as(nlbound.ETRS, "SpatialLines")))
#VALIDATION
pred.raw= overlay(k.c, pm10.validproj)
pred.raw$mean=log10(pm10.validproj$mean)
dif.sq.error=(pred.raw$mean-pred.raw$PM10.pred)^2
SSE=sum(dif.sq.error)

```

```
RMSE= (SSE/152) ^0.5  
ME= (sum(pred.raw$mean-pred.raw$PM10.pred))/152  
cor(pred.raw$mean,pred.raw$PM10.pred)
```

---

## LIST OF REFERENCES

---

- Annon, A., Luzet, C., Gubler, E., & Ihde, J. (2001). Map projections for Europe. *Institute for Environment and Sustainability*, 1-132.
- Armstrong, M. (1984). Problems with universal kriging. *Mathematical Geology*, 16(1), 101-108.
- Atkinson, P. M. (2008). Issues of Uncertainty in Super-Resolution Mapping and the Design of an Inter-Comparison Study. *Proceedings of the 8th International Symposium on Spatial Accuracy Assessment in Natural Resources and Environmental Sciences Shanghai, P. R. China, June 25-27, 2008*, pp. 145-154.
- Atkinson, P. M., Pardo Iguzquiza, E., & Chica Olmo, M. (2008). Downscaling cokriging for super-resolution mapping of continua in remotely sensed images. *IEEE Transactions on Geoscience and Remote Sensing*, 46(2), 573-580.
- Atkinson, P. M., Webster, R., & Curran, P. J. (1992). Cokriging with ground-based radiometry. *Remote Sensing of Environment*, 41(1), 45-60.
- Bayraktar, H., & Turalioglu, F. (2005). A Kriging-based approach for locating a sampling site—in the assessment of air quality. *Stochastic Environmental Research and Risk Assessment*, 19(4), 301-305.
- Beelen, R., Hoek, G., Pebesma, E., Vienneau, D., de Hoogh, K., & Briggs, D. J. (2009). Mapping of background air pollution at a fine spatial scale across the European Union. *Science of The Total Environment*, 407(6), 1852-1867.
- Bourennane, H., King, D., & Couturier, A. (2000). Comparison of kriging with external drift and simple linear regression for predicting soil horizon thickness with different sample densities. *Geoderma*, 97(3-4), 255-271.
- Cinzia Mazzetti, & Todini, E. (2002). Development and application of the block Kriging technique to rain-gauge data. [University of Bologna].
- Denby, B., Schaap, M., Segers, A., Bultjes, P., & Horálek, J. (2008). Comparison of two data assimilation methods for assessing PM10 exceedances on the European scale. *Atmospheric Environment*, 42(30), 7122-7134.
- Dickey, J. H. (2000). Selected topics related to occupational exposures Part VII. Air pollution: Overview of sources and health effects. *Disease-a-Month*, 46(9), 566-589.
- Diem, J. E., & Comrie, A. C. (2002). Predictive mapping of air pollution involving sparse spatial observations. *Environmental Pollution*, 119(1), 99-117.
- Emili, E., Popp, C., Petitta, M., Riffler, M., Wunderle, S., & Zebisch, M. (2010). PM10 remote sensing from geostationary SEVIRI and polar-orbiting MODIS sensors over the complex terrain of the European Alpine region. *Remote Sensing of Environment*, In Press, Corrected Proof.
- European-Topic-Centre-on-Air-and-Climate-Change. (2011). AirBase - xml and raw data file downloads. Retrieved 27th March, 2011, from <http://acm.eionet.europa.eu/databases/airbase/airbasexml/index.html>
- Fischer, H., Brunekreef, B., & Lebret, E. (2004). Air pollution related deaths during the 2003 heat wave in the Netherlands. *Atmospheric Environment*, 38(8), 1083-1085.
- Goovaerts, P. (1999). Using elevation to aid the geostatistical mapping of rainfall erosivity. *Catena*, 34(3-4), 227-242.
- Goovaerts, P. (2000). Geostatistical approaches for incorporating elevation into the spatial interpolation of rainfall. *Journal of Hydrology*, 228(1-2), 113-129.
- Hengl, T., Heuvelink, G. B. M., & Rossiter, D. G. (2007). About regression-kriging: From equations to case studies. *Computers and Geosciences*, 33(10), 1301-1315.
- Hengl, T., Heuvelink, G. B. M., & Stein, A. (2004). A generic framework for spatial prediction of soil variables based on regression-kriging. *Geoderma*, 120(1-2), 75-93.
- Hutchison, K. D., Smith, S., & Faruqui, S. J. (2005). Correlating MODIS aerosol optical thickness data with ground-based PM2.5 observations across Texas for use in a real-time air quality prediction system. *Atmospheric Environment*, 39(37), 7190-7203.
- Olea, R. (1991). Reply to comments on “book review: An Introduction to Applied Geostatistics”. *Mathematical Geology*, 23(4), 683-685.
- Pardo Iguzquiza, E., Chica Olmo, M., & Atkinson, P. M. (2006). Downscaling cokriging for image sharpening. *Remote Sensing of Environment*, 102(1-2), 86-98.
- Schaap, M., Manders, A. M. M., Hendriks, E. C. J., Cnossen, J. M., Segers, A. J. S., Denier van, H. A. C., et al. (2009a). Regional Modelling of Particulate Matter for the Netherlands. [Technical background report BOP]. *Netherlands Research Program on Particulate Matter (BOP), Report 500099008*.
- Schaap, M., Renske, T., & Henk, E. (2009b). LOTOS EUROS. *Macc, Report D\_R-ENS\_1.4.1* (September 2009).

- Singh, V., Carnevale, C., Finzi, G., Pisoni, E., & Volta, M. (2011). A cokriging based approach to reconstruct air pollution maps, processing measurement station concentrations and deterministic model simulations. *Environmental Modelling and Software, In Press, Corrected Proof*.
- Stedman, J. R. (2004). The predicted number of air pollution related deaths in the UK during the August 2003 heatwave. *Atmospheric Environment*, 38(8), 1087-1090.
- Stein, A., & Corsten, L. C. A. (1991). Universal kriging and cokriging as regression procedure. *Biometrics*, 47(2), 575-587.
- van de Kasstele, J. (2006). *Statistical air quality mapping: PhD thesis*. Wageningen University, Wageningen.
- van de Kasstele, J., & Stein, A. (2006). A model for external drift kriging with uncertain covariates applied to air quality measurements and dispersion model output. *Environmetrics*, 17(4), 309-322.
- van de Kasstele, J., Stein, A., Koelemeijer, R., Dekkers, A., Schaap, M., & Homan, C. (2006). Statistical mapping of PM10 concentrations over Western Europe using secondary information from dispersion modeling and MODIS satellite observations. *Stochastic Environmental Research and Risk Assessment*, 21(2), 183-194.
- Webster, R., & Oliver, M. A. (2008). *Geostatistics for environmental scientists : e-book* (Second edition ed.). United Kingdom: Wiley & Sons, Ltd.
- Wenxia, T., Li, J., & Li, Y. (2008). Rasterizing airborne laser scanning point clouds by block kriging. [ISPRS Congress Beijing 2008, Proceedings of Commission III]. *The International Archives of the Photogrammetry, Remote Sensing and Spatial Information Sciences.*, Vol. XXXVII Part B3b., 687-692.
- Zhang, D., Aunan, K., Seip, M. H., Larssen, S., Liu, J., & Zhang, D. (2010). The assessment of health damage caused by air pollution and its implication for policy making in Taiyuan, Shanxi, China. *Energy Policy*, 38(1), 491-502.